Lbx1-expressing cells lacking the repellent EphA4 receptor are involved in axonal midline crossing in the spinal cord and evoke a minor gait defect

Inauguraldissertation

zur

Erlangung der Würde eines Doktors der Philosophie
vorgelegt der
Philosophischen-Naturwissenschaftlichen Fakultät
der Universität Basel

von

Christiane Pudenz
aus Jena, Deutschland

Basel, 2014

Genehmigt von der Philosophisch-Naturwissenschaftlichen Fakultät

auf Antrag von

Prof. Dr. Silvia Arber

(Dissertationsleitung)

Prof. Dr. Peter Scheiffele

(Korreferat)

Basel, den 20.05.2014

Prof. Dr. Jörg Schibler
(Dekan)

Namensnennung-Keine kommerzielle Nutzung-Keine Bearbeitung 3.0 Schweiz
(CC BY-NC-ND 3.0 CH)

Sie dürfen: **Teilen** — den Inhalt kopieren, verbreiten und zugänglich machen

Unter den folgenden Bedingungen:

Namensnennung — Sie müssen den Namen des Autors/Rechteinhabers in der von ihm festgelegten Weise nennen.

Keine kommerzielle Nutzung — Sie dürfen diesen Inhalt nicht für kommerzielle Zwecke nutzen.

Keine Bearbeitung erlaubt — Sie dürfen diesen Inhalt nicht bearbeiten, abwandeln oder in anderer Weise verändern.

Wobei gilt:

- **Verzichtserklärung —** Jede der vorgenannten Bedingungen kann **aufgehoben** werden, sofern Sie die ausdrückliche Einwilligung des Rechteinhabers dazu erhalten.
- **Public Domain (gemeinfreie oder nicht-schützbare Inhalte) —** Soweit das Werk, der Inhalt oder irgendein Teil davon zur Public Domain der jeweiligen Rechtsordnung gehört, wird dieser Status von der Lizenz in keiner Weise berührt.
- **Sonstige Rechte —** Die Lizenz hat keinerlei Einfluss auf die folgenden Rechte:
    - Die Rechte, die jedermann wegen der Schranken des Urheberrechts oder aufgrund gesetzlicher Erlaubnisse zustehen (in einigen Ländern als grundsätzliche Doktrin des **fair use** bekannt);
    - Die **Persönlichkeitsrechte** des Urhebers;
    - Rechte anderer Personen, entweder am Lizenzgegenstand selber oder bezüglich seiner Verwendung, zum Beispiel für **Werbung** oder Privatsphärenschutz.
- **Hinweis —** Bei jeder Nutzung oder Verbreitung müssen Sie anderen alle Lizenzbedingungen mitteilen, die für diesen Inhalt gelten. Am einfachsten ist es, an entsprechender Stelle einen Link auf diese Seite einzubinden.

Quelle: http://creativecommons.org/licenses/by-nc-nd/3.0/ch/ Datum: 12.11.2013

Contents

1. Summary

Most limbed animals, including mice and human beings, show alternating hindlimb movement mediated by neuronal circuits in the spinal cord. However, when the repulsive EphA4 receptor expressed by subsets of spinal neurons is mutated, hindlimbs lose their typical left-right alternating pattern and as a consequence, mice exhibit a hopping gait. EphA4 tyrosine kinase receptor binds to its ligand ephrinB3 at the midline of the spinal cord resulting in axonal growth cone collapse. Therefore, in wild type mice, EphA4-expressing axons are prevented from crossing the midline towards the contralateral side. In full *EphA4*$^{-/-}$ mutants, it has been suggested that the hopping gait is caused by an increased number of axons derived from excitatory neurons crossing the spinal midline (Kullander 2003, Restrepo 2011). However, it remained unclear, which subpopulations of spinal interneurons are misguided towards the contralateral side and are involved in the observed hopping gait phenotype. Hence, we aim to determine the cellular origin contributing to axon misguidance and hopping gait in *EphA4*$^{-/-}$ mutant mice, by influencing the balance between excitation and inhibition across the spinal midline. Among 11 main neuron populations in the spinal cord, the interneurons derived from the progenitor domain territory dorsal dI4-6 and marked by the transcription factor Lbx1, were targeted in this study. Here, we investigated the premotor interneuron distribution of motor neurons targeting specific hindlimb muscles in *EphA4* mutant mice by means of monosynaptic rabies tracing technique. We also assessed the gait behavior on a treadmill in the conditional *EphA4* mutant mice, whose *EphA4* receptor was deleted in Lbx1-expressing neurons. We found that a deletion of *EphA4* in Lbx1-positive neurons resulted in aberrant axon guidance of dorsal neurons across the spinal midline and minor gait defects such as a hopping gait at low velocities on the treadmill and a reduced swing time during alternating gait. Moreover, 3-week old conditional *EphA4* mutants perfomed a slight aberrant hopping gait at higher velocities compared to adults. Therefore, Lbx1-expressing interneurons appear to be partially responsible for the phenotypes observed in full *EphA4* mutant mice. In conclusion, we show that the EphA4 receptor plays an important role in preventing axons of Lbx1-expressing interneurons from crossing the spinal midline. Further, EphA4-expression in Lbx1-positive neurons is essential to conserve a complete alternating gait. Lbx1-expressing neurons might be one component of several cell types contributing to the locomotor CPG. Moreover, we also found that

deletion of the *EphA4* receptor in all inhibitory neurons of conditional *EphA4*$^{flox/-}$*vGAT*$^{Cre/+}$ mutant mice caused a partial hopping gait demonstrating that proper axon guidance of inhibitory neurons beside excitatory neurons is important to maintain alternating gait. Finally, although α2chimaerin was shown to be an EphA4 downstream effector and full *α2chimaerin* mutant mice exhibited a hopping gait (Beg 2007; Wegmeyer 2007), we found no anatomical and gait behavioral defects in the conditional *α2chimaerin* mutant mice, lacking α2chimaerin in Lbx1-positive cells. In addition, full *α2chimaerin*$^{-/-}$ mutants displayed significantly decreased synchronous hindlimb movement compared to the full *EphA4*$^{-/-}$ mutant. These findings suggests that deletion of a single EphA4 effector has less effect on the anatomical and gait behavioral phenotypes than it was observed for the EphA4 receptor itself.

2. Introduction

2.1 Locomotion

Locomotion in animals is essential for their survival. Animals require movement in order to seek for food or hunt for prey, to escape an enemy and to find a sexual partner. Their locomotion is adapted to their environment; consequently, they swim, fly, crawl or walk on the ground. Most terrestrial animals require limbs enabling them to move faster on land. Therefore, a coordination of limbs is essential. During evolution, different species have developed a variety of gait patterns to move forward, such as the walk, trot, pace and gallop. The gait pattern depends on balance, body shape, agility, speed and energy expenditure (Hildebrand 1989). Locomotor behaviors are additionally essential for maintaining posture, eye movements, breathing, chewing, vocalizing, reaching and grasping. Neuronal circuits for breathing, chewing and swallowing can be found in the brain stem whereas circuits involved in locomotion are thought to be located at least partially in the spinal cord (Grillner 1975; Jordan 1992; Grillner 2006). Appropriate locomotion requires the activation of different muscles. Each muscle is innervated by a group of motor neurons in the ventral horn of the spinal cord, called motor neuron pools (Romanes 1964; McHanwell 1981). To move one limb forward, muscles act in opposite manner to bend joints, therefore, certain muscles are contracted and its opposing partners are flexed. A step cycle or stride can be divided into swing and stance phase. During the swing phase, the feet are in the air and move forward, whereas during stance phase, the feet are placed on the ground and move backwards in relation to the body. Contraction of flexor muscles mainly occurs during the swing phase, whereas contraction of extensor muscles is activated during the stance phase (Engberg 1969; Shik 1976).

2.2 Central pattern generator in the spinal cord

Limb locomotion is perpetuated by motor circuits in the spinal cord. Brown (1914) was the first who suggested that intrinsic networks in the spinal cord of cat evoke itself rhythmic locomotor-like behavior of limbs. He observed rhythmic bursts of reciprocal activity in flexor

and extensor motor neurons in isolated spinal cords, suggesting a model of two systems of neurons called half-centers that inhibit each other (Brown 1914). Likewise in invertebrates, a neuronal network in the spinal cord was found that generated a normal coordinated motor output pattern independently of sensory inputs (Wilson 1965). Furthermore, recent studies of isolated vertebrate spinal cord preparations from newborn rodents showed that locomotor-like rhythmic activity can be evoked by applying intrinsic neurotransmitters (Kudo 1987; Cazalets 1992; Kjaerulff 1996). These findings of an intrinsic network in the spinal cord gave rise to the idea of the central pattern generator (CPG).

In swimming animals, a constant phase lag of the cycle duration is produced between rostral and caudal segments in the spinal cord emerging a mechanical wave along the the body (Grillner 2006). However, in rodents, the CPG network is located in the cervical and lower thoracic/lumbar enlargement of the spinal cord involved in forelimb and hindlimb locomotion, respectively (Kiehn 2006). Each limb is thought to contain a separate spinal CPG to evoke a standard pattern of muscle activation (Kiehn 2006). In the vertebrate spinal cord, the CPG is essential for two major functions, the rhythm generation and the pattern generation, in order to activate limb muscles in a coordinated manner (Kiehn 2011). The rhythm generation functions as a clock providing rhythmic drive to motor neurons and other CPG neurons, whereas pattern generation is essential for the rhythmic activation of motor neurons involved in left-right alternation and flexor-extensor coordination (Kiehn 2006; Kiehn 2011). A modified model of the mammalian CPG was proposed consisting of two layers: a rhythm-generating layer that is two or several synapses upstream to motor neurons and project directly to the pattern-generating layer which in turn is monosynaptically connected to motor neurons (reviewed in Kiehn (2006)). Various studies have shown that CPG neurons are located in laminae VII, VIII and X of the ventral spinal cord (Kjaerulff 1996; Tresch 1999; Dai 2005). In the CPG of swimming animals, rhythm- and pattern-generators are thought to comprise only one layer (Grillner 2003).

It is still not known whether locomotor behavior functions by the recruitment of multiple CPGs that require various combinations of neurons in the spinal cord for different behaviors or whether the CPG is reconfigured in a task dependent manner by shared interneurons (Goulding 2009). The mammalian locomotor CPG has been proposed to comprise multiple distributed rhythm-generating core networks along the spinal cord emerging in a flexible

activation of the limb CPGs (Grillner 1981; Grillner 2003; Kiehn 2006). This suggests that each limb CPG can be activated alone or in combination resulting in different gait patterns such as alternating or in-phase coordination of the limbs (Grillner 2006). On the contrary, the shared interneuron hypothesis was mainly reported in crustacean and turtle whose pools of multipotent CPG interneurons are recruited in a different combination for various motor behaviors (Meyrand 1991; Berkowitz 2008). In general, CPG output is adaptable and flexible and can be influenced by sensory afferents, descending supraspinal input and by neuromodulators in the spinal cord (Fig. 1).

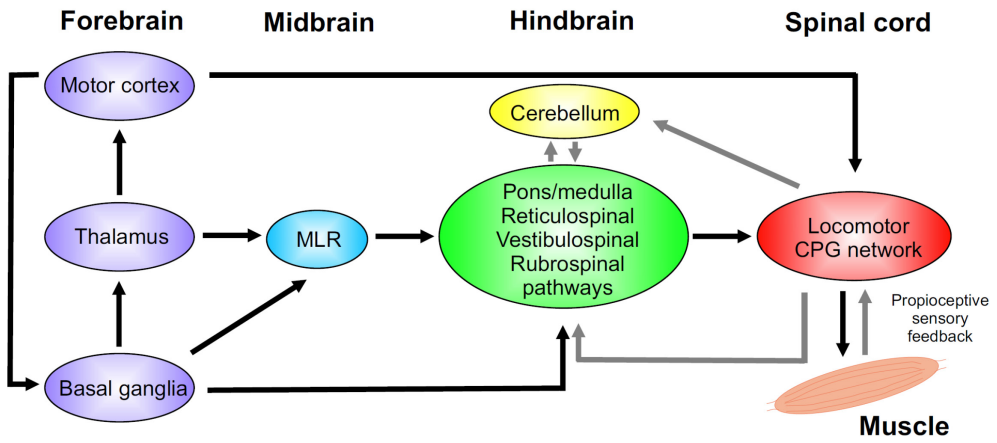

Figure 1. Supraspinal and sensory input to the locomotor CPG in rodent

Motor pathways in vertebrates involving forebrain, midbrain, hindbrain and spinal cord. The spinal cord contains the locomotor CPG network. Propioceptive sensory feedback from muscles modulates the motor output. Moreover, descending reticulospinal, rubrospinal and vestibulospinal pathways from the hindbrain control the CPG in the spinal cord. The cerebellum also influences the spinal CPG via supraspinal motor pathways. The reticulospinal pathway is activated by the mesencephalic locomotor region (MLR), which receives input from thalamus and basal ganglia. The motor cortex has a direct input on the spinal CPG via the corticospinal tract and thereby refines and initiates locomotion. (Adapted from Goulding (2009)).

2.2.1 Influence of sensory afferent on CPG networks

Somatosensory information of touch, temperature, pain, itch, stretch is relayed by sensory afferent fibers to interneurons in the spinal cord (reviewed in Gross (2002)). Small $TrkA^{+}$ nociceptive sensory neurons innervate interneurons in laminae I-III (Snider 1998), whereas medium sized mechanosensory neurons connect to interneurons in laminae III, IV

and V (reviewed in Gross (2002)). Furthermore, the spinal CPG receives proprioceptive input from muscle spindles and tendon organs in muscles that provide feedback in spinal reflexes (Smith 1988; Pearson 1993; Proske 2012). Reflexes are complex and adaptable to specific motor tasks.

The stretch reflex detects a lengthening contraction of the muscle and is mediated by Ia afferent fibers forming monosynaptic contacts to motor neurons in the spinal cord (Hulliger 1984). Additionally, Ia afferents contact Ia inhibitory interneurons innervating antagonistic muscles that are essential for reciprocal innervations for the coordination of muscle contractions (Hultborn 1971; Feldman 1975). Alterations in muscle tension detected by Golgi tendon organs are mediated by Ib afferents that connect to Ib inhibitory interneurons in the spinal cord (Swett 1975; Crago 1982; Pearson 1995). Motor neurons are silenced by Ib inhibitory interneurons resulting in precise spinal control of muscle force. Both Ia and Ib afferents influence the timing of locomotor activity via disynaptic and polysynaptic pathways (Pearson 1995).

It has been suggested that sensory feedback involved in rhythmic locomotion exhibits three functions as follows (Pearson 1993). First, sensory afferents are important for strengthening of CPG activities, e.g. for activation of the hindlimb extensor muscles during stance phase. Second, timing of sensory feedback enables an appropriate motor output during locomotion, e.g. adaption of position of the body, force of muscle activity and direction of movement. Third, sensory input facilitates phase transitions in rhythmic movements, e.g. CPG program switches from stance to swing phase at the end of the stance phase by muscles spindles in the hip flexor muscles (Grillner 1978; Kriellaars 1994). Moreover, somatosensory signals from the limbs regulate the step cycle as it was observed that the rate of stepping in spinal and decerebrate cats increases with the speed of the treadmill belt, the stance phase decreases while the swing phase remains relatively constant (Barbeau 1987).

2.2.2 Supraspinal influence on CPG networks

Descending pathways from the hindbrain control the CPG network in the spinal cord, including reticulospinal, rubrospinal and vestibulospinal pathways (Lakke 1997; Goulding

2009). Serotonergic neurons located in the parapyramidal region (PPR) of the medulla were shown to be involved in rhythm-generation of the CPG via descending pathways (Jordan 2008). The medullary reticular formation via reticulospinal pathway initiates locomotor activity by glutamatergic descending signals (Hagglund 2010). The reticulospinal neurons in the pons and medulla are themselves activated by the mesencephalic locomotor region (MLR) and the lateral hypothalamus (Garcia-Rill 1987; Jordan 1998). The mesencephalic locomotor region in turn receives input from the basal ganglia and thalamus (reviewed in Jordan (1998) and Goulding (2009)). Both basal ganglia and cerebellum are thought to be involved in the timing of muscle activation (Wichmann 1996). The cerebellum fine-tunes motor output according to the task through sensory and internal feedback from the spinal cord via spinocerebellar pathways and in turn influences the CPG through various descending pathways (reviewed in Goulding (2009)). In general, feedback pathways from the spinal cord and input from other brain regions converge in the brainstem and are important to stabilize the locomotor rhythm (Grillner 1991; Cohen 1996). It has been shown that decerebrated cats are able to perform purposeful locomotion similar in pattern to that of cats with intact cortex (Bjursten 1976). In these animals, speed and mode of locomotion (walking, trotting, galloping) were dependent on the strength of electrical stimulation of the brainstem (Bjursten 1976). Theses findings indicate the importance of subcortical control during adaptive locomotion. However, the motor cortex is directly connected to CPG interneurons in the spinal cord via the corticospinal tract (Stanfield 1992), and is thereby thought to be involved in adaptation of locomotion for complex locomotor ability tasks requiring a high degree of visuomotor coordination e.g. walking over obstacles (Rossignol 1996; Drew 2008; Asante 2010). Furthermore, it has been shown that the posterior parietal cortex plays additionally an important role in planning and adjustment of precise stepping over obstacles (Drew 2008).

In general, several functions of supraspinal control on locomotion have been suggested by Orlovsky (reviewed in MacKay-Lyons (2002)): the activation of spinal locomotor CPGs, control of intensity of CPG activity, maintaining equilibrium during locomotion, adaptation of limb movement to external conditions and coordination of locomotion with other motor acts. Spinal CPGs are only responsible for the perpetuation of patterns of muscle activity required for locomotion.

2.2.3 Influence of neuromodulators on CPG networks

The output of the CPG network can be additionally influenced by neuromodulators. Neuromodulators are neurotransmitter-like substances transmitted by synaptic terminals or blood vessels. Neuromodulators co-exist in nerve terminals and, therefore, increase or decrease the effect of classical neurotransmitters. Neuromodulation can have an intrinsic influence within the CPG but also an extrinsic effect of descending pathways from the brain (Katz 1995). The locomotor CPG output was shown to be influenced by neurotransmitters like glutamate, GABA and glycine and neuromodulators such as serotonin and dopamine (Cazalets 1992; Grillner 1995; Katz 1995). Moreover, peptides like neurotensin, somatostatin, substance P exhibit neuromodulatory effect on the CPG (Parker 1996; Barthe 1997).

Most of the serotonergic input to the spinal cord originates from brain stem raphe nuclei and the parapyramidal region (Lakke 1997). In various studies, it was shown that serotonine can modulate left-right and flexor-extensor alternation during fictive locomotion (Pearlstein 2005; Liu 2009). Hence, serotonin has an effect on motor neurons or premotor interneurons in order to influence the the final motor output. Like serotonin, noradrenaline modulates sensory and descending inputs to spinal interneurons in the cat (Jankowska 2000; Hammar 2004; Hammar 2007). Furthermore, inhibitory interneurons releasing GABA and/or gycine were shown to play an essential role in alternating left-right locomotion pattern and between flexor and extensor motor neurons (Butt 2003; Lanuza 2004).

2.3 Assembly of interneurons in the spinal cord

During development of the spinal cord, roof plate and floorplate of the neural tube provide a dorsal-ventral axis of two morphogen gradients. The highest dose of Sonic hedgehog (Shh) is produced in the ventral floorplate whereas more dorsally the Shh dose is lowest (Jessell 1989; Jessell 2000). In contrast, the roof plate secrets bone morphogenetic proteins (BMPs) generating an opposing dorsal to ventral gradient of BMP (Lee 1999). The two opposing gradients of Shh and BMP establish a spatially restricted pattern of progenitor domains along the dorsal to ventral ventricular zone (Goulding 2002). Six dorsal progenitor

domains generate early-born dI1-dI6 neurons (E10-E12.5) and two late-born classes of dorsal interneurons dIL_A and dIL_B (E11-E13) (Goulding 2002; Gross 2002; Muller 2002). The majority of dorsal cells differentiate as sensory interneurons and -relay neurons that receive sensory information from the periphery ((Bermingham 2001; Julius 2001), reviewed in Grossmann (2010) and Helms (2003)). In the ventral part of the neural tube, progenitor cells give rise to five classes of neurons, V0, V1, V2, V3 and motor neurons (Jessell 2000; Goulding 2009; Alaynick 2011; Kiehn 2011). The ventral interneuron classes are located in ventral laminae VII and VIII in the spinal cord considered to be involved in the locomotor CPG in quadrupedal mammals (Kiehn 2006; Goulding 2009). Besides, some dorsally born neurons migrate ventrally during development suggesting a participation in the ventral-located CPG (Pierani 2001; Gross 2002; Lanuza 2004).

The progenitor domains express different combination of transcription factors during neurogenesis (Jessell 2000). The ventral domains can be further subdivided according to their transcription factors, function, projection and expression of neurotransmitter type (Jessell 2000; Alaynick 2011). V0, V1, V2a, V2b and V3 interneurons are marked by the expression of the transcription factors Evx1/2, En1, Chx10, Gata2/3 and Sim1, respectively (reviewed in Jessell (2000); Goulding (2009); Grossmann (2010); Alaynick (2011)). The dorsal dI1 and dI2 interneurons are marked by Math1 and Ngn1/2, respectively (Helms 1998; Bermingham 2001; Gowan 2001). Mash1 defines progenitors that give rise to dI3-dI5 and late-born $dIL_{A/B}$ interneurons (Gross 2002; Muller 2002). Moreover, Lbx1 marks progenitors of the early-born dI4-dI6 interneurons and late-born $dIL_{A/B}$ neurons located adjacent to the Mash expressing progenitor domain (Gross 2002; Muller 2002) (Fig. 2).

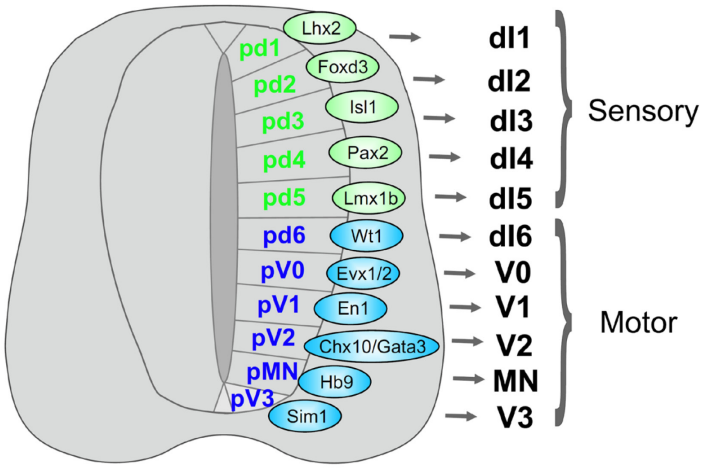

Figure 2. Pattern of progenitor domains in the developing mouse spinal cord

At embryonic stage, eleven early postmitotic neuron types are patterned in the embryonic spinal cord (pd1-6, pV0-3 and pMN). The dorsally derived dI1-dI5 neurons mainly contribute to sensory spinal pathways. The dorsally derived dI6, the ventrally derived V0-V3 interneurons and motor neurons (MN) are involved in the locomotor network. Dorsal and ventral interneurons are marked by specific transcription factors indicated in the scheme. (Adapted from Goulding (2009)).

2.3.1 Lbx1-expressing interneurons in the spinal cord

The gene encoding the homeodomain factor Lbx1 is expressed in postmitotic neurons in the spinal cord (Jagla 1995; Schubert 2001). The expression of Lbx1 is essential for the specification of two early postmitotic populations, a dorsal Lbx1-negative population that gives rise to dI1-dI3 neurons and a ventral Lbx1-positive population that generates dI4-dI6 neurons (Gross 2002; Muller 2002). Lbx1 is expressed in early born dI4-6 neurons and late born dIL_A and dIL_B neurons in the dorsal spinal cord (Gross 2002; Muller 2002). Late born Lbx1-expressing neurons that arise from the dI4 domain differentiate as ipsilaterally projecting association interneurons, form the substantia gelatinosa and also migrate laterally. The dI5 and dI6 neurons migrate laterally and ventrally and are finally located in the nucleus propius and ventral horn (Gross 2002; Muller 2002). Taken together, Lbx1-expressing neurons at embryonic stage E16.5 can be found mainly in the substantia gelatinosa, but also in deeper layers (lamina III-V) and in the medial ventral spinal cord (Gross 2002; Muller 2002). Furthermore, Lbx1 is expressed by both excitatory glutamatergic and inhibitory GABAergic/glycinergic neurons in the embryonic spinal cord (Cheng 2005).

2.4 Neuronal networks involved in left-right coordination

Left-right coordination requires commissural interneurons whose axons cross the spinal midline in order to coordinate the activity of the limbs on both sides of the body. Most limbed animals, including mice and human beings, show alternating locomotion of their hindlimbs. Inhibitory and excitatory interneurons are suggested to be involved in alternating and hopping gait. In a model of a left-right alternating circuit, contralateral motor neurons are inhibited either directly by inhibitory commissural interneurons or indirectly by excitatory commissural interneurons, which in turn activate ipsilateral inhibitory interneurons on the contralateral side (Kjaerulff 1997; Butt 2002; Butt 2003; Rabe 2009; Kiehn 2010; Kiehn 2011; Wu 2011). However, left-right synchrony is generated by excitatory commissural interneurons that monosynaptically innervate contralateral motor neurons (Quinlan 2007; Rabe 2009; Kiehn 2010; Kiehn 2011; Rybak 2013). Synchronous locomotor activity can also be evoked by blocking fast inhibitory transmission in the isolated spinal cord suggesting an important role for ipsilateral neurons for left-right alternation (Cowley 1995). Moreover, ipsilateral interneurons such as Rhenshaw cells and Ia inhibitory interneurons directly inhibit motor neurons (Kiehn 2010). In the model of Rybak et al. (2013), it was suggested that inhibitory and excitatory commissural interneurons receive excitatory inputs from ispilateral interneurons. Some of the excitatory ipsilateral interneurons are thought to express the EphA4 receptor important for ispilateral axonal projections (see chapter 2.5.3.3) and only innervate ipsilateral commissural interneurons (Rybak 2013). They propose that the balance between different interneurons defines the gait. In a previous model, Kiehn et al. (2010) suggested that an yet unidentified rhythm-generating neuron provide rhythmic drive to several ipsilateral and commissural interneurons (Fig. 3). Additionally, ipsilateral excitatory EphA4-positive neurons might project directly to motor neurons. In general, Kiehn (2011) proposed that excitatory neurons of the CPG network are responsible for rhythm generation and inhibitory commissural interneurons are involved in left-right alternation.

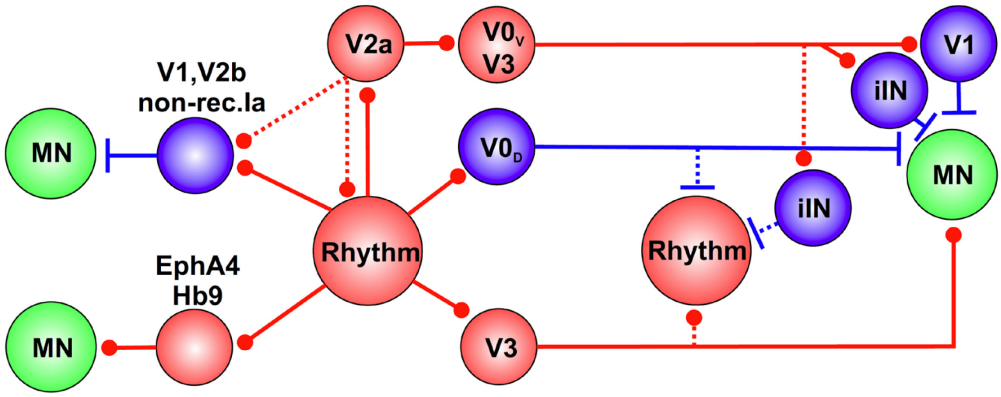

Figure 3. Model of the organization for left-right coordination in the rodent CPG

Motor neurons (MNs) are generally innervated by alternating excitation and inhibition. Rhythm-generating neurons might activate several ipsilateral and commissural interneurons such as inhibitory $V0_D$ and excitatory V3 that project either directly or indirectly onto MNs. Ipsilaterally projecting inhibitory neurons (iIN) are thought to be V2b, V1 such as non-reciprocal Ia inhibitory and Rhenshaw cells that directly activate MNs. In addition, excitatory EphA4-positive and Hb9 neurons innervate MNs. The excitatory V2a neurons were shown to project on excitatory commissural neurons $V0_V$ and V3, might also project on ipsilateral inhibitory interneurons and are dispensable for rhythm-generation. (Adapted from Kiehn (2010)).

2.4.1 Commissural interneurons

Commissural interneurons consist of both excitatory and inhibitory populations important for left-right coordination (Butt 2003; Grillner 2003; Quinlan 2007; Rabe 2009), whereas inhibitory commissural neurons are thought to be more abundant (Weber 2007; Restrepo 2009). Retrograde tracing experiments of commissural interneurons in the lumbar regions of neonatal rat revealed distinct projection patterns and can be grouped into long range and short range commissural interneurons (Eide 1999; Stokke 2002). Long range commissural interneurons exhibit ascending, descending or bifurcating axons with both ascending and descending projections (Eide 1999; Stokke 2002). In general, commissural interneurons are located in the superficial lamina, in the deep dorsal horn and the ventromedial area in the spinal cord. All four groups can be found in the ventromedial area (laminae VII, VIII, X), where the locomotor CPG is thought to be located (Kjaerulff 1996) and, therefore, it is thought that commissural interneurons are involved in the left-right alternation.

Commissural interneurons are proposed to consist of the dI1-dI3, dI5, dI6, V0 and V3 cell subpopulations (Serafini 1996; Rabe 2009). V0 interneurons are derived from Dbx1-

expressing progenitors whose major subset consist of excitatory and inhibitory commissural interneurons (Pierani 2001; Lanuza 2004) and a minor subset are $V0_C$ interneurons, cholinergic partition cells, located close to the central canal (Zagoraiou 2009). Rabe et al. (2009) revealed that the majority of dorsal V0 interneurons consist of commissural interneurons, whereas the ventral V0 interneurons project mainly ipsilaterally. In another study of Tapalar et al. (2013), dorsal V0 neurons were shown to constitute predominantly of inhibitory neurons while ventral V0 are predominantly glutamatergic. Ablation of V0 neurons and recording of locomotor-like activity revealed intermittent periods of synchronous coordination between both hindlimbs in *Dbx1*$^{-/-}$ mutants (Lanuza 2004) or a complete hindlimb hopping in vitro and vivo of conditional *Hoxb8*^{Cre} *Dbx1*^{DTA} mutants, in which Cre recombination is restricted to spinal segments caudal to C4 (Talpalar 2013). Talpalar et al. (2013) found a frequency-dependent hopping gait. Regarding the dorsal and ventral V0 interneurons, the authors revealed that inhibitory dorsal V0 neurons are required at slow locomotion and excitatory ventral V0 neurons at fast locomotion in order to enable left-right alternating modes at different speeds. Therefore, excitatory commissural interneurons besides the inhibitory commissural neurons are essential for the maintance of left-right alternation.

The V3 population constitutes the majority of excitatory commissural interneurons in the mouse spinal cord (Zhang 2008). Blocking of V3 neuronal activity resulted in an increased variability in the locomotor burst amplitude and period, and in an imbalance between the left-right activity. The authors showed that V3 interneurons are essential to maintain a stable and balanced locomotor rhythm but may play a minor role in left-right alternation. Moreover, it was suggested that V3 commissural interneurons might be active during left-right synchrony as they project directly to contralateral motor neurons (Kiehn 2010; Kiehn 2011) and remain completely unaffected by the loss of alternating gait and the absence of inhibitory commissural interneurons in *Netrin1*$^{-/-}$ mutants (Rabe 2009).

The dorsally derived dI6 neurons are thought to be inhibitory commissural neurons additionally contributing to left-right alternation (Andersson 2012). The authors deleted a subpopulation of dI6 interneurons marked by the transcription factor Dmrt3. *Dmrt3*$^{-/-}$ mutant mice showed a loss of alternating hindlimb movement accompanied by increased uncoordinated step movements at P4. As adult, the stride time was increased and they

displayed difficulties walking at higher velocities. The authors suggested that Dmrt3-expressing neurons have a critical role for left-right coordination but also for the coordination between fore- and hindlimbs.

2.4.2 Ipsilateral ventral interneurons

Ipsilaterally projecting interneurons were mainly investigated in the ventral spinal cord. The inhibitory V1 interneurons are located in close proximity to motoneuron pools and can be subgrouped into Ia inhibitory interneurons, Renshaw cells and likely many other subtypes (Sapir 2004; Alvarez 2005). Ia inhibitory interneurons play an important role in the reflex pathway and Renshaw cells are shown to mediate feedforward inhibition onto motor neurons (Alvarez 2007). According to the review of Alaynick et al. (2011), there still remains an unidentified inhibitory V1 subgroup. An inactivation or deletion of V1 interneurons in isolated spinal cords resulted in a significantly increased step cycle (Gosgnach 2006). Hence, V1 interneurons are required for fast motor bursting and, therefore, play an essential role in regulating locomotor speed (Gosgnach 2006).

The glutamatergic V2a interneurons are confined to the ipsilateral side but are part of the commissural pathway involved in left-right alternation since they project on excitatory V0 commissural interneurons (Crone 2008). In a study by Crone et al. (2008), V2a interneurons were selectively ablated by dipheria-toxin A resulting in a partial uncoupling of left-right alternation. V2a interneurons might also be involved in rhythm generation as the ablation of V2a evoked increased variability of the step cycle period (Crone 2008). However, the inhibitory V2b interneurons mainly project ipsilaterally and can be found in lamina VII (Lundfald 2007). In adult mice, cFos expression was increased in V2 interneurons following locomotion, indicating that V2 neurons play a role in locomotor behavior (Al-Mosawie 2007). The authors suggested that V2-derived interneurons might receive primary afferent input and probably mediate disynaptic reflexes. Moreover, it has been suggested that the p2-domain generates a third subpopulation of V2 interneurons, the V2c neurons, marked by the expression of Sox1 (Panayi 2010). Further investigation of V2 interneurons in their anatomy and function still remains to be performed in future.

Moreover, Wilson et al. (2005) revealed that another ipsilaterally projecting interneuron type, the glutamatergic Hb9-expressing interneuron, is located adjacent to the ventral commissure of the spinal cord. These cells are thought to play a role in rhythm generation and were shown to be activated during locomotion.

2.5 Axon guidance in the spinal cord

During development of the spinal cord, newborn neurons send out their axons towards target neurons. Local interneurons possess short axons that form synaptic contacts to neurons in their vicinity, whereas projection neurons send out long axons to distant targets. Peripheral sensory neurons send out axons into the central nervous system where they diverge on different neurons. However, motor neurons receive convergent input from various neurons. Therefore, axons need to migrate a long way to find their targets and need the help of molecular cues that influence the direction in which growth cones will travel (Tessier-Lavigne 1996). Each of short-range and long-range cues can be attractive or repulsive. In the short-range, an increase in adhesivity of one cellular substrate causes axons to turn pathways towards the substrate, or to turn away or collapse in the presence of repulsive membrane molecules (Kolodkin 1996; Tessier-Lavigne 1996). In the long range, growth cones migrate towards or turn away from the concentration gradients of certain diffusible molecules originating at distant sources (Gundersen 1979; Zheng 1994; Tessier-Lavigne 1996). In the nervous system, a variety of cues and receptors are involved in axon guidance information along the entire way of growing axons.

2.5.1 Eph receptors and their ligands

The Eph receptors are one of several receptors involved in axon guidance and are part of the largest subgroup of receptor tyrosine kinases that bind to specific ligands, the ephrins. Both Eph receptors and ephrins play important roles in developmental processes such as axonal pathfinding, neural crest cell migration, vascular development and, generally, in cell to cell recognition events (Flanagan 1998; Frisen 1999; Xu 2000). Furthermore, Eph receptors and their ligands ephrins are also involved in embryonic patterning such as the

regulation of hindbrain segmentation (Xu 1995), retinal axon guidance to topographically appropriate targets within the optic tectum (Cheng 1995; Drescher 1995), brain commissure formation (Henkemeyer 1996) and forebrain patterning (Xu 1996). In vertebrates, 14 different Eph receptors and 8 different ephrins are known and can be divided into two subclasses A and B (Eph Nomenclature Committee (1997)). All ephrin ligands are membrane-bound. Ephrin-A ligands are attached to the cell membrane via a glycosylphosphatidylinositol (GPI) anchor, whereas ephrin-B ligands possess a transmembrane domain and a short cytoplasmic tail. In general, EphA receptors bind ephrin-A ligands and EphB receptors bind ephrin-B ligands with one exception for the EphA4 receptor which binds additionally ephrinB2 and ephrinB3 (Gale 1996; Gale 1997; Bergemann 1998). Furthermore, each ephrin ligand shows a different set of affinity for their Eph receptors. EphA4 binds a variety of ephrins whereas EphA1 exhibits a restricted affinity to only ephrin-A1 (Gale 1997). Moreover, ephrin ligands themselves can also act as receptors since they are able to transduce intracellular signals upon binding to their cognate Eph receptors (Holland 1996; Bruckner 1997; Davy 1999).

2.5.2 Axon guidance of commissural interneurons

During spinal cord development, commissural interneurons, expressing the receptor DCC, are attracted towards the ventral cord by the diffusible signal Netrin-1 in the floor plate (Kennedy 1994; Serafini 1996; Fazeli 1997). In addition, BMPs act as repellents from the roof plate on commissural interneurons (Augsburger 1999). Since commissural axons cross the ventral midline but not the dorsal, various short-range cell adhesion molecules are transiently up- and down-regulated. During the migration of the growth cone towards the midline, commissural interneurons are guided by the expression of adhesion molecules as Axonin-1 and TAG-1 that bind to the local NrCAM floor plate signal (Dodd 1988; Stoeckli 1997). When the commissural interneurons have crossed the midline, a variety of chemorepellents such as Slit, L1, neuropilin and EphB receptors are upregulated in order to avoid a recrossing of the axons (Brose 1999; Imondi 2000; Tran 2000; Kaprielian 2001).

The deletion of *Netrin-1* in mice resulted in a complete synchrony between the left and right side during fictive locomotion suggesting an involvement in GPG of left-right

alternation (Rabe 2009). Furthermore, the absence of Netrin-1 also revealed a misguidance of dorsal commissural interneurons and thereby a decrease of axons crossing the spinal midline (Serafini 1996; Rabe 2009). The dI1-dI3, dI5, dI6 and dorsal V0 interneurons exhibited a 75-80% reduction of commissural axons whereas the ventral V3 interneurons remained unaffected. A greater number of inhibitory than excitatory commissural interneurons was lost in the *Netrin-1*$^{-/-}$ mutant (Rabe 2009). Moreover, a genetic inactivation of the vesicular glutamate transporter 2 (vGLUT2) in mouse is not required for locomotor CPG (Gezelius 2006; Wallen-Mackenzie 2006). Therefore, it has been suggested that inhibitory commissural interneurons are essential for left-right coordination (Cowley 1995; Kiehn 2006). Likewise, a lack of the DCC receptor in mice resulted in a loss of commissural interneurons (Rabe Bernhardt 2012). However, a completely uncoordinated left-right ventral root activity was observed in the *DCC*$^{-/-}$ mutants by a fictive locomotion assay whereas a hopping gait was seen in adulthood (Finger 2002; Rabe Bernhardt 2012). Furthermore, crossing of all corticospinal tract axons was disrupted resulting in a persistence of ipsilateral corticospinal tracts in hindbrain and spinal cord. Since the phenotype in full *Netrin*$^{-/-}$ mutants is more severe than in *DCC*$^{-/-}$ mutants, Netrin-1 might, therefore, attract several inhibitory commissural interneuron populations normally involved in left-right alternation (Rabe 2009). Even in humans, a mutation of the *DCC* gene was found to cause mirror movements (Srour 2010). Mirror movement is defined as an involuntary movement in one side of the body which mirrors voluntary movement performed in the contralateral side of the body (Armatas 1994).

2.5.2.1 EphrinB3 ligand as midline repellent in the spinal cord

EphB-receptors are expressed on segments of commissural axons that have crossed the midline in the embryonic mouse spinal cord (Imondi 2000). Commissural interneurons are repelled from recrossing the spinal midline by EphB receptor interaction with its ligand ephrinB3 at the midline of the spinal cord resulting in commissural growth cone collapse (Imondi 2000; Kadison 2006). EphrinB3 is expressed on floor plate cells and in the ventral midline at embryonic stages where they function as repellent ligand for EphB and EphA4 receptor-bearing axons (Dottori 1998; Imondi 2000).

2.5.3 Interaction of EphA4 receptor and its ligand ephrinB3

The EphA4 receptor possesses a high affinity with ephrin-A5, -A1, -A2 and -A6 (Flanagan 1998; Menzel 2001) and especially ephrinB3 binds to EphA4 with the highest affinity since ephrin ligands have been shown to induce signaling on receptor binding (Gale 1996; Holland 1996; Bergemann 1998; Dottori 1998).

2.5.3.1 Expression of the EphA4 receptor in mouse

During development, EphA4 expression displays a defined spatiotemporal pattern (Nieto 1992; Mori 1995). At the end of embryogenesis, expression of EphA4 is found mainly in regions of cerebral cortex, striatum, thalamus, hippocampus, hindbrain (rhombomeres 3 and 5; superior colliculus, red nucleus and sensory trigeminal nucleus), cerebellum, cochlea, eye and spinal cord (Nieto 1992; Kullander 2001b; Greferath 2002). In the spinal cord, EphA4 expression was found in all regions with a slight increase in the medio-lateral regions at E11, whereas by E13.5 until P6, high EphA4 expression was confined to the intermediate and ventral spinal cord (Dottori 1998; Greferath 2002). Motor neurons in the ventral horn require EphA4 for axon guidance in muscles (Kania 2003). EphA4 expression remained similar at all levels of the spinal cord and persisted through the development of the corticospinal tract (Coonan 2001; Greferath 2002).

2.5.3.2 EphA4-ephrinB3 interaction on axons of corticospinal tract

The EphA4 receptor and its ligands ephrinB3 play an essential role in axon guidance of corticospinal tract fibers at the midline of the spinal cord. Corticospinal tract axons, originating from layer V neurons in the neocortex, descend ipsilaterally through the internal capsule, basis pedunculi in the midbrain, pons and medullary pyramids (Stanfield 1992). In the medulla, corticospinal axons cross the ventral midline since ephrinB3 expression is restricted to the dorsal part of the midline (Kullander 2001a). Finally, the axons descend on the contralateral side along the dorsal funiculus into the gray matter of the spinal cord during the first postnatal week where their branches terminate predominantly in the dorsal

horn contralateral to the cells of origin in the motor cortex (Schreyer 1982; Stanfield 1992; Dottori 1998). In rodents, axons from the corticospinal tract make synaptic contacts onto interneurons in the spinal cord which in turn innervate motor neurons (Dottori 1998). The repellent ligand ephrinB3, expressed at the spinal midline, prevents EphA4-expressing corticospinal tract fibers (Martone 1997; Flanagan 1998; Coonan 2001; Yokoyama 2001; Canty 2006) from recrossing to the ispilateral side during postnatal development (Kullander 2001a; Yokoyama 2001; Egea 2005).

In both full *EphA4*$^{-/-}$ and *ephrinB3*$^{-/-}$ mutant mice, the descending course of corticospinal tract axons through the medulla until the spinal cord appeared normal; however, corticospinal axons in both mutants showed an abnormal collateral fiber branching from the dorsal funiculus into the gray matter of both ipsilateral and contralateral side, and additionally recross the spinal midline (Coonan 2001; Kullander 2001a; Kullander 2001b; Yokoyama 2001). On the contrary, Dottori et al. (1998) found additionally an abnormal corticospinal pathway in the medulla in which axons terminated instead of crossing the midline in the full *EphA4*$^{-/-}$ mutant. Furthermore, an aberrant ventrally shifted termination pattern of the corticospinal tract fibers was found within the intermediate and ventral horn (Dottori 1998; Coonan 2001; Canty 2006). Developing corticospinal axons in wild type were suggested to express additionally ephrinB3 that would repel corticospinal tract fibers from intermediate and ventral regions with a high EphA4 expression in the spinal cord (Dottori 1998; Coonan 2001; Kullander 2001b). A dynamic dual expression of EphA4 on corticospinal tract fibers and surrounding gray matter was suggested to be activated at different time points providing a correct termination of axons (Coonan 2001). Hence, the expression of EphA4 in the intermediate zone plays an important role for an appropriate termination of corticospinal tract axons (Coonan 2001). Furthermore, the EphA4 receptor is also essential for an appropriate development of the topography of the hindlimb corticospinal tract. The branching of the hindlimb corticospinal tract into the spinal cord is regulated by the EphA4 receptor. The EphA4 expression in the spinal cord is high at the time of forelimb branching but low at the time of hindlimb branching suggesting that EphA4 in the gray matter controls the time and termination of the hindlimb corticospinal tract axons in the spinal cord (Canty 2006). Hindlimb axons only branch into the spinal cord when EphA4 expression in the cord is down-regulated (Canty 2006). In the full *EphA4*$^{-/-}$ mutant, hindlimb axons enter the cervical cord, whereas a significant reduction of corticospinal tract axons was found in the lumbar

spinal cord (Dottori 1998; Canty 2006). Moreover, both full *EphA4*$^{-/-}$ and *ephrinB3*$^{-/-}$ mutants displayed a shallower and widened dorsal funiculus compared to wild type mice (Dottori 1998; Kullander 2001a; Kullander 2001b; Restrepo 2011).

Regarding the gait behavior, both full *EphA4*$^{-/-}$ and *ephrinB3*$^{-/-}$ mutants displayed an abnormal hopping gait, moving their hindlimbs synchronically (Dottori 1998; Kullander 2001a; Yokoyama 2001). In addition, the full *EphA4*$^{-/-}$ mutants showed hesitation in initiating locomotion (Dottori 1998). The synchronous hindlimb locomotion defects in full *EphA4*$^{-/-}$ and *ephrinB3*$^{-/-}$ mutant mice have been initially suggested to originate from the defect of recrossed corticospinal tract axons (Dottori 1998; Kullander 2001a). This conclusion, however, has proven to be wrong as several following studies revealed that the hopping gait results from aberrantly midline crossing axons of spinal neurons (see in more detail below; Kullander (2003), Borgius (2014), Retrepo (2011), Vallstedt (2013)). Recent findings by Borgius et al. (2014) showed that the specific deletion of the *EphA4* gene from cortical neurons maintained an alternating gait, whereas a restricted deletion of *EphA4* in the spinal cord caused a hopping gait at all frequencies of locomotion.

2.5.3.3 EphA4-ephrinB3 interaction on axons of ipsilateral spinal interneurons

Beside commissural interneurons, ispilaterally projecting interneurons in the spinal cord are found to posses either longitudinal or local axons. Longitudinal ipsilateral axons project either ascending to the brain or caudally and contribute to the ventral, lateral and dorsal funiculus (reviewed in Sakai (2012)). Paixao et al. (2013) showed that the EphA4-ephrinB3 interaction is required for the formation of ipsilateral ascending axon tracts in the dorsal funiculus of the dorsal dIL_B (Zic^{2+}) neurons since a deletion of *EphA4* in dorsal neurons caused axonal midline-crossing of dIL_B cells. The authors further displayed that additionally to the misguidance of axons, the cell bodies of dIL_B neurons moved to the midline resulting in a gap between ephrinB3 expression and the dorsal funiculus. This gap of ephrinB3 expression causes spinal and corticospinal axons to cross the midline.

However, some populations of spinal cord interneurons form local connections in segments located close to their cell bodies (Kullander 2003; Kiehn 2006). Excitatory ipsilateral interneurons were shown to express EphA4 and are components of the ipsilateral

CPG network in which excitatory EphA4-positive cells fire in-phase with the ipsilateral motor neurons (Kullander 2003; Butt 2005). In isolated spinal cord preparations, full *EphA4*$^{-/-}$ mutant mice revealed an abnormal synchronous rhythmic activity of both hindlimbs whereas the flexor and extensor activity remained alternating (Kullander 2003). A strengthening of inhibition by sarcosine induced a reversal of synchronous to alternating fictive locomotion in full *EphA4*$^{-/-}$ mutant mice suggesting that a reinforcement of inhibitory commissural interneurons can restore stronger aberrant excitatory innervations in the contralateral side (Kullander 2003). In contrast to previous studies in the full *EphA4*$^{-/-}$ mutant (see chapter 2.5.3.2), it has been revealed that the abnormal hopping gait originates from an increase in the number of excitatory spinal neurons and a decreases in the number of inhibitory neurons crossing the midline in the spinal cord, suggesting the hopping phenotype is the result of a change in the balance between excitatory and inhibitory signals across the midline (Kullander 2003; Restrepo 2011). Deletion of *EphA4* in mice causes an overexcitation between the two sides of the spinal cord as it was also seen in the *Netrin1*$^{-/-}$ mutant with a decrease in inhibitory commissural neurons and a hopping gait (Rabe 2009) (Fig. 4). Restrepo et al. (2011) further revealed that the synchronous left-right activity of ventral roots in the full *EphA4*$^{-/-}$ mutant resulted from an aberrant axon crossing through the ventral but not the dorsal commissure. In contrast, Vallstedt et al. (2013) showed that a deletion of *EphA4* in the dorsal progenitor domain of the spinal cord exhibited a synchronous hindlimb gait whereas mice affected in the ventral spinal cord displayed an almost synchronous gait but to a lesser extend. Therefore, dorsally derived ipsilateral interneurons, when misguided, have an additional effect on locomotion beside the ventral derived interneurons.

EphA4 was revealed to be expressed in ipsilateral neurons; only very few commissural neurons might exhibit the EphA4 receptor (Kullander 2003). The interneuron population expressing EphA4 is a heterogeneous population with the majority of EphA4-positive neurons that are excitatory and some are also inhibitory (Butt 2005; Restrepo 2011), e.g. inhibitory V2b neurons were shown to express EphA4 (Lundfald 2007). In addition, the majority of the ipsilateral excitatory V2a neurons express the EphA4 receptor, although no misguided axons across the midline were observed in the full *EphA4*$^{-/-}$ mutant (Lundfald 2007). Furthermore, the ipsilateral excitatory Hb9 interneurons did not express EphA4. In total, approximately 30% of EphA4-expressing cells were accounted for motor neurons and V2 interneurons, thereby, remaining circa 70% for other ipsilateral interneuron populations

to be identified (Lundfald 2007). Hence, the EphA4 receptor is thought to be expressed in ipsilateral projecting neurons in the spinal CPG in order to prevent aberrant midline crossing and to provide ipsilateral topography (Egea 2005).

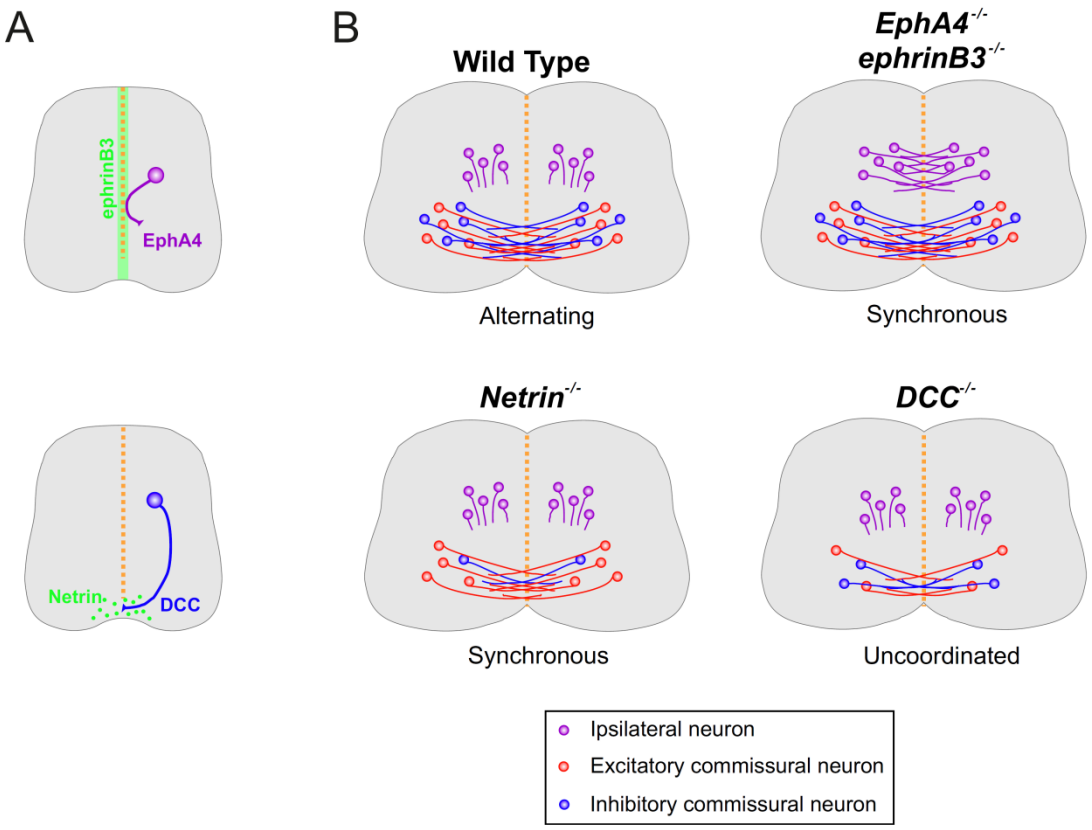

Figure 4. Models of CPG neurons involved in mutant mice with axon guidance defect

A: EphA4-ephrinB3 interaction repels the axon from the spinal midline whereas Netrin-DCC interaction guides the axon through the ventral midline. B: In the full *EphA4*$^{-/-}$ and *ephrinB3*$^{-/-}$ mutants, excitatory ipsilateral interneurons aberrantly cross the midline and cause a synchronous hopping gait in comparison to wild type mice. However, in the full *Netrin*$^{-/-}$ mutant, a reduced number of inhibitory commissural interneurons cross the midline resulting in synchronous left-right coordination, but the synchrony is not reversible by pharmacological strengthening as it was observed in the full *EphA4*$^{-/-}$ mutant. In both *EphA4*$^{-/-}$ and *Netrin*$^{-/-}$ mutants, an overexcitation on both sides of the spinal cord occurs. In the *DCC*$^{-/-}$ mutant, the number of both excitatory and inhibitory commissural interneurons crossing the midline is reduced causing uncoordinated activity between the left and right side. (Adapted from Vallstedt (2013)).

2.5.3.4 EphA4 receptor and its downstream effectors α2chimaerin and ephexin

The Eph receptor signaling during axon guidance requires a multistep process that involves ephrin-binding, activation of the tyrosine kinase activity, autophosphorylation and higher-order clustering (Egea 2005). An inactive Eph monomer receptor is dimerized by binding ephrin following a trans-autophosphorylation. Specific biological functions require an organization into an active oligomer by higher-order clustering of the Eph-ephrin complex (Egea 2005). Eph receptors are only activated by membrane bound ligands but not by soluble monomeric ligands (Davis 1994). The Eph-ephrin interaction induces bidirectional signaling, ephrin-Eph forward signaling and an Eph-ephrin reverse signaling (Noren 2004). In both forward and reverse signaling, activated Eph receptors couple to various downstream effectors, the Rho GTPase-activating proteins (GAPs), that inactivate Rho-GTPases, and the guanosine nucleotide exchange factors (GEFs), that activate Rho-GTPases (Shamah 2001; Wong 2001; Luo 2002; Cowan 2005; Yang 2006). Activation and inactivation of Rho-GTPases such as RhoA, Rac and Cdc42, are important regulators of actin dynamics in the growth cones involved in cell-cell detachment and reorganization of the actin cytoskeleton (Luo 2000; Etienne-Manneville 2002; Noren 2004). Activation of RhoA induces growth cone collapse, whereas activation of Rac and Cdc42 evoke axonal extension (Luo 2000; Etienne-Manneville 2002).

One of the EphA4 downstream effectors are ephexin1 and Vav2 (GEFs) which in turn activate RhoA resulting in growth cone collapse (Shamah 2001; Cowan 2005; Sahin 2005). Egea et al. (2005) suggested that ephrins trigger EphA4 signaling by higher-order clustering that in turn evokes the phosphorylation of ephexin1. Ephexin1 interacts with EphA4 kinase domain and induces RhoA activation and inhibition of Rac1 and Cdc42 (Shamah 2001). Shamah et al. (2001) showed that ephexin interacts with EphA4 but poorly with EphB receptors resulting in a specificity of the EphA4-ephexin interaction. Another downstream effector of EphA4 is α-chimaerin, a Rho-GAP, that specifically inactivates Rac (Beg 2007; Iwasato 2007; Wegmeyer 2007). Both pathways of ephexin and α-chimaerin result in growth cone retraction (Cowan 2005; Sahin 2005; Beg 2007; Iwasato 2007; Wegmeyer 2007). The α-chimaerin effector exhibits two isoforms α1 and α2 that both comprise diacylglycerol-binding (C1) and Rac-GAP domains (Hall 1990; Hall 1993). α2chimaerin binds with its

additional SH2-domain and another binding site to the kinase domain of the EphA4 receptor (Beg 2007; Wegmeyer 2007). Iwasato et al. (2007) suggested a cooperative action of ephexin1-induced RhoA activation and α-chimaerin-induced Rac inactivation in order to evoke growth cone retraction in various circuits and possibly also at the spinal midline (Fig. 5). Moreover, Nck adaptor protein was suggested to be another downstream effector of EphA4 involved in the control of axon guidance of the spinal CPG (Fawcett 2007). Nck was shown to bind α-chimaerin and interacts with actin-regulatory protein complex members (Wells 2006; Fawcett 2007; Wegmeyer 2007). Therefore, α-chimaerin and Nck might inactivate Rac in concert.

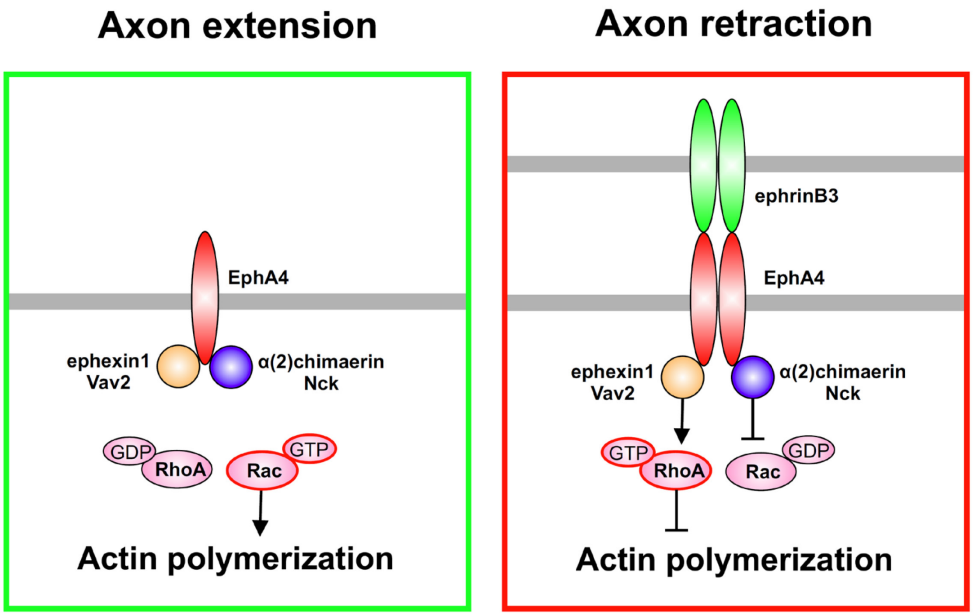

Figure 5. Model of EphA4 forward signaling of corticospinal tract axons at the spinal midline

In the absence of ephrinB3 (green box), RhoA remains inactivated and Rac is activated resulting in actin polymerization and axonal extension. However, binding of ephrinB3 (red box) causes an EphA4 dimerization and forward signaling that activates several EphA4 downstream effectors such as ephexin1, Vav2, α-chimaerin and Nck. The effector α-chimaerin inhibits Rac whereas ephexin and Vav2 might activate RhoA causing inhibition of actin polymerization. Both pathways might be involved in a cooperative action inducing axonal retraction of growth cones. (Adapted from Iwasato (2007)).

2.5.3.4.1 The α2chimaerin effector

In mice, α2chimaerin was found to be co-localized with EphA4 in the spinal cord, motor cortex and the developing growth cone of corticospinal tract fibers (Beg 2007; Wegmeyer

2007). Furthermore, α2chimaerin was expressed throughout the gray matter in the spinal cord (Beg 2007; Wegmeyer 2007). A deletion of *α-chimaerin* or specifically *α2chimaerin* in mice resulted in a hopping gait, abnormal CPGs, aberrant midline crossing of CPG axons and aberrantly recrossing of corticospinal tract fibers and, thereby, resembles the phenotypes of the full *ephrinB3*$^{-/-}$ and *EphA4*$^{-/-}$ mutants (Dottori 1998; Kullander 2001a; Yokoyama 2001; Kullander 2003; Beg 2007; Iwasato 2007; Wegmeyer 2007). Therefore, α(2)chimaerin is essential for the correct formation of the corticospinal tract fibers, of the CPG in the spinal cord and the maintenance of left-right alternation (Beg 2007; Iwasato 2007; Wegmeyer 2007). Taken together, the EphA4 receptor requires an intrinsic kinase activity to mediate forward signaling for the correct formation of the corticospinal tract and CPG in the spinal cord (Kullander 2001b; Yokoyama 2001; Egea 2005; Beg 2007; Iwasato 2007).

2.6 Aims of the thesis

Various previous studies (Pierani 2001; Lanuza 2004; Wilson 2005; Gosgnach 2006; Lundfald 2007; Crone 2008; Zhang 2008; Rabe 2009; Andersson 2012; Paixao 2013; Talpalar 2013) have started to reveal the function and connection of specific interneurons in the locomotor CPG in mammals by means of genetic markers and loss of function studies. In full *EphA4*$^{-/-}$ mutant mice, it has been shown that ipsilateral excitatory neurons aberrantly crossed the spinal midline and caused a hopping gait (Kullander 2003; Butt 2005; Restrepo 2011). Nevertheless, it remained unclear, which interneuron populations in the spinal cord are involved in the misguidance of axons and contribute to the synchronous hindlimb movement in the full *EphA4*$^{-/-}$ mutant mouse. Since deletion of *EphA4* in a certain interneuron population can provide the identification of ipsilateral components in the normal locomotor CPG, therefore, we investigated whether a conditional ablation of the EphA4 receptor or its ligand α2chimaerin in the dorsal derived Lbx1-expressing neurons would result in similar phenotypes as observed in the full *EphA4*$^{-/-}$ mutant. Here, we examined the premotor interneuron distribution of specific muscles and the gait behavior on treadmill in conditional *EphA4* and *α2chimaerin* mutant mice, in which the EphA4 receptor and its effector α2chimaerin was ablated in Lbx1-expressing neurons, respectively.

3. Results

3.1 Conditional *EphA4* (*EphA4*$^{flox/-}$*Lbx1*$^{Cre/+}$) mutant mice

3.1.1 Aberrant axon misguidance revealed by premotor interneuron distribution

Previous studies revealed a hopping gait in the full *EphA4* mutant (*EphA4*$^{-/-}$) mouse that is thought to be evoked by numerous crossing axons through the midline of the spinal cord (Dottori 1998; Kullander 2003; Restrepo 2011). In the beginning of this study, we wanted to compare the premotor interneuron distribution between full *EphA4* knock out and wild type mice by means of retrograde rabies tracing that would visualize possible interneurons involved in locomotion. We expected to identify a different subset of premotor interneurons in the full *EphA4* mutant located in the ventral contralateral side of the spinal cord and aberrantly crossing the spinal midline since Kullander et al. (2003) showed that misguided axons in the full *EphA4* mutant originated from cells in the ventral cord that normally express *EphA4*. In this way, we were hoping to identify a premotor interneuron population which could be further investigated in a conditional mutant model in which the *EphA4* gene is deleted in this specific interneuron type.

3.1.1.1 Variability of the premotor interneuron distribution in full *EphA4* mutant mice

To investigate premotor interneuron distribution of a single motor neuron pool in full *EphA4* mutant mice, we used a rabies virus tracing technique allowing the visualization of monosynaptically connected neurons presynaptic to infected neurons (Wickersham 2007a; Wickersham 2007b; Stepien 2010). Rabies virus normally retrogradely infects numerous synaptically connected neurons as it can be transferred through synapses (Ugolini 1995; Ugolini 2008; Ugolini 2010). However, when a modified rabies virus, lacking its glycoprotein gene needed for further transport across synapses, was injected into a muscle, motor neurons were taking up the virus by their axon endings and rabies could not be transferred

through further synapses (Fig. 6A). For this study, the modified rabies virus was injected together with AAV (adeno-associated virus), expressing the glycoprotein gene, into the Quadriceps (Q) muscle of young mice aged P5-7. Both viruses were taken up by the axon endings of motor neurons. Given that glycoprotein was expressed in motor neurons in these experiments, the rabies virus was transported across the first synapse but not further as the connected interneurons lacked the glycoprotein gene (Fig. 6B). Therefore, the premotor interneuron distribution pattern of Q motor neurons could be visualized in the lumbar spinal cord.

The position of the premotor interneurons in the spinal cord was defined by their distribution along the dorsal-ventral and lateral-medial axis (Fig. 6E). Moreover, ipsi- and contralateral positions were defined to the side of virus injection. The central canal was set as the 0.0 coordinate. In wild type, the Q premotor interneuron distribution revealed the majority of interneurons located in the ipsilateral spinal cord in Rexed`s laminae VI, VII and X (Fig. 6C and E). A smaller number of cells was found in the ventral contralateral side, especially in Rexed`s lamina VIII and ventro-medial lamina VII (Stepien 2010). Single cells were found in the dorsal contralateral side in Rexed`s laminae IV, V and VI. According to Stepien et al. (2010), the contralateral interneuron population consisted of both excitatory and inhibitory neurons.

We injected seven full *EphA4* mutant mice into the Q muscle. The premotor interneuron pattern revealed high variability among these mice (Fig. 6D). Interestingly, two of seven spinal cords showed a high increase of interneurons in the dorsal contralateral side connecting to ipsilateral motor neurons compared to wild type mice (Fig. 6F). The other five spinal interneuron distributions displayed a similar pattern as it was found in wild type (% dorsal contralateral cells [WT: 4.27, 3.78, 3.13, 2.67; full *EphA4*: 24.85, 8.1, 6.22, 4.59, 4.45, 4.16, 4.12]).

Furthermore, it has been shown that EphA4 is not exclusively expressed in the spinal cord but also very broadly in the whole brain (Greferath 2002), which might have additionally resulted in complex changes in the neuronal network above the spinal cord caused by the deletion of the *EphA4* gene in mice. We also observed that most full *EphA4* mutant mice had problems in keeping equilibrium when walking. Furthermore, an appropriate connection from motor neurons to muscles could have been also affected by the lack of *EphA4* (Kania

2003; Luria 2008). As the deletion of *EphA4* apparently affected the whole organism, it was therefore difficult to study the role of spinal interneurons involved in axonal midline crossing and hopping gait in the full *EphA4* mutant mouse. Therefore, the *EphA4* gene needs to be knocked out in different interneuron populations in order to obtain a clear picture of connectivity phenotypes.

Against our expectations, we observed a striking increase of premotor neurons in the dorsal contralateral part of the spinal cord in few full *EphA4* mutant mice and not in the ventral contralateral cord; therefore, we assumed that dorsal interneurons were misconnected in the full *EphA4* mutant. Due to the location of the dorsal contralateral neurons in Rexed`s laminae IV to VI, we reasoned that the dorsal dI4 to dI5 interneurons expressing Lbx1 might be involved. Lbx1 is a homeodomain transcription factor and is expressed during embryonic stages in the spinal cord (Gross 2002; Muller 2002). DI4 neurons among other cells form the substantia gelatinosa in the dorsal horn, dI5 neurons are located in the nucleus proprius close to the central canal and dI6 interneurons are situated in the ventral medial spinal cord. Besides, dI6 neurons are commissural interneurons thought to be involved in left-right alternation (Lanuza 2004; Goulding 2009; Wu 2011; Andersson 2012; Vallstedt 2013). Therefore, we wanted to obtain a conditional *EphA4* knock out mouse whose Lbx1-expressing cells lack the EphA4 receptor in order to study the premotor interneuron distribution.

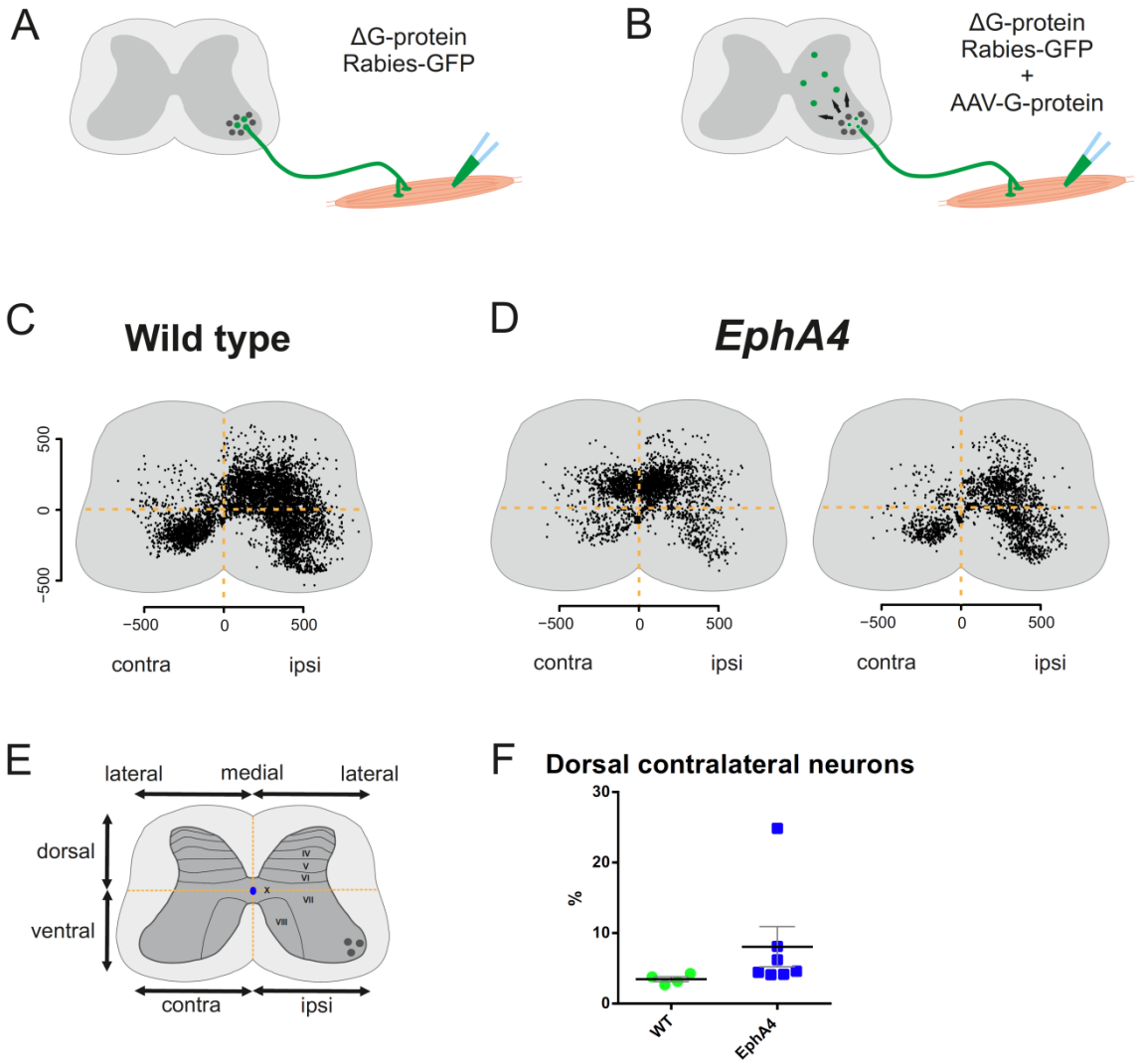

Figure 6. Monosynaptic rabies tracing in the spinal cord of full *EphA4* mutants in comparison to wild type

A: Rabies-GFP lacking its glycoprotein G (G-protein enables transsynaptic viral transfer) was injected in a specific muscle and only infected motor neurons. B: Complementation by AAV-G-protein resulted in mono synaptic spread of rabies to premotor neurons. C and D: Examples of premotor interneuron distribution pattern from T11 until S1 segments of Quadriceps motor pool in wild type and full *EphA4* mutant. In wild type, only few cells were located in the dorsal contralateral spinal cord (C). However in full *EphA4* mutants, variability in the premotor interneuron distribution was found (D). Two examples are illustrated; one pattern showing an increase in dorsal contralateral cells and the other pattern was comparable to wild type. Scale in µm. E: Scheme illustrating orientation and Rexed lamina position in the spinal cord. Infected motor neurons are located in the ipsilateral spinal cord. Central canal is marked in blue. Adapted by Stepien (2010). F: Percentage of dorsal contralateral cells of premotor interneuron distribution indicating each value of wild type (green) and full *EphA4* mutant (blue) mice. Mean (black line) and SEM (grey lines) are shown. Variability in the dorsal contralateral quadrant was found in the full *EphA4* mutant compared to wild type mice.

3.1.1.2 Shorter and wider shaped dorsal funiculus in conditional *EphA4* mutants

The aim was to delete the EphA4 receptor in Lbx1-expressing neurons. We, therefore, obtained conditional *EphA4*$^{flox/-}$*Lbx1*$^{Cre/+}$ mutant mice. Because of simplification, I will use the abbreviation "conditional *EphA4* mutant mice" in the following chapters to refer to these mice.

The overall observation of the dorsal funiculus revealed a different shape between wild type and both *EphA4* mutant mice (Fig. 7D). Hence, we quantified the dorsal funiculus by calculating the ratio of length/width and the dorsal gray matter by examining the ratio of length of dorsal spinal cord/length of dorsal gray matter (Fig. 7A). The quantification of the dorsal funiculus and dorsal gray matter in the lumbar spinal cord of wild type mice displayed a narrow and long shaped dorsal funiculus (Fig. 7B and C; mean of ratios in Table 1.1 of Appendix). However, the dorsal funiculus in the full *EphA4* mutant mice revealed a wider and shorter shape and, thereby, leaving an increased gray matter between dorsal funiculus and central canal in comparison to wild type mice. These findings were already described previously (Dottori 1998; Kullander 2001b; Restrepo 2011; Borgius 2014). Regarding the conditional *EphA4* mutant mice, the shape of the dorsal funiculus resembled the one of full *EphA4* mutants with its wider shape (ratio of dorsal funiculus: $P=0.94$ and ratio of dorsal gray matter: $P=0.99$; see Table 2.1). The ratios of the dorsal funiculus and dorsal gray matter of both *EphA4* mutants were significantly decreased in comparison to wild type mice (ratio of dorsal funiculus: $P<0.0001$; see all P values in Table 2.1). Taken together, both conditional and full *EphA4* mutant mice exhibited a shorter and wider shaped dorsal funiculus in comparison to wild type mice.

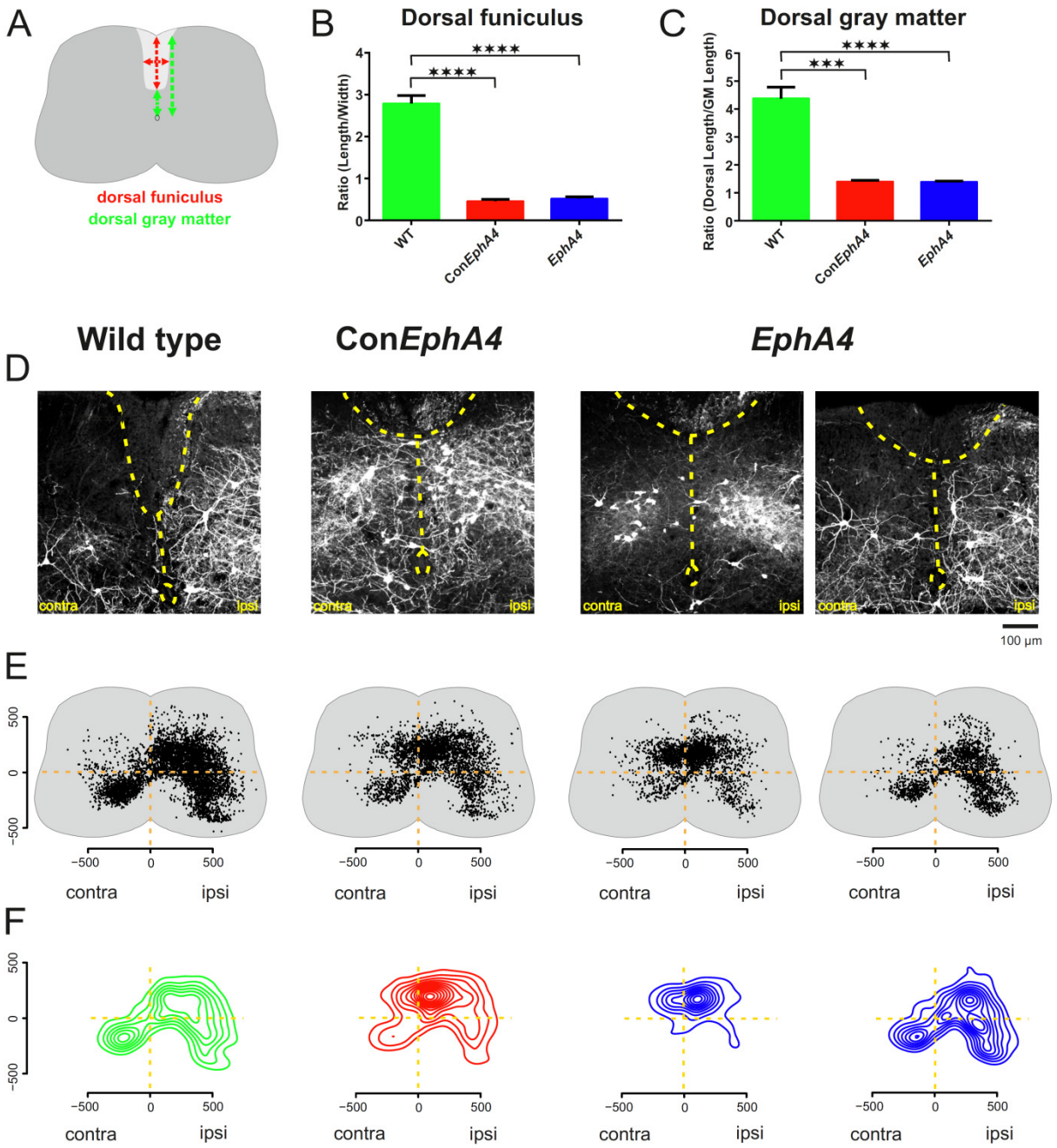

Figure 7. Premotor interneuron distribution of Q motor neurons in comparison between wild type, conditional and full *EphA4* mutant mice

A: Scheme of quantification of the dorsal funiculus and the dorsal gray matter. B: The dorsal funiculus was quantified by the ratio of the length divided by the width. Both conditional and full *EphA4* mutants showed a significantly decreased ratio of the shorter and widened dorsal funiculus in comparison to wild type mice. C: The quantification of the dorsal gray matter displays the ratio of the length of the dorsal spinal cord divided by the dorsal gray matter above the central canal. The ratio of the dorsal gray matter is significantly decreased in both *EphA4* mutant mice compared to wild type mice. D: Confocal pictures (20x) of the dorsal part in the lumbar spinal cord of rabies-infected premotor interneurons in wild type, conditional and full *EphA4* mutant mice. Quadriceps was specifically injected. Yellow dotted line displays the dorsal funiculus, midline and central canal. In conditional and full *EphA4* mutants, the dorsal funiculus showed a wider and

To Figure 7:

shorter shape compared to wild type mice. In the first example of the full *EphA4* mutant and the conditional *EphA4* mutant, rabies-infected cells were also found in the dorsal contralateral spinal cord. E: Examples of premotor interneuron distribution patterns from T11 to S1 segments. Yellow dotted line divides the spinal cord into four quadrants: dorsal ispilateral, dorsal contralateral, ventral ispilateral and ventral contralateral. F: Contour plot of premotor interneurons. Scale in µm.

3.1.1.3 Increased number of dorsal contralateral neurons in conditional *EphA4* mutants compared to wild type mice

3.1.1.3.1 Dorsal contralateral neurons of Q premotor interneuron distribution

As described above for full *EphA4* mutant mice, conditional *EphA4* mutant pups were injected in the Q at P5-7 by rabies GFP complemented with AAV glycoprotein. We examined the premotor interneuron distribution in conditional *EphA4* mutant mice in comparison to wild type and full *EphA4* mutants, and we reconstructed premotor interneurons from the whole lumbar spinal cord (T11 to S1 segment). In conditional *EphA4* mutant mice, the interneuron distribution as transverse projection (along the lateral-medial axis) revealed a striking increase of premotor interneurons in the dorsal contralateral spinal cord in contrast to wild type (see median values in Table 1.2 and below) and resembled the increased dorsal distribution of a few full *EphA4* mutants (Fig. 7E) (% dorsal contralateral neurons [Con*EphA4* (n=2): 12.8, 15.1; full *EphA4* (n=2): 24.85, 8.1]). The transverse interneuron distribution is additionally illustrated in a three-dimensional density plot, as contour plot (Fig. 7F). In Figure 8, two examples of a longitudinal projection (along the rostral-caudal axis) of premotor interneurons in wild type and conditional *EphA4* mutant are illustrated showing the dorsal and ventral premotor interneuron distribution seperately. Like the transverse projection, difference in premotor interneuron distribution between conditional *EphA4* mutant and wild type mice was observed in the contralateral side of the dorsal spinal cord (see median values of all animals in Table 1.2 and below).

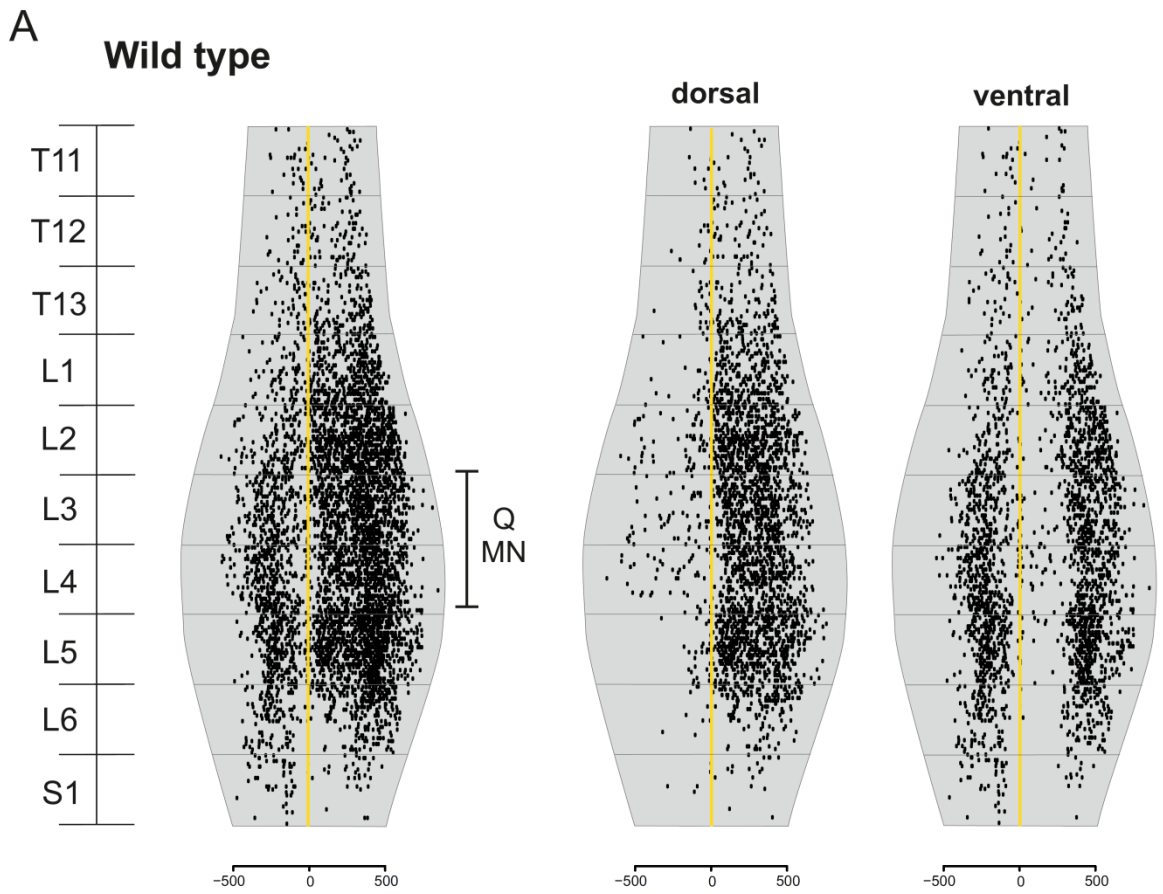
A
Wild type
dorsal
ventral
T11
T12
T13
L1
L2
L3
L4
L5
L6
S1
Q
MN
−500
0
500

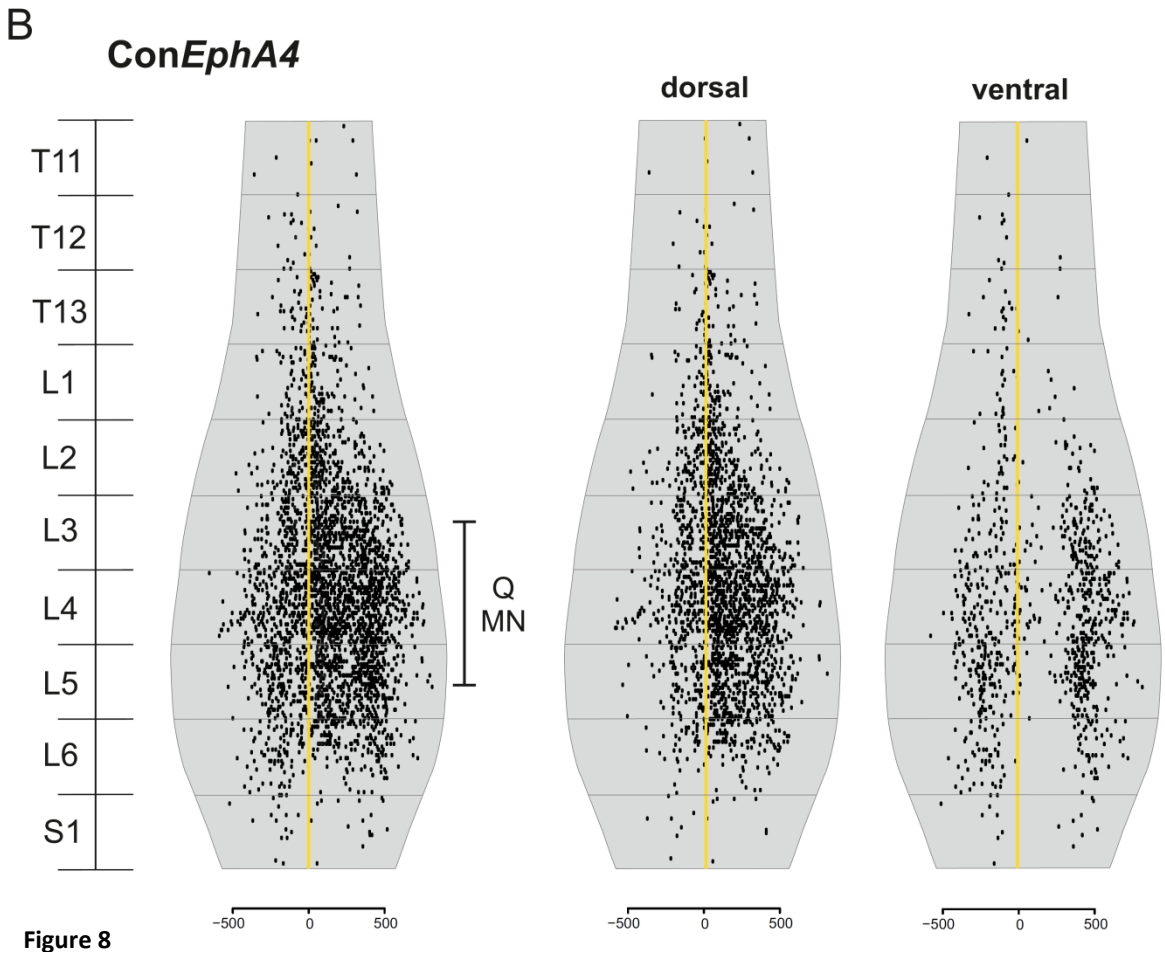
B
ConEphA4
dorsal
ventral
T11
T12
T13
L1
L2
L3
L4
L5
L6
S1
Q
MN
−500
0
500

Figure 8

Figure 8. Longitudinal plot of the premotor interneuron distribution of Q motor neurons

Longitudinal plots from T11 to S1 segments are displayed in the whole spinal cord and are shown separately in the dorsal and ventral cord. A: In an example of wild type, the majority of cells were located in the dorsal ipsilateral side. B: However in an example of conditional *EphA4* mutant, many neurons were found in the contralateral side of the dorsal spinal cord. Spinal midline is indicated by the yellow line. Quadriceps motor neuron pool is indicated by Q MN. Scale in µm.

In two-dimensional density plots, the transverse interneuron distribution of wild type versus conditional *EphA4* mutant mice (Fig. 9A and D), conditional versus full *EphA4* mutants (Fig. 9B and E) and wild type versus full *EphA4* mutant mice was plotted (Fig. 9C and F). The highest density of premotor interneurons was located in the lateral part of the ipsilateral spinal cord in wild type mice (n=4) (Fig. 9A). However, in conditional *EphA4* mutant mice (n=2), a shift of the density peak towards the medial side occurred (Fig. 9B). Full *EphA4* mutant mice (n=7) showed a range of density peaks from the lateral to the medial part of the ipsilateral spinal cord and, thereby, reflecting a high variability of premotor interneuron distribution (Fig. 9B and C). In a closer look at the contralateral side, the majority of interneurons were located in the ventral part in wild type mice (Fig. 9D), whereas the interneuron density of the two conditional *EphA4* mutants was equally distributed in the dorsal and ventral spinal cord (Fig. 9D). The density distribution in the dorsal contralateral side of two full *EphA4* mutants (showing the high peaks of density distribution in blue) resembled more the one of conditional *EphA4* mutant mice (Fig. 9E). However, the density plot of the other five full *EphA4* mutants was comparable with the one of wild type mice (Fig. 9F).

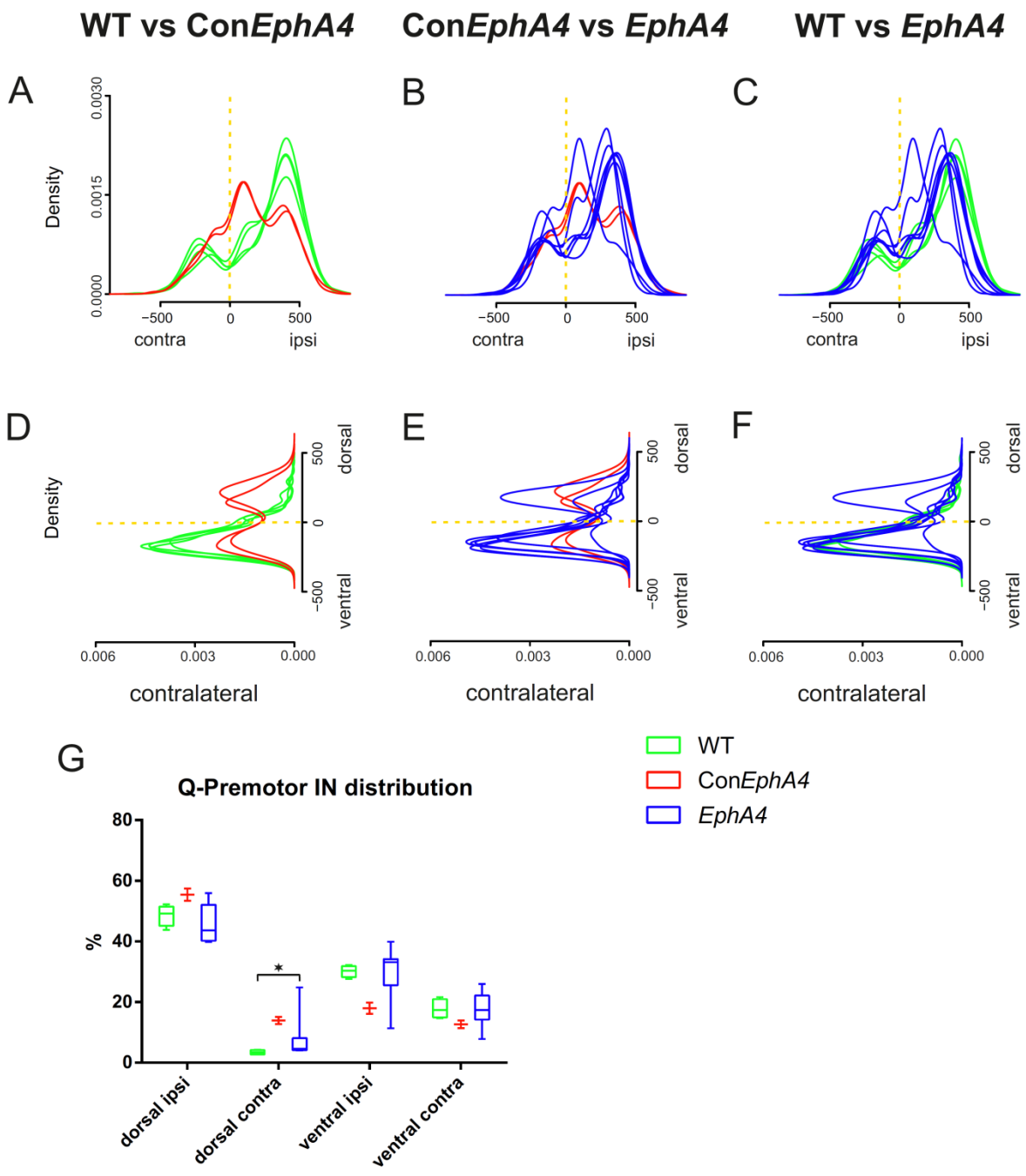

Figure 9. Premotor interneuron distribution of Q motor neurons in four quadrants of the spinal cord

A-C: Density plot of ipsi- and contralateral spinal cord comparing distribution densities between wild type (n=4) and conditional *EphA4* mutant (n=2), conditional and full *EphA4* mutant (n=7) and between wild type and full *EphA4* mutant mice. D-F: Density plot of the contralateral side comparing distribution densities between wild type and conditional *EphA4* mutant, conditional and full *EphA4* mutant and between wild type and full *EphA4* mutant mice. Scale in µm. G: Box and whisker plot showing the percentages of premotor interneurons in four quadrants of the spinal cord. Percentages of interneurons in the dorsal contralateral and ventral ipsilateral parts were tested by a Kruskal Wallis rank sum test with a post-hoc paired Wilcoxon test (significant difference when FDR<0.05).

We next calculated percentages of interneurons in the spinal cord divided into four parts: dorsal ipsilateral, dorsal contralateral, ventral ipsilateral and ventral contralateral (see all median values in Table 1.2), which are illustrated as box and whisker plot in Figure 9G. We focused on the dorsal contralateral part of the lumbar spinal cord for statistical analysis since the most differences in interneuron distribution between wild type and mutants were observed in that quadrant (median of % dorsal contralateral cells [WT: 3.45; Con*EphA4*: 13.95; *EphA4*: 4.59]). A Kruskal Wallis test revealed significant differences between all three genotypes (P=0.025; significant difference when P<0.05). Applying a post hoc pairwise Wicoxon test, the number of premotor interneurons was significantly increased in the full *EphA4* mutant in comparison to wild type mice (FDR=0.023; see P and FDR values in Table 2.2). Regarding the conditional *EphA4* mutant, no significant difference was found (wild type versus conditional *EphA4*: FDR=0.064; conditional versus full *EphA4* mutant: FDR=0.143). However, in the graph in Figure 9G, it is clearly obvious that the median of the percentages of dorsal contralateral neurons are highest in the conditional *EphA4* mutant. Therefore, the reason for a non-significant difference could have been the low number of two conditional *EphA4* mutant mice. In conclusion, there is a tendency of an increase of premotor interneurons in the contralateral side of conditional *EphA4* mutants in comparison to wild type mice. Further Q injections in the conditional *EphA4* mutant will have to approve these findings.

3.1.1.3.2 Dorsal contralateral neurons of TA and GS premotor interneuron distribution

Moreover, we wanted to investigate the premotor interneuron distribution from additional muscles in order to verify the findings of an increase of neurons in the dorsal contralateral quadrant of the Q premotor interneuron distribution in the conditional *EphA4* mutant. Complemented rabies injection with AAV-glycoprotein was continued into the flexor muscle Tibialis anterior (TA) and the extensor muscle Gastrocnemius (GS) by Dr. Daisuke Satoh. Premotor interneuron distribution of Q and TA motor neurons in wild type mice, displayed as contour plots, revealed a similar pattern with the majority of neurons on the ipsilateral side and some neurons in the ventral contralateral part of the spinal cord (compare Fig. 7F and 10A). However, the contour plot of the GS premotor interneuron distribution showed a decrease in cells in the whole ventral spinal cord compared to TA

premotor interneuron pattern in wild type mice (Fig. 10A). Regarding the contour plot of conditional *EphA4* mutant mice, an increase in both TA and GS premotor interneurons in the contralateral side of the spinal cord was observed in conditional *EphA4* mutant mice compared to wild type mice (Fig. 10A).

In order to compare the premotor interneuron distributions between wild type and conditional *EphA4* mutant mice, we plotted the data as two-dimensional density plots of interneuron distribution separately for the contralateral and ipsilateral part of the spinal cord (Fig. 10B-E). In the contralateral spinal cord, an increase of the density of TA premotor interneurons in the dorsal part and a decrease of density in the ventral part was observed in the conditional *EphA4* mutant compared to wild type mice (Fig. 10B). This resulted in an equal distribution of the density in the dorsal and ventral part of the conditional *EphA4* mutant, whereas a unique high density peak was located in the ventral part in wild type mice. In contrast, the density of GS premotor interneurons in the conditional *EphA4* mutant was slightly increased in the dorsal contralateral spinal cord compared to wild type (Fig. 10C).

Percentages of TA and GS premotor interneurons in the four parts of the spinal cord (dorsal ipsilateral, dorsal contralateral, ventral ipsilateral and ventral contralateral) are illustrated for conditional *EphA4* mutants and wild type mice in a box and whisker plot in Figure 10F and G (see also Table 1.3). Regarding the TA premotor interneuron distribution, a significant increase of the percentage of interneurons in the dorsal contralateral part was found in the conditional *EphA4* mutant in comparison to wild type mice (Fig. 10F; median of % dorsal contralateral cells [WT: 1.92; Con*EphA4*: 14.41]; P=0.016; see also Table 2.3). Likewise, the box and whisker plot of GS premotor interneurons in Figure 10G revealed a significant augmentation of interneurons in the dorsal contralateral quadrant of the spinal cord (median of % dorsal contralateral cells [WT: 3.68; Con*EphA4*: 6.77]; P=0.036).

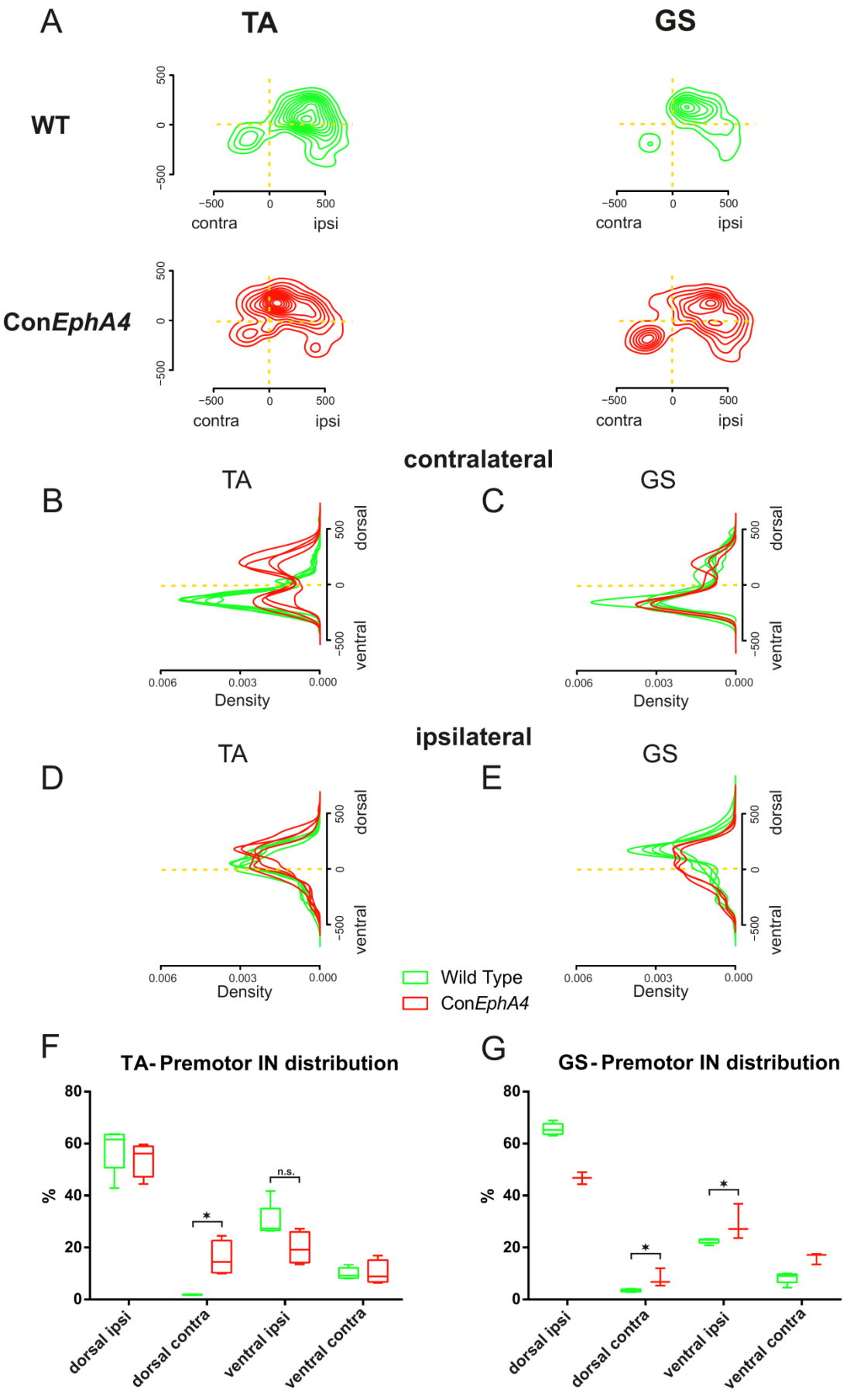
A
TA
GS
WT
ConEphA4
contra
ipsi
contralateral
ipsilateral
B
C
D
E
dorsal
ventral
Density
Wild Type
ConEphA4
F
G
TA- Premotor IN distribution
GS- Premotor IN distribution
%
dorsal ipsi
dorsal contra
ventral ipsi
ventral contra
n.s.

Figure 10

Figure 10. Premotor interneuron distribution of TA and GS motor neurons in comparison between wild type and conditional *EphA4* mutant mice

A: Contour plots of premotor interneuron distribution of TA and GS motor neurons in wild type and conditional *EphA4* mutants. B and C: Density plots of the contralateral spinal cord comparing distribution densities between wild type and conditional *EphA4* mutant mice of TA and GS premotor interneuron distribution. D and E: Density plots of the ipsilateral side comparing distribution densities between wild type and conditional *EphA4* mutant mice of TA and GS premotor interneuron distribution. Scale in µm. F and G: Box and whisker plots showing the percentages of pre-motor interneurons, projecting either to TA or GS motor neurons, in the four quadrants of the spinal cord. Percentages of interneurons in the dorsal contralateral and ventral ipsilateral part were tested by a Mann Whitney rank sum test (significant difference when $P<0.05$). TA and GS muscle injections and interneuron reconstructions were performed by Dr.Daisuke Satoh.

In summary, the conditional *EphA4* mutant exhibited an enhancement of premotor interneurons of Q, TA and GS motor neurons in the dorsal contralateral part of the spinal cord in comparison to wild type mice. Our findings of the Q premotor interneuron distribution were confirmed by the data of TA and GS premotor interneurons revealing likewise an increase of interneurons in the dorsal contralateral spinal cord in the conditional *EphA4* mutant. A more pronounced increase in the neuron density in this quadrant was found in the Q and TA premotor interneuron distribution of the conditional *EphA4* mutant. Indeed, axons of dorsal contralateral interneurons cross the midline and mis-connect to the contralateral motor neurons in conditional *EphA4* mutant mice whose Lbx1-positive cells lack the EphA4 receptor.

3.1.1.4 Change of ipsilateral interneuron distribution in conditional *EphA4* mutants compared to wild type mice

Additionally, we wanted to investigate a possible change in the premotor interneuron distribution in the ipsilateral spinal cord of conditional *EphA4* mutant mice. In the box and whisker plot of the Q premotor interneuron distribution in Figure 9G, a decrease of interneurons in the ventral ipsilateral spinal cord in the conditional *EphA4* mutant was observed in comparison to wild type mice (median of % ventral ispilateral neuron [WT: 30.35; Con*EphA4*: 17.94; *EphA4*: 33.14]). However, no significant difference between all three genotypes was found by a Kruskal Wallis test ($P=0.217$; all four quadrants cannot be

statistically tested, see also chapter 5.4). Like the statistical comparison of the dorsal contralateral quadrant, the number of conditional *EphA4* mutant mice might have been too small for a complete statistical test. Further Q injections in the conditional *EphA4* mutant will have to be performed to verify these findings.

Furthermore, the contour plots of GS and TA premotor interneuron distribution of the ipsilateral spinal cord in wild type showed that GS premotor interneurons were located more medially whereas TA premotor interneurons were found more laterally (Fig. 10A; previously described by Tripodi et al. (2011) and Dougherty et al. (2013)). In addition, the density plot and the box and whisker plot of GS premotor interneuron distribution in the conditional *EphA4* mutant revealed an increase of cells in the ventral ipsilateral spinal cord compared to wild type mice (Fig. 10E and G). This finding was confirmed to be significantly different by a Mann Whitney rank sum test (median of % ventral ipsilateral cells [WT: 22.99; Con*EphA4*: 27.1]; P=0.036; see also Table 2.3). In contrast, no significant difference was found in the ventral ipsilateral part of the TA premotor interneuron distribution between wild type and conditional *EphA4* mutant mice (Fig. 10F; median of % ventral ipsilateral cells [WT: 27.31; Con*EphA4*: 19.18]; P=0.064). Furthermore, the box and whisker plot of the GS premotor interneuron distribution in Figure 10G showed an increase of interneurons in the ventral contralateral part of the spinal cord and a decrease of interneurons in the dorsal ipsilateral part of the conditional *EphA4* mutant compared to wild type mice. Taken together, a shift of GS premotor interneuron distribution in all four parts of the spinal cord occurred in the conditional *EphA4* mutant with an increase of neurons in the dorsal contralateral quadrant and in the whole ventral cord, and a decrease of cells in the dorsal ipsilateral part in comparison to wild type mice. GS premotor interneuron distribution was shifted more extensively in all four quadrants than it was seen for TA premotor interneurons in the conditional *EphA4* mutant.

In summary, a tendency of an increase of Q premotor interneurons and a significant decrease of GS premotor interneurons were found in the ventral ipsilateral quadrant of the spinal cord in conditional *EphA4* mutant mice in comparison to wild type mice. This implies that the ipsilateral spinal cord is also affected in the conditional *EphA4* mutant. Further investigation of the shift of premotor interneuron distribution in the ipsilateral spinal cord needs to be performed in future.

3.1.1.5 Ectopic dorsal contralateral interneurons express Lbx1

To verify whether the misguided dorsal contralateral neurons of the Q premotor interneuron distribution expressed indeed Lbx1 in conditional and full *EphA4* mutant mice, we performed immunohistochemical stainings against rabies GFP and Lbx1 in spinal cords of wild type (n=4), conditional (n=2) and full (n=6) *EphA4* mutant mice at P13-15. Lbx1 is mainly expressed during embryonic stages, therefore, Lbx1-expression was already declined at P13-15. The highest Lbx1 expression was found in the dorsal horn. However, no Lbx1-positive cells were observed in the ventral medial spinal cord although Lbx1 expression pattern was observed in the dorsal and ventral medial spinal cord according to Gross et al. (2002). Lbx1-expression in the ventral spinal cord ceased as it was previously reported (Gross 2002). Overall, few dorsal contralateral interneurons were found in wild type mice. Thereby, a co-localization of rabies GFP- and Lbx1-positive cells was only seen in the dorsal ipsilateral spinal cord (Fig. 11). On the contrary, in conditional and full *EphA4* mutant mice, some of the dorsal contralateral ectopic neurons showed co-localization of rabies GFP and Lbx1-staining. In conclusion, axons of dorsal Lbx1-expressing neurons, lacking the EphA4 receptor, were misguided across the midline in the spinal cord and connected monosynaptically to motor neurons. The deletion of *EphA4* in a subset of interneurons, the Lbx1-expressing cells, resulted in a misconnected spinal network.

It is to assume that the majority or even all ectopic dorsal contralateral neurons express Lbx1. This project will be continued in the laboratory. Conditional *EphA4* mutant mice containing a lacZ reporter gene (*EphA4*$^{flox/-}$*Lbx1*$^{Cre/+}$*Tau*$^{lox\text{-}stop\text{-}lox\text{-}SynGFP\text{-}INLA}$ and *EphA4*$^{flox/-}$*Lbx1*$^{Cre/+}$*Tau*$^{lox\text{-}stop\text{-}lox\text{-}FlpO\text{-}INLA}$ mutant mice) were already obtained and will be additionally injected in specific muscles in order to visualize all Lbx1-expressing cells in the spinal cord at postnatal age.

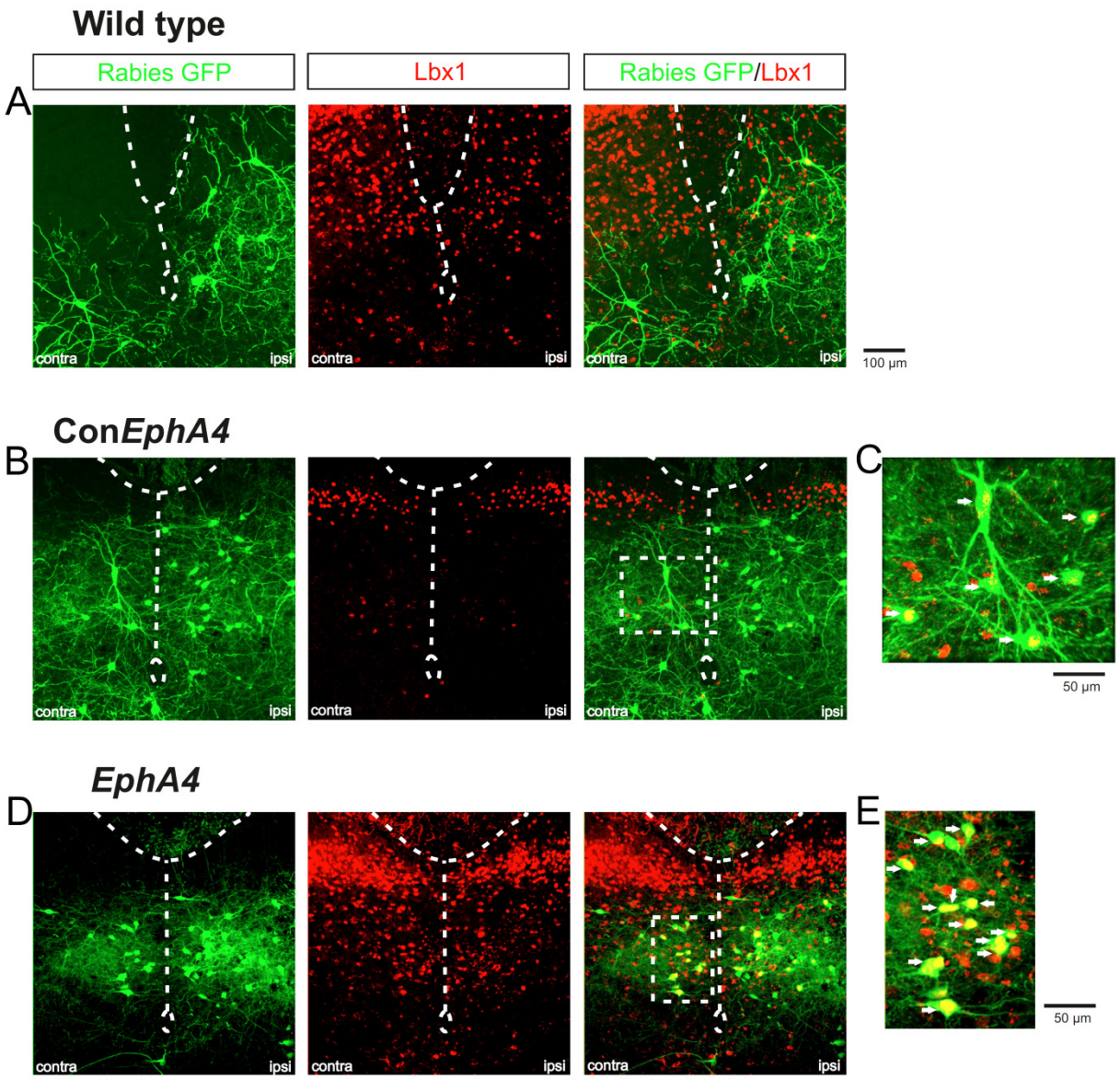

Figure 11. Ectopic dorsal contralateral interneurons are Lbx1-positive

Immunohistochemical stainings of rabies GFP and Lbx1 in the dorsal spinal cord in wild type, conditional and full *EphA4* mutant mice. The homeodomain transcription factor Lbx1 is expressed in dorsal dI4-6 interneurons. A: In an example of wild type, hardly any interneurons in the dorsal contralateral side were found. Some of the dorsal ipsilateral neurons were Lbx1-positive. B and D: On the contrary in examples of conditional and full *EphA4* mutants, some premotor interneurons in the dorsal contralateral side showed co-labeling of Lbx1 and rabies GFP (higher magnification of rectangle in C and E). White arrows point to co-labeled dorsal contralateral neurons (found in n=2 conditional and n=6 full *EphA4* mutants).

3.1.2 Gait behavior analysis of *EphA4* mutant mice

3.1.2.1 Classification of gait types on TreadScan

We have shown that deletion of *EphA4* in Lbx1-expressing neurons in the spinal cord resulted in an anatomical phenotype. Moreover, we wanted to study whether the misconnected Lbx1-positive neurons were also involved in an aberrant gait phenotype comparable to the hopping gait in full *EphA4* mutants.

Hence, the gait of adult wild type, conditional and full *EphA4* mutant mice was investigated on the TreadScan apparatus consisting of a treadmill with a transparent walking belt for camera detection from underneath. 20 second long trials were recorded at different belt speeds and then visually analyzed. The observed gait types were classified into four different groups mainly by the position of the hindlimbs to each other on the treadmill and additionally by a time difference between both hindlegs. The gait classification is as following: Alternating (ALT), Transitional Step (TS), Mixture (MIX) and synchronous Hopping (synHOP) (Fig. 12A). Mix and synHOP gait types were further grouped together into Hopping gait (HOP). Observing the full *EphA4* mutant mice walking with a hopping gait on the TreadScan, we found that some of their hopping steps did not show synchronicity between both hindlegs during the swing phase. Therefore, we distinguished the HOP gait into MIX and synHOP gait types since we wanted to separate real synchronous hindlimb movement during swing and stance phase from a more asynchronous hindlimb movement. The aim at the beginning of the gait type analysis was to investigate a correlation between anatomy and gait behavior. That meant, whether an increase of midline crossing axons of Lbx1-expressing cells in the *EphA4* mutants would correlate with an increase of synHOP gait frequency. It appeared that there was a continuum from MIX until synHOP gait and, therefore, a criterion distinguishing the two gait types was selected by the time difference between both hindlimbs. The time difference was measured by the frame difference between both hindlegs when starting into the swing phase.

A detailed description of the four gait types can be found in the following paragraph. The first observed gait type is Alternating gait (ALT). While one hindleg is in the middle of the stance phase, the other leg is in the middle of the swing phase. The position of both hindlegs on the treadmill is alternated. The second gait type, we found, is a Transitional Step (TS).

That means, both hindlegs are coming from an alternating step and end in a parallel or slightly shifted (one foot is shifted half of the length of the other foot) position to each other on the treadmill. TS was used to stop walking or to prepare for MIX or synHOP gait types. The third gait is described as Mixture gait (MIX) which appears as a gait between ALT and synHOP. Both hindlimbs start and end a stride in a parallel or slightly shifted position on the treadmill. The two hindlegs are some time but not always synchronous during stance and swing phase. One leg starts earlier in the swing and stance phase followed by the other leg; e.g. while one leg is already bended in the middle of the swing phase, the other leg is just starting into the swing phase and is still stretched. That means, both hindlegs are in average more than ca. 30% apart during the swing phase time. We classified the fourth gait type as synchronous Hopping gait (synHOP). Here, both hindlegs are in a parallel position on treadmill and move synchronously in swing and stance phase. That means, both hindlegs are in average less than ca. 30% apart during the swing phase time.

Wild type mice showed mainly ALT gait, whereas the full *EphA4* mutant exhibited mainly synHOP gait and in addition some MIX gait (Fig. 12B). In the conditional *EphA4* mutant, the majority of steps were ALT and MIX gait types. A detailed gait type analysis is described in the following chapters.

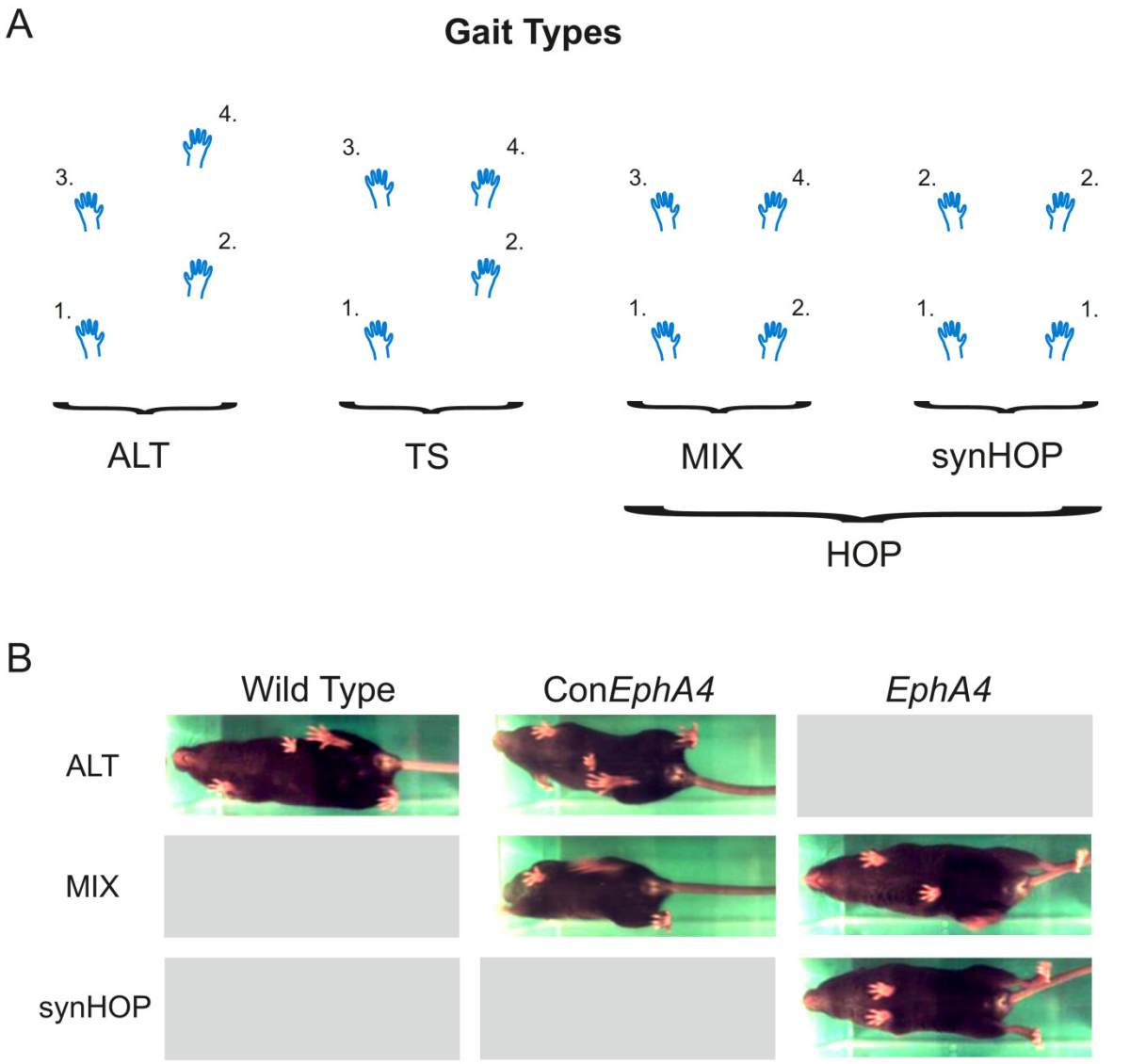

Figure 12. Classification of gait types on TreadScan

A: Wild type, conditional and full *EphA4* mutant mice exhibited four gait types on treadmill classified by position and time of both hindlimbs to each other. ALT: alternating gait, TS: transitional step, MIX: mixture gait and synHOP: synchronous hopping gait. MIX and synHOP can be grouped together as HOP (hopping gait). B: Wild type mice walked with ALT gait. Conditional *EphA4* mutants showed mainly ALT but also MIX gait types. On the contrary, solely synHOP and MIX gait types were found in full *EphA4* mutants. Pictures on TreadScan at belt speed of 16cm/s.

3.1.2.2 Obtaining conditional *EphA4* mutant mice with reporter allele

We performed the TreadScan gait type analysis with three sets of conditional *EphA4* mutant mice starting with the first and second set. The gait type analysis displayed a higher frequency of synHOP gait per trial of the first set of conditional *EphA4* mutants than it was observed for the second set of mutants. We have then realized that the Cre recombination did not specifically occur in Lbx1-expressing cells when the female of the breeding pair contained the $Lbx1^{Cre}$ allele. In further test matings between $EphA4^{+/-}Lbx1^{Cre}$ males and $Tau^{lox\text{-}stop\text{-}lox\text{-}mGFP\text{-}INLA}$ females (likewise $Tau^{lox\text{-}stop\text{-}lox\text{-}SynGFP\text{-}INLA}$ females), the Lbx1-expression pattern of the offspring was mainly observed in the dorsal spinal cord with some cells in the ventral medial part as it was previously described by Gross et al. (2002). However, when $EphA4^{+/-}Lbx1^{Cre}$ females and $Tau^{lox\text{-}stop\text{-}lox\text{-}mGFP\text{-}INLA}$ male were mated, Lbx1-expression in the pups was additionally found in the whole ventral lateral part. Therefore, in further matings, solely $EphA4^{+/-}Lbx1^{Cre/+}$ males were used to obtain conditional *EphA4* mutant offspring. In order to verify the Lbx1-expression pattern in the spinal cord postmortem in the following conditional *EphA4* mutants, they should additionally contain a reporter allele, either $Tau^{lox\text{-}stop\text{-}lox\text{-}SynGFP\text{-}INLA}$ or $Tau^{lox\text{-}stop\text{-}lox\text{-}FlpO\text{-}INLA}$. Hence, the third set of conditional *EphA4* mutant mice, $EphA4^{flox/-}Lbx1^{Cre/+}$ $Tau^{lox\text{-}stop\text{-}lox\text{-}SynGFP\text{-}INLA}$ and $EphA4^{flox/-}Lbx1^{Cre/+}$ $Tau^{lox\text{-}stop\text{-}lox\text{-}FlpO\text{-}INLA}$, were obtained and recorded. As the gender of the $Lbx1^{Cre}$ expressing parent of the first set of conditional *EphA4* mutant mice (n=4) could not be identified afterwards, the data was not included in the analysis. Furthermore, the second set of mice (n=4) were identified as offspring from $EphA4^{+/-}Lbx1^{Cre/+}$ males but their frequency of HOP gait during a trial was significantly increased compared to the third set of conditional *EphA4* mutant mice (by t-student test) and, therefore, could not be pooled together. Hence, the data of the second set of mice was also not included in the analysis. The final gait behavior analysis (shown in this thesis) was solely performed with the third set of conditional *EphA4* mutant mice (n=6).

3.1.2.3 HOP gait at low frequency locomotion in adult conditional *EphA4* mutant mice

In the gait type analysis, we compared the counted gait types per trial of adult conditional *EphA4* mutant mice with wild type and full *EphA4* mutants at belt speeds of 12, 16, 20, 30, 40 and 50 cm/s. The full *EphA4* mutant mice were not able to walk at 50 cm/s. The gait types of all three genotypes were analyzed according to the gait classification as described above in chapter 3.1.2.1.

In Figure 13, the percentages of the four gait types were plotted in a box and whisker graph at the different speeds separately for wild type, conditional and full *EphA4* mutant mice. Comparing the graphs, a striking difference of the four gait types between wild type and full *EphA4* mutant mice were obvious. At all tested speeds, wild type mice showed mainly an alternating gait, sometimes TS, but hardly any MIX and synHOP gait types (Fig. 13A; see all median values in Table 1.4). On the contrary, the majority of the steps exhibited by the full *EphA4* mutant mice were synHOP gait types and some steps of MIX gait at all tested speeds (Fig. 13C; see Table 1.6). We hardly observed any ALT and TS gait types. Overall, the gait types of the conditional *EphA4* mutant mice resembled mainly the ones of wild type (Fig. 13B; see Table 1.5). Like in wild type mice, conditional *EphA4* mutants mostly displayed ALT and sometimes TS gait types. In addition, the frequency of MIX gait was slightly increased at lower speeds of 12, 16 and 20 cm/s compared to higher speeds of 30, 40 and 50 cm/s. SynHOP gait was found very rarely.

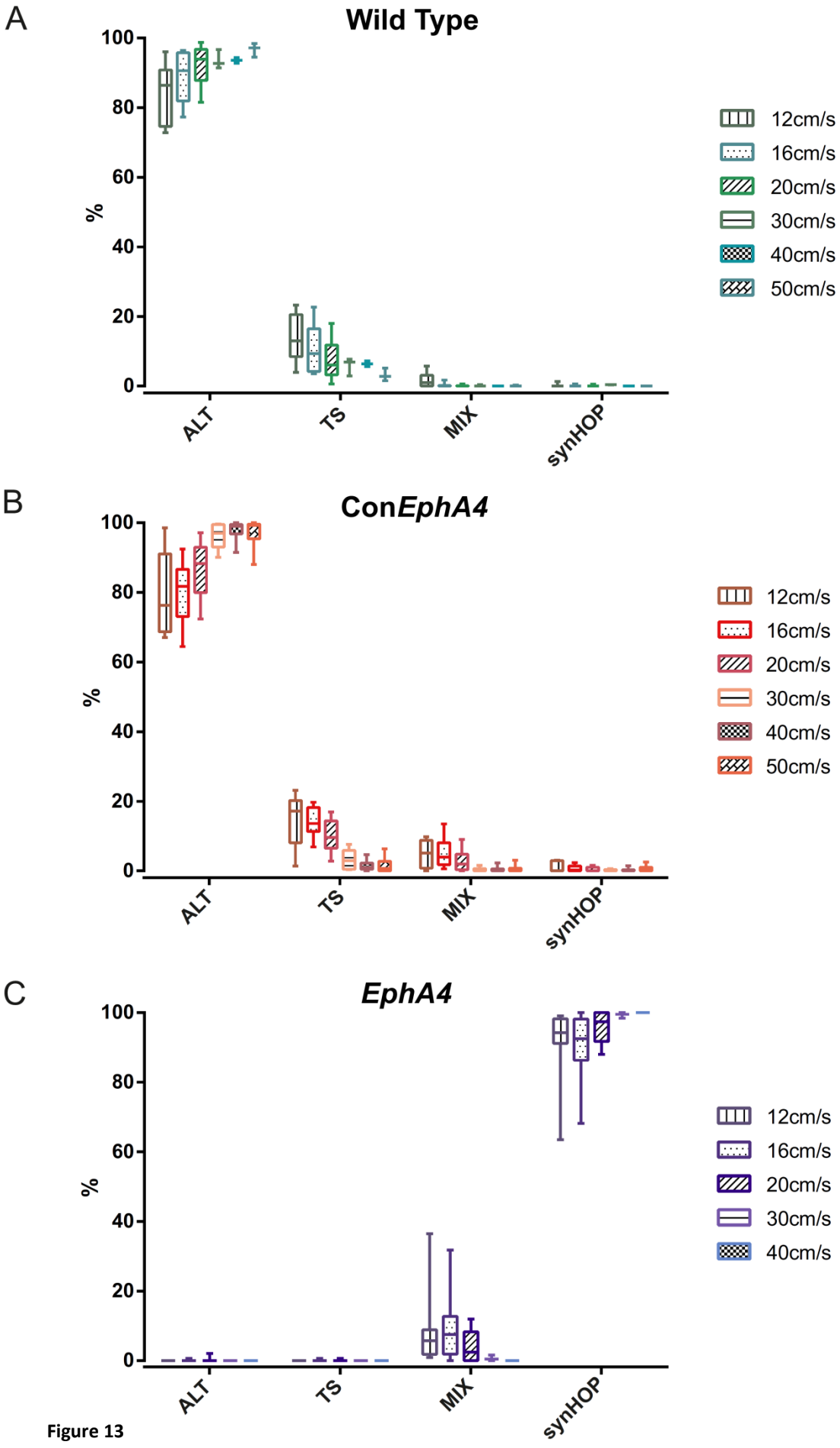
A
Wild Type
100
80
60
40
20
0
%
ALT
TS
MIX
synHOP
12cm/s
16cm/s
20cm/s
30cm/s
40cm/s
50cm/s
B
ConEphA4
100
80
60
40
20
0
%
ALT
TS
MIX
synHOP
12cm/s
16cm/s
20cm/s
30cm/s
40cm/s
50cm/s
C
EphA4
100
80
60
40
20
0
%
ALT
TS
MIX
synHOP
12cm/s
16cm/s
20cm/s
30cm/s
40cm/s

Figure 13

Figure 13. Percentage of gait types during a 20s trial of adult wild type, conditional and full *EphA4* mutant mice

Box and whisker graphs showing the percentages of ALT, TS, MIX and synHOP gait types at belt speeds of 12, 16, 20, 30 , 40 and 50 cm/s on the TreadScan apparatus of wild type (A), conditional (B) and full *EphA4* (C) mutant mice.

We observed a continuum from MIX until synHOP gait type and, therefore, the percentages of both gait types were pooled together as HOP gait for further statistical tests. In order to compare statistical differences of the gait types between the genotypes and speeds, HOP gait types were solely selected for a statistical test (reason see chapter 5.4). Hence, percentages of HOP gait were plotted in a box and whisker graph (Fig. 14; median values see Table 1.9). A Kruskal Wallis rank sum test was performed to compare the frequency of HOP gait between the belt speeds within each genotype (Table 2.4). No significant difference was found between the speeds of wild type (P=0.074) and of full *EphA4* mutant (P=0.818) mice. However, an overall significant difference between the speeds was obtained in the conditional *EphA4* mutant (P=0.012), but when single pairs of speeds of HOP gait type were compared with the post-hoc pairwise Wilcoxon test, no significant difference was found between the speeds. Regarding the false discovery rate (FDR) values in Table 2.4, a tendency of an increase in HOP frequency at lower speeds (12 to 20 cm/s) was observed in comparison to higher speeds (30 to 50 cm/s).

Moreover, a Kruskal Wallis rank sum test was conducted in between the three genotypes within each belt speed (Table 2.5). There was an overall significant difference between wild type, conditional and full *EphA4* mutant mice at 12 (P<0.0001), 16 (P<0.0001), 20 (P<0.0001), 30 (P=0.0104) and at 40 cm/s (P=0.0242). Within all recorded speeds, a pronounced significant increase in the frequency of HOP gait occurred in the full *EphA4* mutant compared to wild type and to conditional *EphA4* mutant mice (Fig. 14; FDR values see Table 2.5). Exclusively at the speeds of 16 and 20 cm/s, conditional *EphA4* mutants exhibited a slight significant increase in the frequency of HOP gait in comparison to wild type mice. In summary, adult conditional *EphA4* mutant mice augmented the frequency of HOP gait when walking at lower belt speeds compared to higher speeds. Besides, their frequency of HOP gait at lower speeds was significantly increased in comparison to wild type mice but showed a striking significant decrease in HOP frequency in comparison to full *EphA4* mutants.

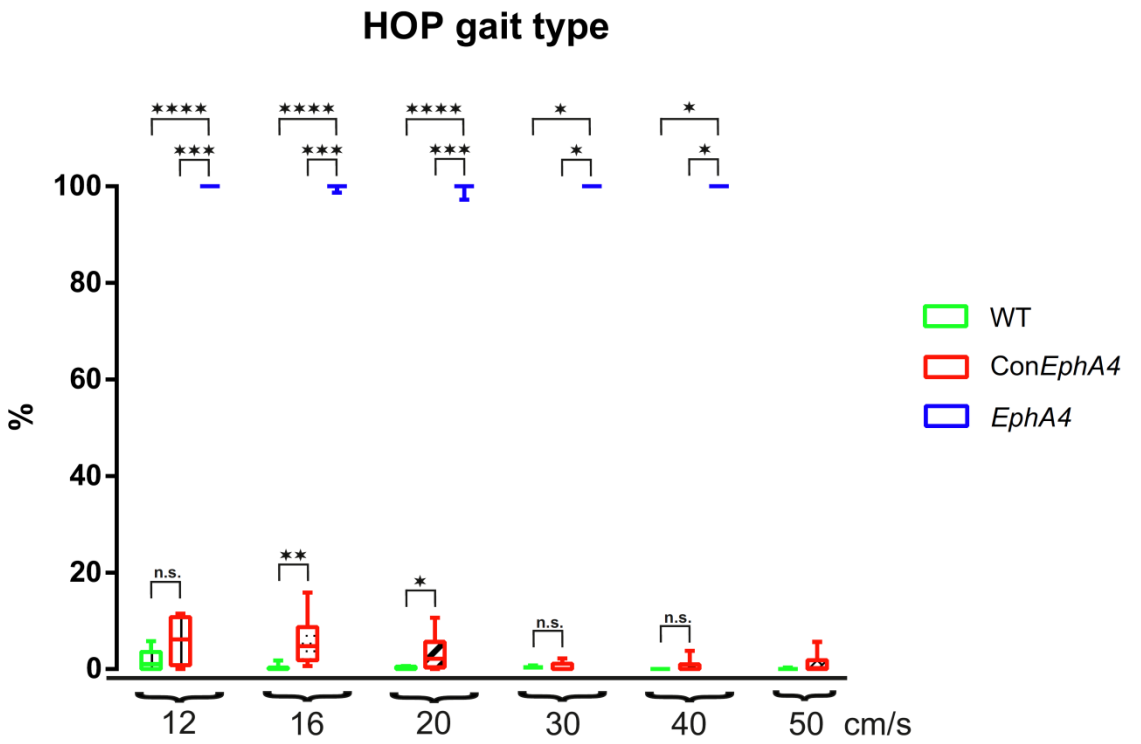

Figure 14. Comparison of HOP frequency between wild type, conditional and full *EphA4* mutant mice

The box and whisker plot shows a significant increase of the frequency of HOP gait in the full *EphA4* mutant at all speeds compared to wild type and conditional *EphA4* mutant mice. However, the conditional *EphA4* mutant displayed a minor increase in HOP gait frequency only at 16 and 20 cm/s in comparison to wild type mice. Kruskal Wallis rank sum test with a post-hoc paired Wilcoxon test was performed (significant difference when FDR<0.05).

3.1.2.4 Difference in HOP gait during development in conditional *EphA4* mutants

The third set of conditional *EphA4* mutant mice was tested on the TreadScan at the age of 3-week old and repeatedly as adults. The gait behavior of adult conditional *EphA4* mutants was already discussed in the previous chapter. We recorded these mice additionally at the age of 3-weeks in order to obtain gait behavior results during late postnatal development.

The 3-week old wild type mice mainly walked with ALT gait and sometimes with TS as it was already observed for adult wild type mice (Fig. 15 and 16A; see median values in Table 1.7). In comparison to the adult mutant, the 3-week old conditional *EphA4* mutant mice walked likewise with ALT gait and with some TS gait steps but additionally showed a slight increase in synHOP gait at higher speeds of 40 and 50 cm/s (Fig. 15 and 16B; median values see in Table 1.8). Providing an overview, a box and whisker plot of percentages of all gait types is shown separately for 3-week old wild type, 3-week old and adult conditional *EphA4* mutant mice in Figure 16.

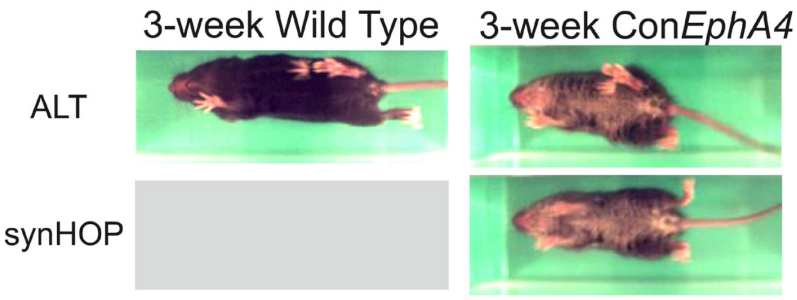

Figure 15. Gait types of 3-week old wild type and conditional *EphA4* mutant mice

3-week old wild type mice walked with ALT gait whereas 3-week old conditional *EphA4* mutant mice displayed ALT and synHOP gait types. Pictures on Treadscan at belt speed of 40 cm/s.

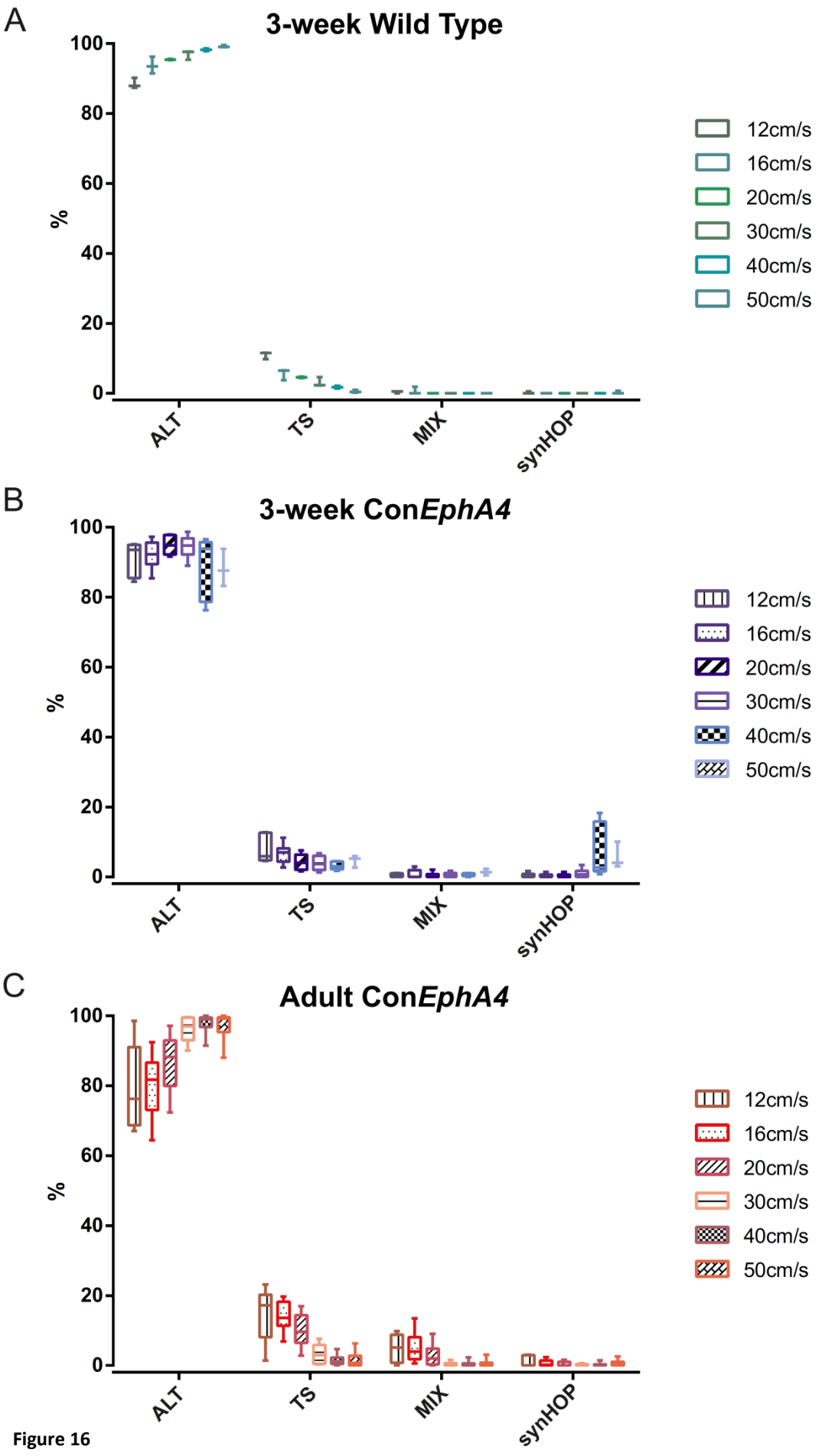
A
3-week Wild Type
100
80
60
40
20
0
%
ALT
TS
MIX
synHOP
12cm/s
16cm/s
20cm/s
30cm/s
40cm/s
50cm/s
B
3-week Con*EphA4*
100
80
60
40
20
0
%
ALT
TS
MIX
synHOP
12cm/s
16cm/s
20cm/s
30cm/s
40cm/s
50cm/s
C
Adult Con*EphA4*
100
80
60
40
20
0
%
ALT
TS
MIX
synHOP
12cm/s
16cm/s
20cm/s
30cm/s
40cm/s
50cm/s

Figure 16

Figure 16. Percentage of gait types during a 20s trial of 3-week old wild type and conditional *EphA4* mutant mice

Box and whisker plots showing the percentage of ALT, TS, MIX and synHOP gait types at belt speeds of 12, 16, 20, 30, 40 and 50 cm/s in 3-week old wild type (A), 3-week old (B) and adult (C) conditional *EphA4* mutant mice on the TreadScan.

Likewise, percentages of MIX and synHOP gait were pooled together as HOP gait for further statistical tests and plotted in box and whisker graphs in Figure 17 (median values in Table 1.9). A Kruskal Wallis rank sum test was performed comparing HOP frequency per trial between the recorded belt speeds within 3-week old wild type and within 3-week old conditional *EphA4* mutant mice (Table 2.6). No significant difference was found within 3-week old wild type mice (P=0.3435). However, an overall significant difference between the speeds was found within the 3-week old conditional *EphA4* mutants (P=0.024). A further post-hoc pairwise Wilcoxon test revealed no significant difference between the different pairs of speeds. According to the FDR values in Table 2.6 of the 3-week old conditional *EphA4* mutant, a tendency of an increase of HOP gait frequency at higher speeds (30 to 50 cm/s) was observed in comparison to lower speeds (12 to 20 cm/s).

Furthermore, percentages of HOP gait were compared between 3-week old wild type and conditional *EphA4* mutant mice within each speed by a Mann-Whitney rank sum test (Fig. 17A). The frequency of HOP gait was only significantly increased at 40 cm/s in 3-week old conditional *EphA4* mutant mice compared to 3-week old wild type mice (P=0.0357). Besides, a tendency of an increase in HOP gait frequency of the conditional *EphA4* mutant was observed at 50 cm/s (P=0.1; see all P values in Table 2.7).

Considering the development in gait behavior, HOP gait frequency between 3-week old and adult conditional *EphA4* mutant mice was compared within each speed by a Mann-Whitney rank sum test (Fig. 17B; Table 2.7). Significant increase of the HOP gait percentages was revealed at 16 cm/s in the adult compared to the 3-week old conditional *EphA4* mutant (P=0.0411). However at higher speeds, a significant augmentation of the HOP gait was found at 40 and 50 cm/s in the 3-week old compared to the adult conditional *EphA4* mutant mouse (40 cm/s: P=0.0216; 50 cm/s: P= 0.0357). Taken together, adult conditional *EphA4* mutants displayed an increase in HOP frequency at lower speeds, whereas 3-week old mutants showed increase in HOP frequency at higher speeds (see median values in Table 1.9).

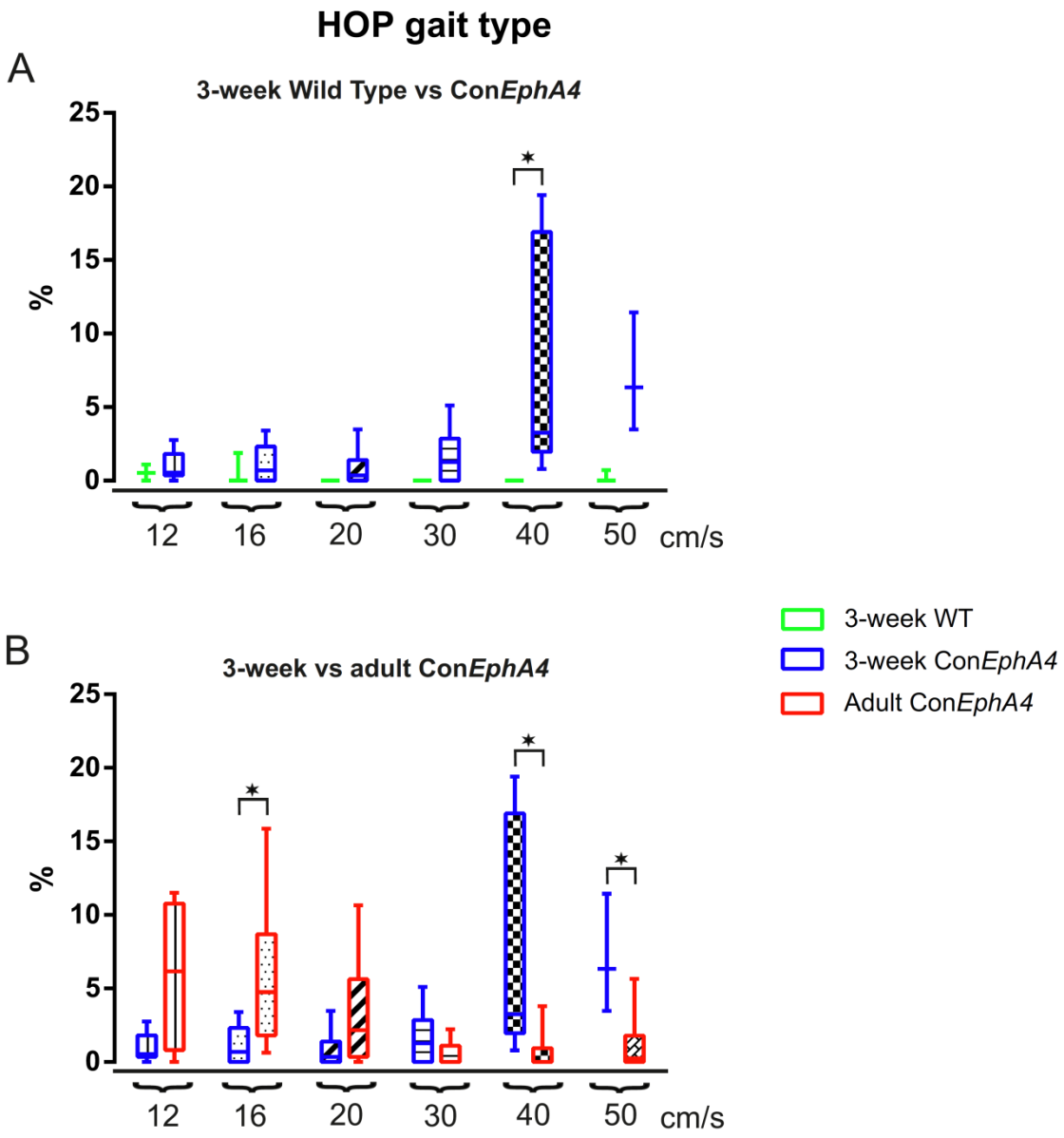

Figure 17. Comparison of HOP frequency between 3-week old wild type, 3-week old and adult conditional *EphA4* mutant mice

A: Frequency of HOP gait during a 20s trial was significantly increased in 3-week old conditional *EphA4* mutants compared to wild type mice at 40 cm/s. B: Comparing 3-week and adult age, adult conditional *EphA4* mutant mice displayed a slight increase in HOP gait frequency at lower speeds whereas 3-week old mutants walked with increased frequencies of HOP gait at higher speeds. Box and whisker plot. Values were compared by a Mann-Whitney rank sum test (significant difference when $P<0.05$).

Next, we wanted to observe the HOP frequency of each animal at the age of 3-week and adulthood (Fig. 18; average % HOP gait per trial in Table 1.10). A Wilcoxon matched-paired signed rank test was performed for each pair of HOP gait percentage comparing between 3-week and adult age of each animal. No significant difference was found for any of the pairs

at all belt speeds (P values in Table 2.7). In Figure 18, a tendency of an increase in HOP frequency at 12 or 16 cm/s from the age of 3-week old until adulthood was observed in some animals whereas the same animals decreased the HOP frequency again at 40 or 50 cm/s until adulthood (note animals in color yellow, blue, green, red and black in Fig. 18).

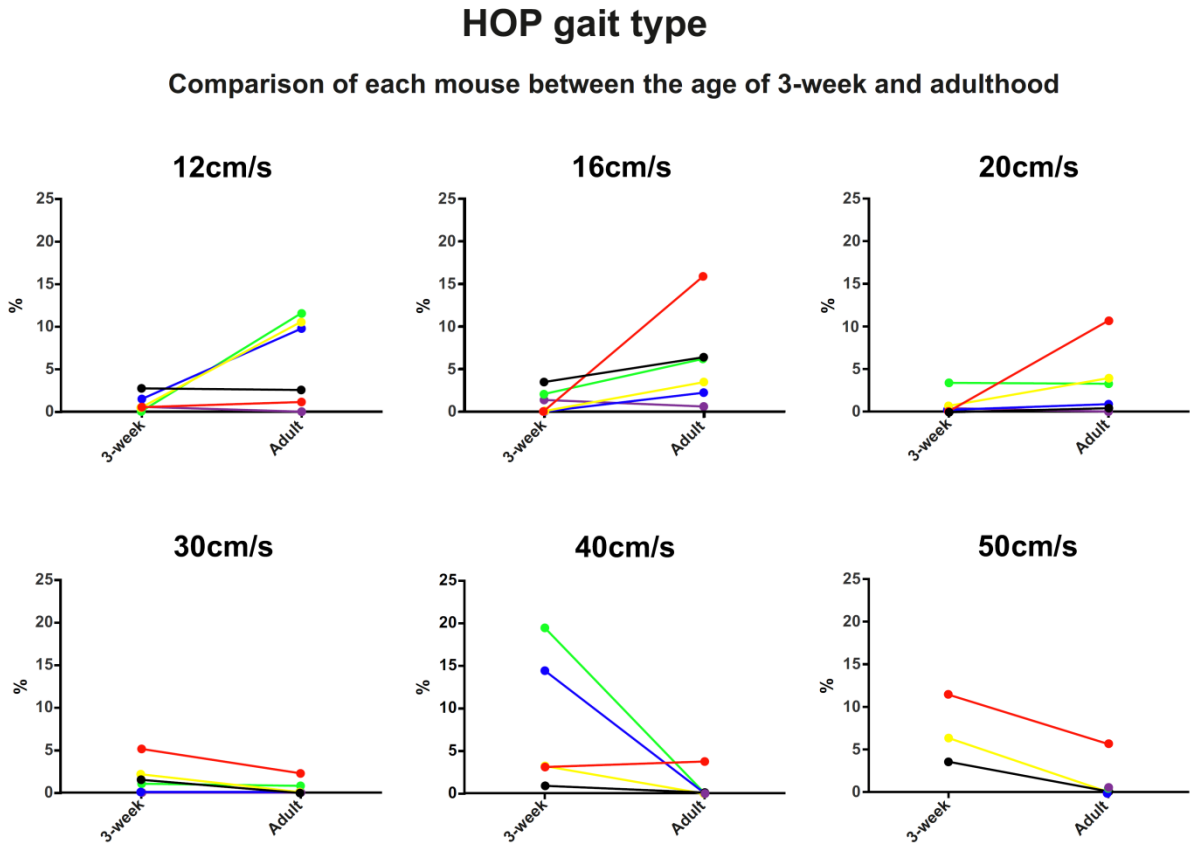

Figure 18. Comparison of HOP gait frequency during a 20s trial of each mouse between 3-week and adult age

Frequency of HOP gait was compared between the age of 3-week and adulthood of each mouse (labeled by a different color) at each belt speed. At 16 cm/s, most of the conditional *EphA4* mutants showed a slight increase in HOP frequency from 3-week until adulthood. However at 40 and 50 cm/s, the majority of mice displayed a decrease in HOP frequency until adulthood. No statistically significant difference was found by a pairwise Wicoxon test (significant difference when $P<0.05$).

In summary, 3-week old conditional *EphA4* mutant mice showed an augmentation in HOP frequency at higher walking speeds in comparison to 3-week old wild type and adult conditional *EphA4* mutant mice. In contrast, during development until adulthood, conditional *EphA4* mutants decreased their HOP frequency at higher speeds but, thereby, slightly increased the frequency of HOP steps at lower speeds.

3.1.2.5 Gait parameter analysis of conditional *EphA4* mutant mice by TreadScan

The TreadScan software (Cleversys, Inc.) enabled an automatic analysis of each stride consisting of stance and swing phase for each of the four limbs. Stance phase is defined as the time when the foot is in contact with the ground, the treadmill; while the swing phase is the time when the foot is in the air. Further gait parameters were automatically calculated by TreadScan software from stance time, swing time and stride length. We selected consistent steps with either ALT or HOP gait of adult animals for the gait parameter analysis. The aim was to compare ALT gait of conditional *EphA4* mutants with the ALT gait of wild type mice and to compare the HOP gait of conditional *EphA4* mutants with the HOP gait of full *EphA4* mutants for the different gait parameters. Furthermore, the gait parameters were compared between the low belt speed of 16 cm/s and the fast belt speed of 40 cm/s. The two belt speeds were exclusively selected as first, the gait type analysis revealed significant differences in the frequencies of HOP gait at 16, 40 and 50 cm/s between wild type mice and conditional *EphA4* mutants. Second, previous gait parameter analysis of the second set of conditional *EphA4* mutant mice showed no striking differences in between the lower speeds. Given that HOP gait frequency was observed very rarely at 40 cm/s in the conditional *EphA4* mutants, solely ALT gait was compared between wild type and conditional *EphA4* mutant mice.

Therefore, first, we compared gait parameters of ALT gait in wild type and conditional *EphA4* mutant mice within 16 and 40 cm/s and parameters of HOP gait in conditional and full *EphA4* mutants were compared at 16 cm/s. Second, gait parameters of ALT gait were compared between the speeds of 16 and 40 cm/s of wild type mice and conditional *EphA4* mutants by a Mann Whitney rank sum test (significant difference when $P<0.05$; see median values of all gait parameters in Table 1.11 and all P values in Table 2.8, 2.9 and 2.10).

The gait parameters, hindlimb, forelimb and diagonal feet couplings, were additionally compared between HOP and ALT gait of conditional *EphA4* mutants in order to verify a difference between both gait types and, therefore, confirming the classification of gait types.

3.1.2.5.1 Less synchronous hindlimb coupling in conditional *EphA4* mutants compared to full *EphA4* mutants

We first analyzed the gait parameter hindlimb coupling that is defined as the coordination of left and right hindlimb by comparing the beginning of the stance phase time. The exact calculation is as following: (Time of first touchdown of one foot after the touchdown of the reference foot – Time of touchdown of reference foot) / (Time of *next* touchdown of reference foot – Time of touchdown of reference foot). Therefore, at least two consistent steps were essential to calculate the hindlimb coupling value. The values ranged between 0.0 for in-phase hindlimb coupling and 0.5 for out-of-phase coupling. We obtained the hindlimb coupling values for the different genotypes in order to investigate whether the classification of gait types was in accordance to hindlimb coupling parameter calculated by TreadScan software.

ALT gait of wild type and conditional *EphA4* mutant mice showed similar hindlimb coupling values close to 0.5 at 16 and 40 cm/s (Fig. 19A; [WT 16 cm/s: 0.46, WT 40 cm/s: 0.48; Con*EphA4* 16 cm/s: 0.44, Con*EphA4* 40 cm/s: 0.46]; 16 cm/s: P=0.262; 40 cm/s: P=0.06). HOP gait of full *EphA4* mutants revealed values close to 0.0 (0.02) and was significantly diminished compared to the coupling value of HOP gait (0.17) in conditional *EphA4* mutant mice at 16 cm/s (P=0.0003). The comparison of hindlimb coupling values of HOP gait with ALT gait of conditional *EphA4* mutant mice revealed a significant decrease of hindlimb coupling values of HOP gait type (P=0.0043). An enhancement of the belt speed to 40 cm/s did not significantly change the hindlimb coupling values in wild type mice and conditional *EphA4* mutants (Fig. 19B; WT: P=0.248; Con*EphA4*: 0.346).

Taken together, the ALT gait of conditional *EphA4* mutant mice is comparable to the one of wild type. Full *EphA4* mutants showed synchronous hindlimb movement, whereas conditional *EphA4* mutants with HOP gait displayed steps in between synchronous and alternating coordination of the both hindlimbs. The analysis of hindlimb coupling parameter with TreadScan software confirmed the gait type classification by position and by time into ALT, MIX and synHOP gait types.

3.1.2.5.2 Uncoupling of diagonal feet in full *EphA4* mutants

Diagonal feet coupling is the coordination of one hindlimb and its diagonally opposite forelimb. The calculation of the value is the same as described above for homologous coupling. In wild type mice with ALT gait, diagonal feet coupling values approximated in-phase coordination (Fig. 19C; [16 cm/s: 0.1; 40 cm/s: 0.03]). Diagonal feet coupling values of ALT gait in conditional *EphA4* mutant mice did not differ significantly to the one of wild type mice at 16 cm/s (P=0.319; [16 cm/s: 0.18]) but displayed a significant increase compared to wild type at 40 cm/s (P=0.0.036; [40 cm/s: 0.08]). Full *EphA4* mutants with HOP gait showed a diagonal feet coupling value of 0.36, thereby, approximating the value 0.5, and were significantly increased to the value of 0.18 in conditional *EphA4* mutant mice with HOP gait (P=0.002). No significant difference was found between ALT and HOP gait of conditional *EphA4* mutants (P=0.134). At a higher speed of 40 cm/s, wild type mice significantly decreased the diagonal coupling values as approximating in-phase values of 0.0, in comparison to 16 cm/s (Fig. 19D; P=0.007 [16 cm/s: 0.12; 40 cm/s: 0.03]).

In summary, HOP gait of full *EphA4* mutants did not display synchronous movement between right hindlimb and left forelimb as it was found for ALT gait, instead showed an uncoupling of diagonal feet. However, conditional *EphA4* mutant mice with HOP gait exhibited increased range of diagonal coupling values between the values of ALT gait and HOP gait of full *EphA4* mutant and, thereby, showing features between alternating and synchronous diagonal feet coordination.

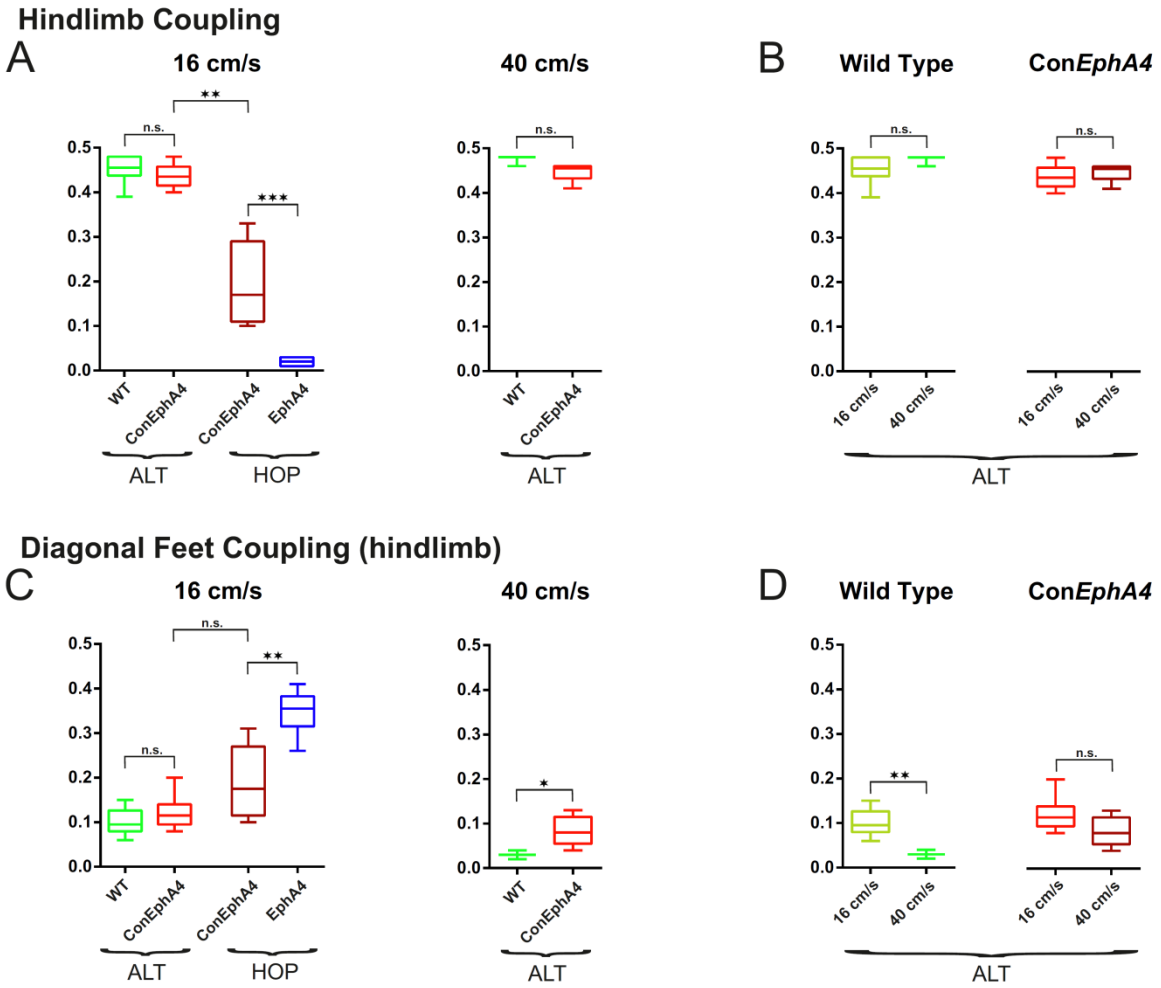

Figure 19. Gait coupling between limbs with ALT and HOP gait on TreadScan

A: Hindlimb coupling is calculated by the time difference between both hindlimbs starting the stance phase. Hindlimbs of wild type and conditional *EphA4* mutant mice walking with ALT gait were almost out-of-phase (values of 0.5) whereas hindlimbs of full *EphA4* mutants with HOP gait were close to in-phase (values of 0.0). Hindlimbs of conditional *EphA4* mutants with HOP gait showed values between 0.0 and 0.5, neither ALT nor synHOP. B: Speed did not affect the hindlimb coupling in wild type and the conditional *EphA4* mutant. C: Diagonal feet coupling describes the coupling between right hindlimb and left forelimb. The diagonal feet were coupled almost out-of-phase in the full *EphA4* mutant with HOP gait whereas the feet of wild type and conditional *EphA4* mutant mice with ALT gait were approximating values close to in-phase coupling. D: Diagonal feet coupling displayed values close to 0.0 for wild type mice at 40 cm/s. Box and whisker plots. Values were compared by a Mann-Whitney rank sum test (significant difference when $P<0.05$).

3.1.2.5.3 No significant differences in stride length of hindlimbs between all genotypes

Stride length signifies the distance between successive strides of the same foot and was calculated by the beginning of the stance phase time. Within the speed of 16 and 40 cm/s, the stride length of ALT and HOP gait in wild type mice and both *EphA4* mutants did not differ significantly between the genotypes and, thereby, providing an equal initial point of calculations for the different gait parameters (Fig. 20A; [WT ALT vs Con*EphA4* ALT: 16 cm/s: P=0.784, 40 cm/s: P=0.619; Con*EphA* HOP vs *EphA4* HOP: P=0.41]; see median values Table 1.11). At a higher speed of 40 cm/s, the stride length significantly increased in wild type and conditional *EphA4* mutant mice (Fig. 20B; [WT: P=0.007; Con*EphA4*: P=0.026]).

3.1.2.5.4 Increased stride frequency of hindlimbs in conditional *EphA4* mutants compared to wild type mice

The ratio of the number of strides to the sum of the stride times of these strides resulted in stride frequency. Conditional *EphA4* mutant mice either with ALT or HOP gait walked with a significant increased stride frequency in comparison to wild type and full *EphA4* mutant mice at 16 cm/s, respectively (Fig. 20C; [WT ALT vs Con*EphA4* ALT: P=0.014; Con*EphA4* HOP vs *EphA4* HOP: P=0.003]; see medians in Table 1.11). In contrast, at 40 cm/s, we found no significant difference in stride frequency of ALT gait between wild type and conditional *EphA4* mutant mice (P=0.5). Stride frequency was significantly augmented at higher belt speed of 40 cm/s compared to 16 cm/s. The frequency increased from 2.78 to 5.05 Hz (wild type) and from 3.46 to 5.55 Hz (conditional *EphA4* mutant) (Fig. 20D; [WT: P=0.007; Con*EphA4*: P=0.0022]).

3.1.2.5.5 Decreased stance time of hindlimbs in conditional *EphA4* mutants with HOP gait compared to full *EphA4* mutants

The stance time of the right hindlimb of ALT gait did not differ significantly between wild type and conditional *EphA4* mutant mice at 16 and 40 cm/s (Fig. 20E; [WT vs Con*EphA4*: 16 cm/s: P=0.172; 40 cm/s: P=0.429]; see median values Table 1.11). However, the stance time of HOP gait in conditional *EphA4* mutants was significantly decreased in comparison to

full *EphA4* mutant mice at 16 cm/s (P=0.042). We also observed a significantly reduced stance time at the higher speed of 40 cm/s compared to 16 cm/s in both wild type (P=0.004) and conditional *EphA4* mutant mice (P=0.002; Fig. 20F).

3.1.2.5.6 Decreased swing time of hindlimbs in conditional *EphA4* mutants with ALT gait compared to wild type mice

The hindlimb swing time of ALT gait was significantly decreased in conditional *EphA4* mutant mice compared to wild type at 16 cm/s (Fig. 20G; P=0.011). On the contrary, at 40 cm/s, swing time of ALT gait of both genotypes did not differ significantly and exhibited similar median values ([WT: 98.18 ms; Con*EphA4*: 83.19 ms]; WT vs Con*EphA4*: P=0.167). Swing time of HOP gait did not differ significantly between conditional and full *EphA4* mutant mice at 16 cm/s (P=0.052). Both mutants displayed decreased median values compared to wild type mice ([WT ALT: 128 ms; Con*EphA4* ALT: 95.73 ms; Con*EphA4* HOP: 77.5 ms; *EphA4* HOP: 88.64 ms]; not statistically tested, reason see 5.4). A significantly diminished swing time in full *EphA4* mutants compared to wild type mice walking on a runway was already described by Akay et al. (2006). Regarding the speed difference, swing time of wild type mice significantly decreased at 40 cm/s compared to 16 cm/s (P=0.049), whereas the swing time of ALT gait of conditional *EphA4* mutants did not differ significantly between 16 and 40 cm/s (P=0.305) (Fig. 20H; all median values Table 1.11).

3.1.2.5.7 Percentage of hindlimb swing time is shorter at lower speeds in all genotypes

Swing time percentage defines the percentage of stride time spent in the swing phase. Within the belt speeds of 16 and 40 cm/s, the percentage of hindlimb swing time of ALT and HOP gait did not differ significantly between the different genotypes (Fig. 20I; [WT ALT vs Con*EphA4* ALT: 16cm/s: P=0.175; 40 cm/s: P=0.381; Con*EphA4* HOP vs *EphA4* HOP 16 cm/s: P=0.48]). However, the median of swing time percentage of ALT gait was 35.92% for wild type and 32.18% for conditional *EphA4* mutant mice at 16 cm/s and significantly rose to 49.66% and 47.17% at 40 cm/s in both wild type and conditional *EphA4* mutant mice, respectively (Fig. 20J; [WT: P=0.007; Con*EphA4*: 0.002]). Taken together, hindlimb swing and

stance time achieved almost half and half of a stride time at higher speeds, whereas the swing time is shorter than the stance time at lower speeds.

3.1.2.5.8 Increased hindlimb track width in full *EphA4* mutants compared to conditional *EphA4* mutants

Moreover, we examined the hindlimb track width that is calculated as the distance between the midpoint of the left hindlimb stride and the midpoint of the right hindlimb stride. It is essentially the distance between both hindlimbs. Hindlimb track width of HOP gait showed a significant enhancement in full *EphA4* mutants in comparison to conditional *EphA4* mutant mice at 16 cm/s (Fig. 20K; P=0.017; [*EphA4*: 22.88 mm; Con*EphA4*: 18.57 mm]). However, hindlimb track width of ALT gait displayed a similar distance between wild type mice and conditional *EphA4* mutants at 16 and 40 cm/s (Fig. 20K; 16 cm/s: P=0.351; 40 cm/s: P=0.262; median at 16 cm/s: [WT: 20.08 mm, Con*EphA4*: 18.76 mm]; at 40 cm/s: [WT: 20.25 mm, Con*EphA4*: 16.24 mm]) and, likewise, between the speeds of 16 and 40 cm/s in wild type (P>0.999) and conditional *EphA4* mutant mice (P>0.999; Fig. 20L). In summary, full *EphA4* mutants with HOP gait walked with an enhanced distance between their hindlimbs, whereas conditional *EphA4* mutants, when walking with HOP gait, extended their hindlimbs to a lower degree than it was observed in the full *EphA4* mutant.

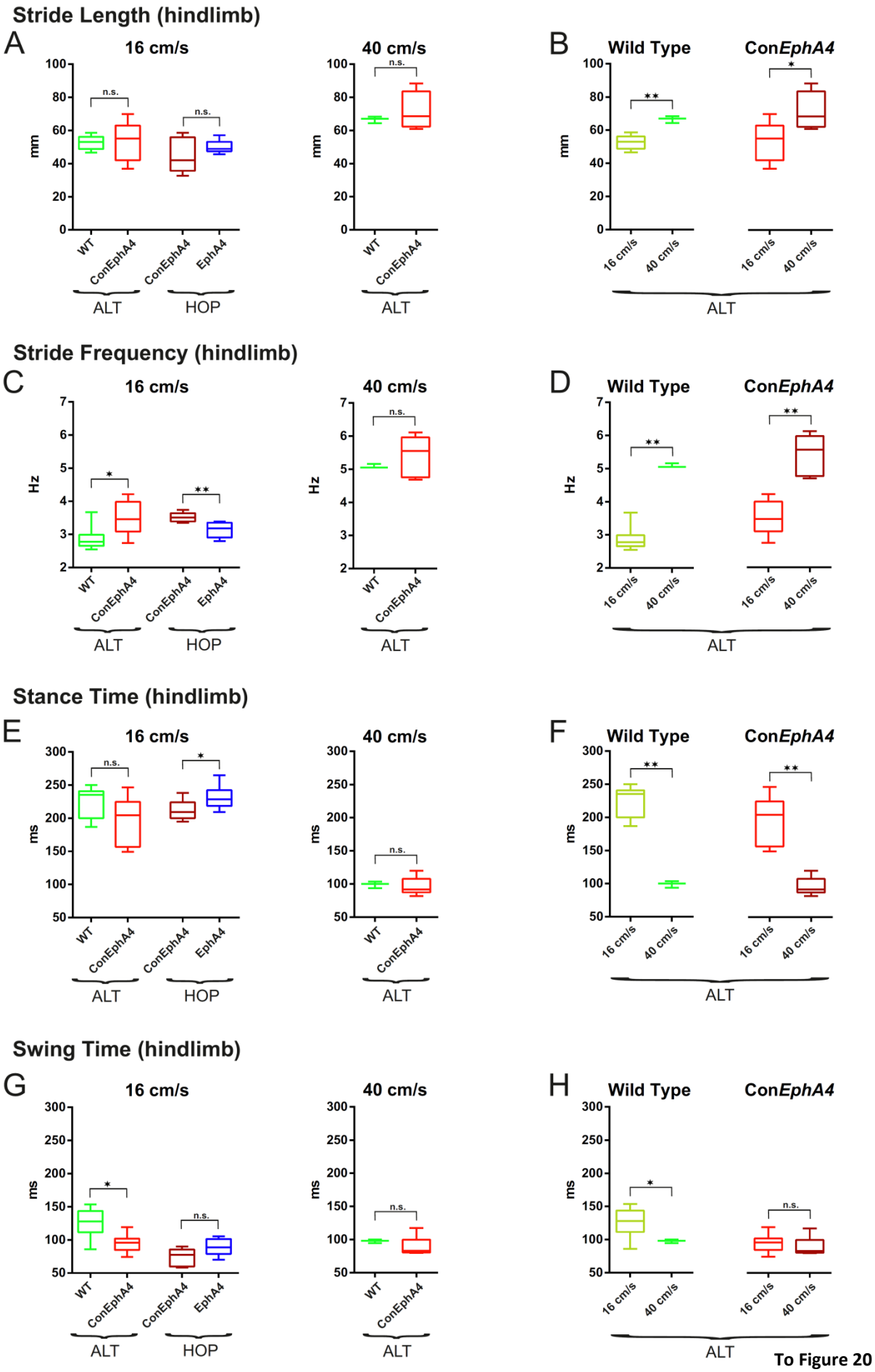
Stride Length (hindlimb)
A
16 cm/s
40 cm/s
B
Wild Type
ConEphA4
mm
n.s.
*
**
WT
ConEphA4
EphA4
16 cm/s
40 cm/s
ALT
HOP
Stride Frequency (hindlimb)
C
D
Hz
Stance Time (hindlimb)
E
F
ms
Swing Time (hindlimb)
G
H

To Figure 20

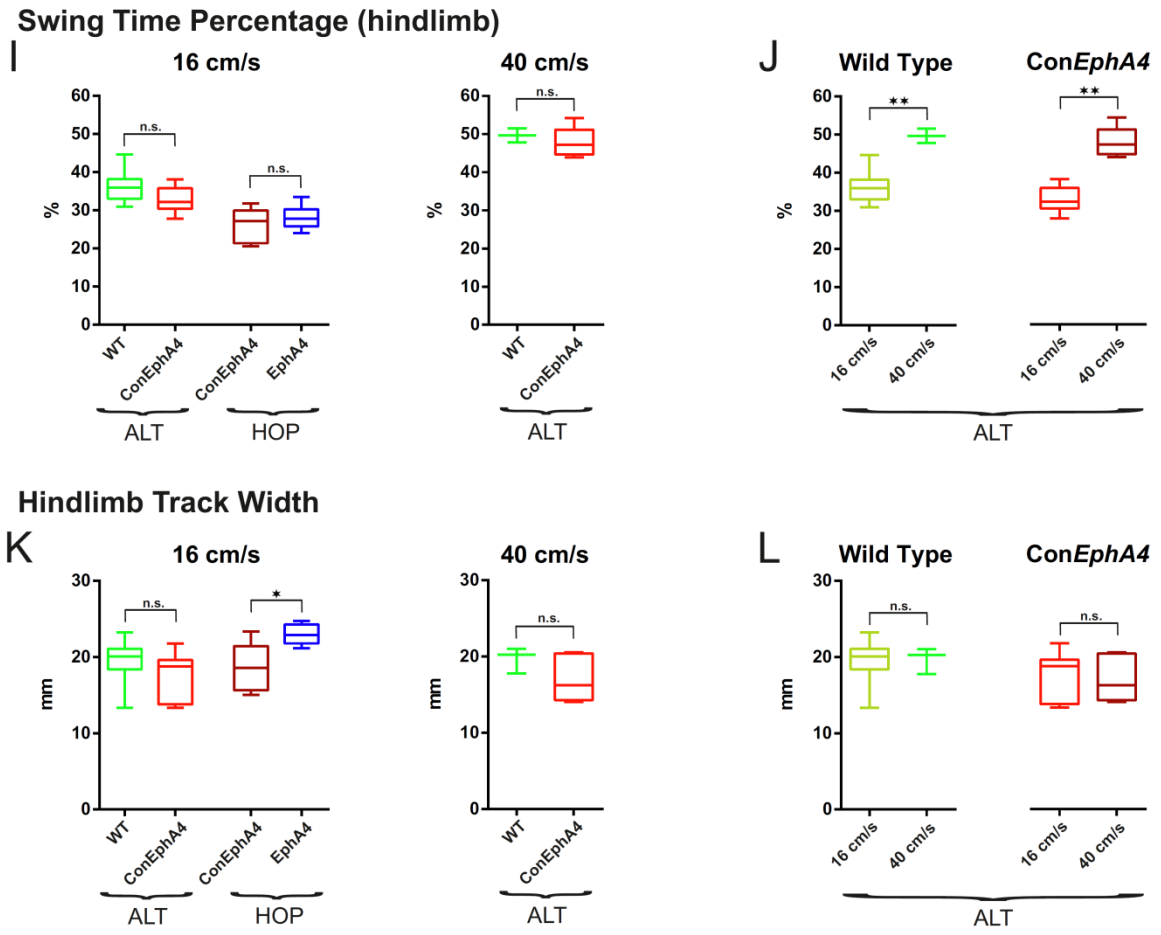

Figure 20. Hindlimb gait parameters of ALT and HOP gait on TreadScan

A,C,E,G,I,K: Comparison of gait parameters between wild type and conditional *EphA4* mutants with ALT gait and between conditional and full *EphA4* mutants with HOP gait at 16 cm/s. As conditional *EphA4* mutant mice showed only constant ALT gait at higher speeds, gait parameters of ALT gait were compared at 40 cm/s. B,D,F,H,J,L: Comparison of gait parameters between the belt speeds of 16 and 40 cm/s within the same genotype, wild type and conditional *EphA4* mutants with ALT gait. All values are given for the right hindlimb. Box and whisker plots. Values were compared by a Mann Whitney rank sum test (significant difference when $P<0.05$).

3.1.2.5.9 Less synchronous forelimb coupling in conditional *EphA4* mutants compared to full *EphA4* mutants

Next, we wanted to investigate whether forelimbs were also affected when conditional *EphA4* mutant mice walked with ALT and HOP gait of their hindlimbs. Forelimb coupling values were calculated in the same manner as for hindlimb coupling values (see above). The forelimb coupling was out-of-phase in wild type (median at 16 cm/s: 0.43) and in conditional *EphA4* mutant mice (median at 16 cm/s: 0.44) with ALT gait as it was also observed for hindlimbs. Comparing forelimb coupling values of ALT gait, there was no significant difference between wild type and conditional *EphA4* mutant mice at 16 and 40 cm/s (Fig. 21A; [16 cm/s: P>0.999; 40 cm/s: P=0.119]). Likewise for hindlimbs, forelimbs of full *EphA4* mutants were coordinated in-phase and, therefore, forelimb coupling (median: 0.02) was significantly decreased compared to the forelimb coupling of HOP gait in conditional *EphA4* mutants (median: 0.22) at 16 cm/s (P=0.0003). Furthermore, regarding ALT and HOP gait of conditional *EphA4* mutant mice, the forelimb coupling values of HOP gait were significantly diminished to the values of ALT gait (P=0.002). Taken together, forelimbs of conditional *EphA4* mutants were coordinated neither out-of-phase nor in-phase and, thereby, lying in between as it was observed for the hindlimbs. When wild type and conditional *EphA4* mutant mice walked with ALT gait at 40 cm/s, the out-of-phase coordination of their forelimbs significantly increased compared to 16 cm/s (Fig. 21B; [WT: P=0.0035; Con*EphA4*: P=0.022]).

3.1.2.5.10 Decreased stance time of forelimbs in conditional *EphA4* mutants compared to wild type and full *EphA4* mutant mice

Conditional *EphA4* mutant mice with either ALT or HOP gait at 16 cm/s showed a significantly reduced stance time of forelimbs in comparison to wild type and full *EphA4* mutant mice, respectively (Fig. 21C; [WT ALT vs Con*EphA4* ALT: P=0.021; Con*EphA4* HOP vs *EphA4* HOP: P=0.019]; see median values Table 1.11). However, at a higher speed of 40 cm/s, the stance time of ALT gait did not differ significantly between wild type mice and conditional *EphA4* mutants (P=0.714), but the stance time significantly decreased at 40 cm/s compared to 16 cm/s in both wild type and conditional *EphA4* mutant mice (Fig. 21D; [WT: P=0.007; Con*EphA4*: P=0.002]).

3.1.2.5.11 Decreased swing time of forelimbs in conditional *EphA4* mutants with ALT gait compared to wild type mice

Swing time of forelimbs was comparable to the swing time of hindlimbs (median values see Table 1.11). Regarding ALT gait, the forelimb swing time of conditional *EphA4* mutant mice significantly decreased in comparison to wild type at 16 cm/s (P=0.023), but no difference between both genotypes was observed at 40 cm/s (P=0.191; Fig. 21E). Swing time of HOP gait did not differ significantly between conditional and full *EphA4* mutant mice (P=0.534). At 40 cm/s, solely the forelimb swing time of wild types was significantly decreased in comparison to 16 cm/s (P=0.049; Fig. 21F).

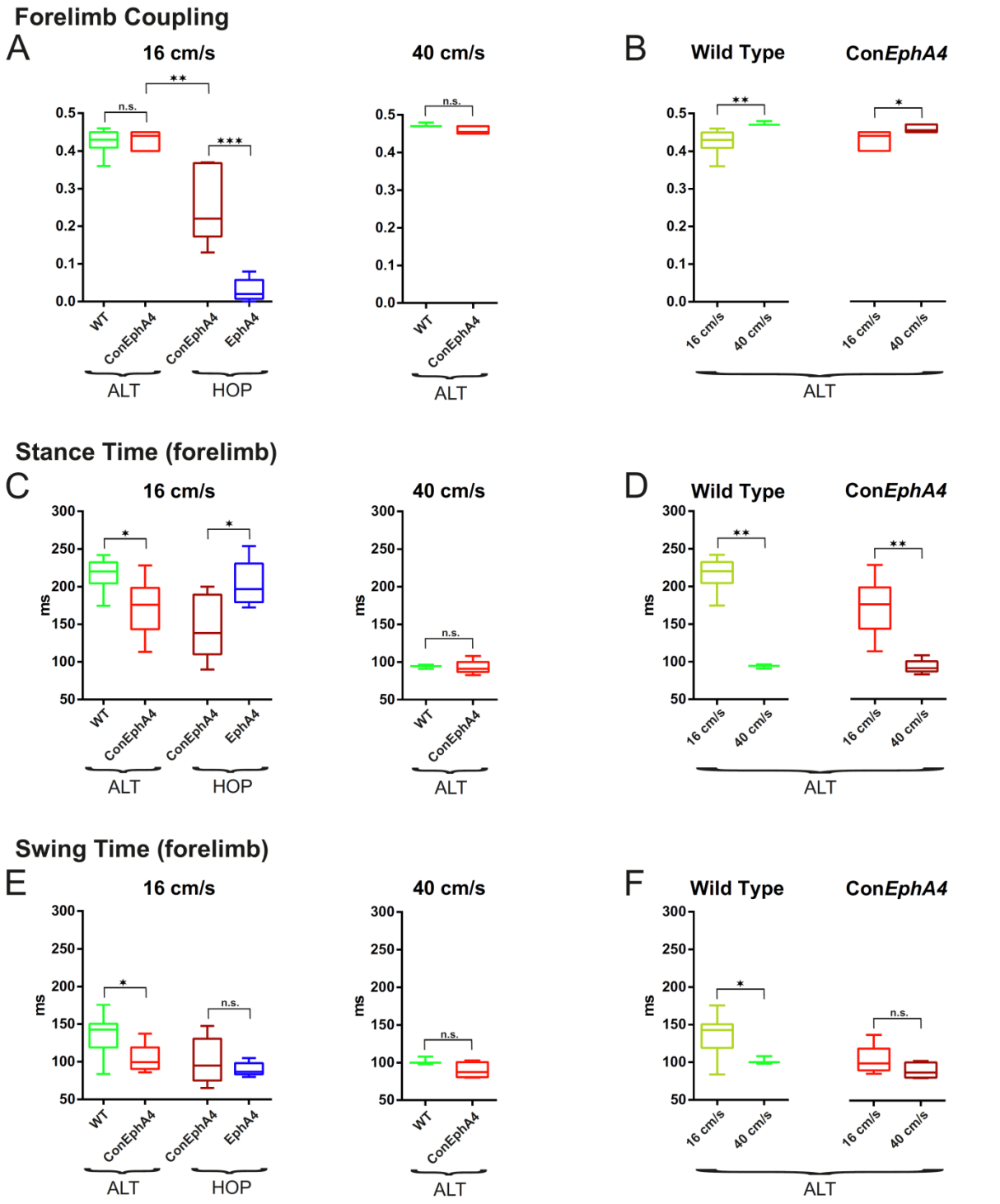

Figure 21. Forelimb gait parameters of ALT and HOP gait on TreadScan

A: Forelimb coupling is calculated by the time difference between both forelimbs starting the stance phase. Forelimbs of wild type and conditional *EphA4* mutants with Alt gait were close to out-of-phase coupling (values of 0.05) whereas the forelimbs of full *EphA4* mutant mice were close to in-phase (values of 0.0). The values of the conditional *EphA4* mutant with HOP gait were lying in between. B: At higher speed of 40cm/s, forelimb coupling approximated the value of 0.5 in wild type and conditional *EphA4* mutant mice. C and E: Comparison of the stance and swing phase time of the right forelimb between genotypes with the same gait type, ALT or HOP, at 16 and 40 cm/s. D and F: Stance and swing time were compared between 16 and 40 cm/s within the same genotype, wild type and conditional *EphA4* mutant. All values are given for the right forelimb. Box and whisker plots. Values were compared by a Mann Whitney rank sum test (significant difference when $P<0.05$).

Summarizing the gait parameter analysis, the different parameters of ALT gait in conditional *EphA4* mutant mice resembled mainly the ones of wild type mice with exception of a reduced swing time and, thereby, an increased stride frequency of conditional *EphA4* mutants. In contrast, HOP gait parameters of conditional *EphA4* mutant mice differed significantly in most of the cases to the HOP gait of full *EphA4* mutants. HOP gait of conditional *EphA4* mutants showed a less synchronous hindlimb movement, a decreased hindlimb track length and decreased hindlimb stance time than it was found in the full *EphA4* mutants. That meant, HOP gait of hindlimbs in conditional *EphA4* mutants was neither alternating nor completely synchronized revealed by the hindlimb coupling parameter and, therefore, could be separated as another gait type. This finding was in accordance with the gait type classification as we distinguished the HOP gait of conditional *EphA4* mutants into MIX gait and the one of full *EphA4* mutants into synHOP gait. The majority of gait parameters changed with an increase in belt speed from 16 to 40 cm/s in wild type and conditional *EphA4* mutant mice. Regarding the overall gait parameter analysis, conditional *EphA4* mutant mice differed mainly to full *EphA4* mutants but also showed a reduced swing time in comparison to wild type mice. This implies that swing phase and, thereby, flexor muscles were affected in the conditional *EphA4* mutant.

Moreover, the coordination between hindlimbs resembled the coordination between forelimbs in wild type, conditional and full *EphA4* mutant mice. Forelimbs showed a less alternating coordination when the hindlimbs walked with HOP gait. A shorter forelimb stance time in conditional *EphA4* mutant mice walking with HOP gait was found compared to full *EphA4* mutants. Furthermore, we revealed a reduced forelimb swing time of conditional *EphA4* mutants with both ALT and HOP gait compared to wild type and full *EphA4* mutants, respectively. Taken together, the gait of forelimbs was additionally affected to the gait of hindlimbs when Lbx1-expressing cells lack the EphA4 receptor in the spinal cord.

3.1.3 No difference in open field behavior of conditional *EphA4* mutants compared to wild type mice

In an open field behavior test, we wanted to investigate whether conditional *EphA4* mutant mice would show a difference in locomotion activity when walking freely for a certain time in comparison to wild type mice. Therefore, wild type and conditional *EphA4* mutant mice were placed in an open field box for ten minutes while the trajectory was measured (Fig. 22A). The average velocity was calculated and resulted in no significant difference between wild type and conditional *EphA4* mutant mice (Fig. 22B; [median: WT: 7.9 cm/s; Con*EphA4*: 6.62 cm/s]; P=0.352; see also Tables 1.12 and 2.11). Likewise, no significant difference was found for the total track length after ten minutes (Fig. 22C; [median: WT: 47.44 m; Con*EphA4*: 39.68 m]; P=0.352). In summary, conditional *EphA4* mutant mice exhibited a comparable locomotion activity to wild type mice during free locomotion.

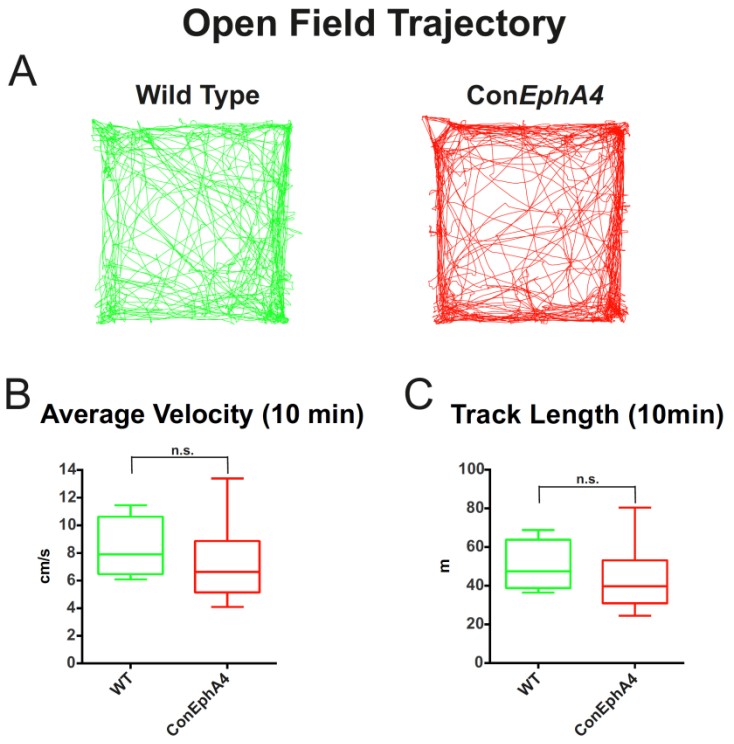

Figure 22. Open field

A: Example trajectories of one wild type and conditional *EphA4* mutant during 10 minutes in an open field box. B and C: Average velocity and total track length during 10 minutes did not differ significantly between adult wild type and conditional *EphA4* mutant mice. Values were compared by a Mann Whitney rank sum test (significant difference when P<0.05).

3.2 HOP and ALT gait of conditional *EphA4*$^{flox/-}$*vGAT*$^{Cre/+}$ mutant mice

Previous studies revealed that ipsilateral excitatory interneurons are misguided across the spinal midline and caused the hopping gait in the full *EphA4* mutant (Kullander 2003; Restrepo 2011). In addition, inhibitory spinal neurons were shown to be essential in left-right alternation (Kiehn 2010; Kiehn 2011; Talpalar 2011) and some inhibitory interneurons also express EphA4 (Lundfald 2007; Restrepo 2011). Therefore, we aimed to investigate a possible role of inhibitory neurons in the aberrant gait behavior of the full *EphA4* mutant mice. Moreover, some of Lbx1-positive neurons, we examined in the conditional *EphA4* mutant, express inhibitory neurotransmitter in the spinal cord (Cheng 2005; Alaynick 2011). Therefore, we obtained two adult conditional *EphA4*$^{flox/-}$*vGAT*$^{Cre/+}$ mutant mice. In those mutants, the EphA4 receptor was deleted in all inhibitory neurons, GABAergic and glycinergic cells, since vGAT (vesicular GABA transporter) is highly concentrated in the nerve endings of GABAergic but also of glycinergic neurons in the spinal cord (Todd 1990; Chaudhry 1998).

The two conditional *EphA4*$^{flox/-}$*vGAT*$^{Cre/+}$ mutant mice were tested on the TreadScan at different belt speeds exhibiting mainly synHOP and MIX gait types in addition to some steps of ALT gait (Fig. 23A; see all values in Table 1.13). At higher belt speeds, the two conditional *EphA4*$^{flox/-}$*vGAT*$^{Cre/+}$ mutants tended to increase their frequency of synHOP gait. The number of conditional *EphA4*$^{flox/-}$*vGAT*$^{Cre/+}$ mice will have to be increased for a further statistical analysis and conclusion. The effect on the gait behavior by the deletion of *EphA4* in inhibitory neurons did not result in an almost complete synHOP gait as it was seen in the full *EphA4* mutant mouse (compare Fig. 23A and B). So far, it appears that the correct connection of inhibitory neurons is important for the conversation of left-right alternation.

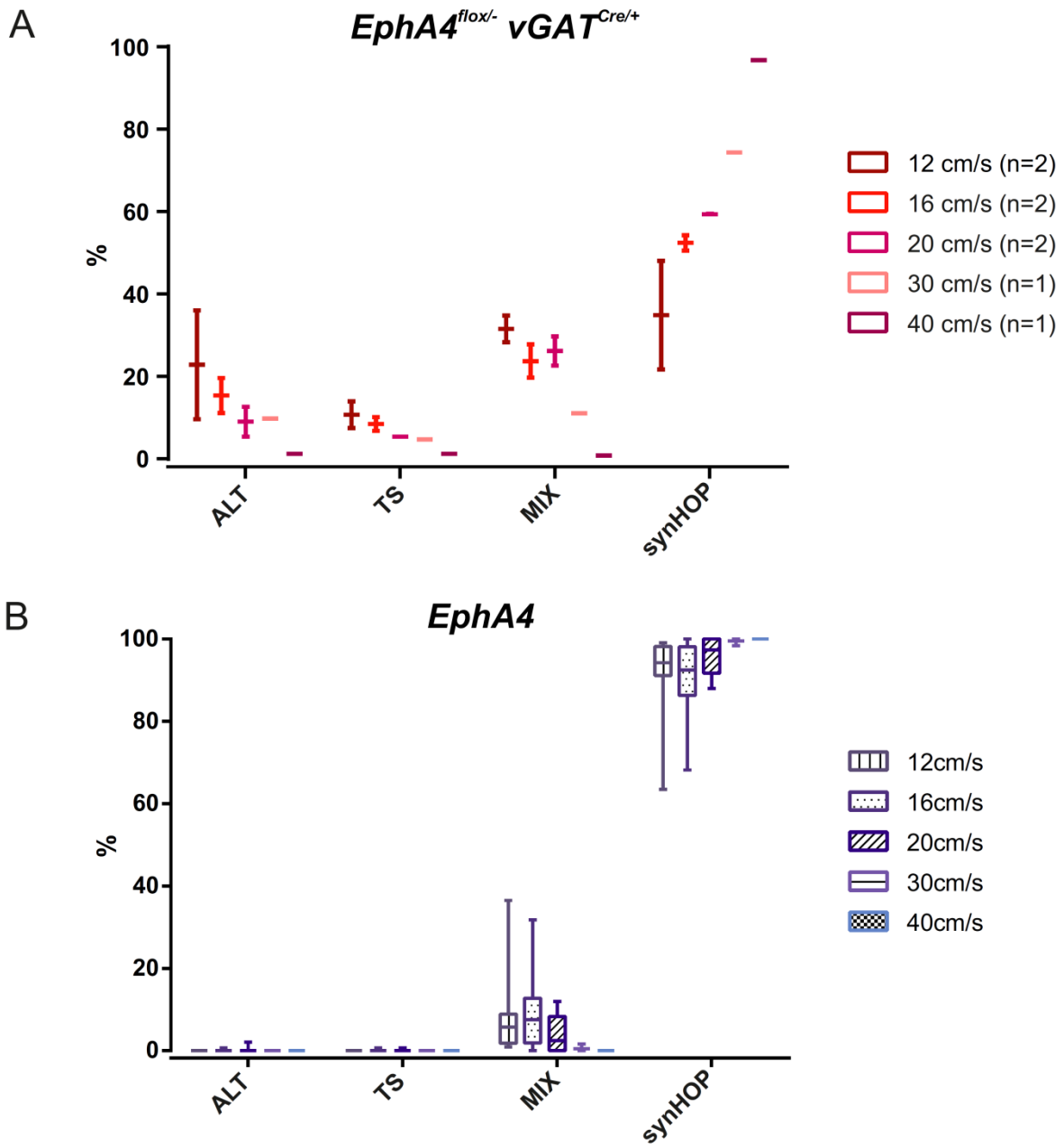

Figure 23. Percentage of gait types during a 20s trial of *EphA4*$^{flox/-}$*vGAT*$^{Cre/+}$ mutant mice on TreadScan

Percentages of ALT, TS, MIX and synHOP gait types at belt speeds of 12, 16, 20, 30, 40 and 50 cm/s of two conditional *EphA4*$^{flox/-}$*vGAT*$^{Cre/+}$ mutant mice (A) in comparison to the full *EphA4* mutant (B).

3.3 Conditional *α2chimaerin* (*α2chimaerin*$^{flox/-}$*Lbx1*$^{Cre/+}$) mutant mice

Previous studies showed that α2chimaerin is a downstream effector of the EphA4 receptor (Beg 2007; Iwasato 2007; Wegmeyer 2007). Deletion of the *α(2)chimaerin* gene in mice resulted in similar anatomical and gait behavioral phenotypes as it was observed for full *EphA4* mutant mice; a hopping gait and aberrant misguidance of numerous fibers across the midline of the spinal cord in comparison to wild type mice were revealed (Dottori 1998; Kullander 2001a; Yokoyama 2001; Kullander 2003; Beg 2007; Iwasato 2007; Wegmeyer 2007). In addition to the conditional *EphA4* mutant, we therefore wanted to study the conditional *α2chimaerin* mutant mouse whose Lbx1-expressing neurons lack the *α2chimaerin* gene. We assumed similar anatomical and gait behavioral phenotypes as it was seen in conditional *EphA4* mutant mice.

3.3.1 No difference in premotor interneuron distribution between conditional *α2chimaerin* mutants and wild type mice

To start with, we wanted to investigate the premotor interneuron distribution in conditional *α2chimaerin*$^{flox/-}$*Lbx1*$^{Cre/+}$ mutant mice. Because of simplicity, I will use the abbreviation “conditional *α2chimaerin* mutant” in the following chapters. Conditional *α2chimaerin* mutant mice of postnatal age P5-7 were injected with rabies GFP complemented by AAV glycoprotein in the Q muscle. In the conditional *α2chimaerin* mutant mouse, the dorsal funiculus displayed a long and narrow shape resembling the one of wild type mice (Fig. 24A-C; mean of ratios in Table 1.1; [dorsal funiculus: P=0.32; dorsal gray matter: P=0.24]; see also Table 2.1). Moreover, premotor interneuron distribution pattern as transverse projection (Fig. 24D) and its contour plot (Fig. 24E) of conditional *α2chimaerin* mutant mice revealed no obvious difference compared to that of wild type mice. In two density plots of the transverse projection and of the contralateral side in Figure 24F and G, the peaks of density in the three conditional *α2chimaerin* mutants overlapped with the ones of the four wild type mice. Percentages of the premotor interneuron distribution were calculated by subdividing the spinal cord into four parts (dorsal ipsilateral, dorsal

contralateral, ventral ipsilateral and ventral contralateral) (Fig. 24H). The median values of interneuron percentages in the four spinal cord quadrants showed comparable values between conditional *α2chimaerin* mutants and wild type mice (median of % dorsal contralateral cells [WT: 3.45; Con *α2chimaerin*: 3.42]; see all median values in Table 1.2). No significant difference of the interneuron percentage in the contralateral spinal cord between conditional *α2chimaerin* mutant and wild type mice was found by applying the Mann Whitney rank sum test ($P > 0.9999$, statistically significant when $P<0.05$; see also Table 2.2).

In summary, deletion of the EphA4 effector, *α2chimaerin*, in Lbx1-expressing neurons resulted in no aberrant anatomical phenotype in the spinal cord resembling, therefore, wild type mice.

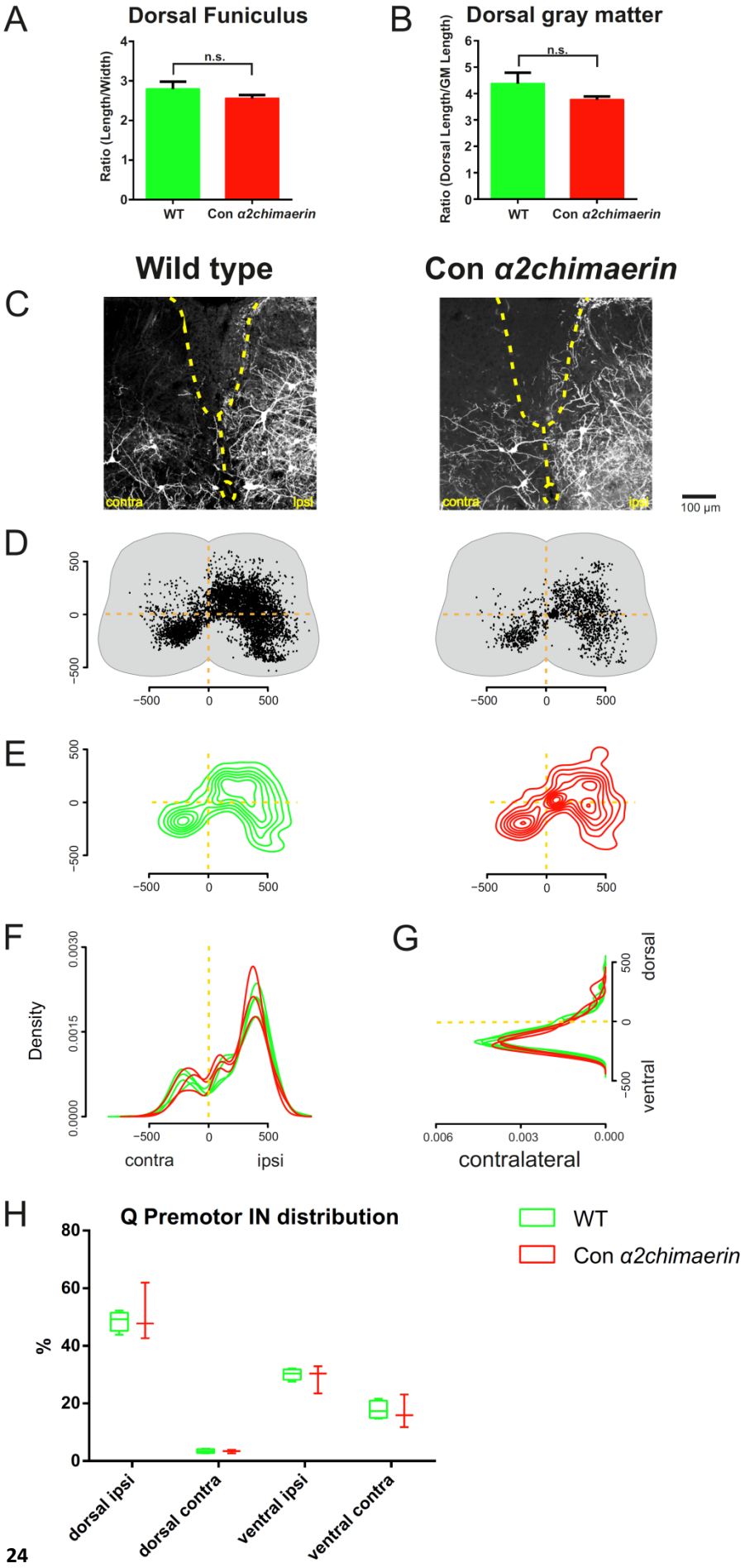
A
Dorsal Funiculus
Ratio (Length/Width)
n.s.
WT
Con α2chimaerin
B
Dorsal gray matter
Ratio (Dorsal Length/GM Length)
n.s.
WT
Con α2chimaerin
Wild type
Con α2chimaerin
C
contra
ipsi
100 µm
D
E
F
Density
contra
ipsi
G
dorsal
ventral
contralateral
H
Q Premotor IN distribution
WT
Con α2chimaerin
%
dorsal ipsi
dorsal contra
ventral ipsi
ventral contra

Figure 24

Figure 24. Premotor interneuron distribution of Q motor neurons in comparison between wild type and conditional *α2chimaerin* mutant mice

A: The ratio of the dorsal funiculus (length/width) of conditional *α2chimaerin* mutants was comparable to the one of wild type mice. B: Likewise, the ratio of the dorsal gray matter of conditional *α2chimaerin* mutant mice did not differ significantly in comparison to wild type mice. C: Confocal photos (20x) of the dorsal spinal cord in the lumbar segment of rabies-infected premotor interneurons in the conditional *α2chimaerin* mutant and wild type. Quadriceps was specifically injected. Note the similar shapes of the dorsal funiculus of wild type and conditional *α2chimaerin* mutant indicated by the yellow dotted line. D: Premotor interneuron distribution patterns from T11 to S1 segments were comparable between wild type and conditional *α2chimaerin* mutant. E: Contour plots of interneuron distribution. F: Density plots of the ipsi- and contralateral side of the spinal cord of wild type and conditional *α2chimaerin* mutant mice. G: Density plot of the contralateral side comparing distribution densities between wild type (n=4) and conditional *α2chimaerin* mutant (n=3) mice. H: Box and whisker plot showing percentages of interneurons in the four quadrants of the spinal cord. No significant difference in the percentages of interneurons in the dorsal contralateral and ventral ipsilateral side was found by a Mann Whitney rank sum test (significant difference when $P<0.05$). Scale in µm.

3.3.2 No difference in gait behavior between conditional *α2chimaerin* mutants and wild type mice

Furthermore, we investigated the gait behavior of conditional *α2chimaerin* mutant mice on the TreadScan apparatus. Full *α2chimaerin* mutant mice were also examined as a full knockout control. Since we have not seen any anatomical phenotypes in the conditional *α2chimaerin* mutant, we therefore assumed to find no gait behavioral defects. In agreement with our expectations, the conditional *α2chimaerin* mutant mice displayed mainly an alternating gait. However, the full *α2chimaerin* mutant showed MIX and ALT gait types additionally to synHOP gait (Fig. 25).

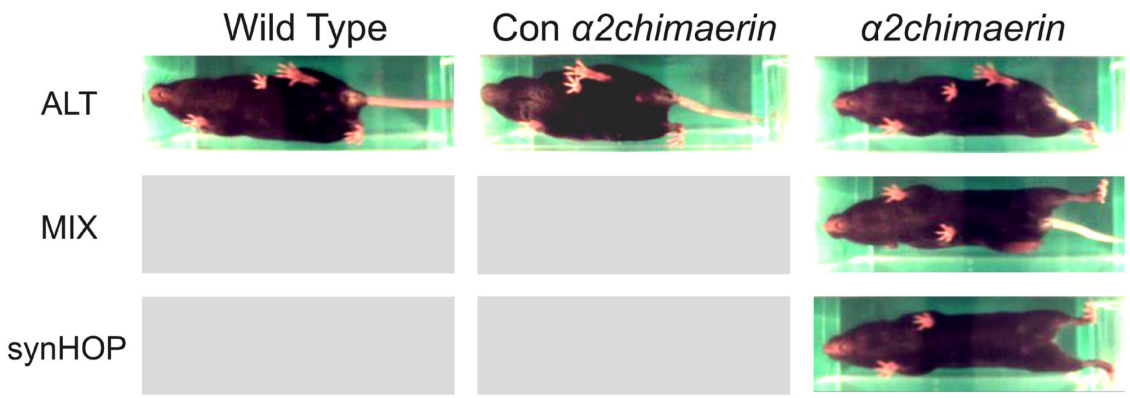

Figure 25. Gait types of wild type, conditional and full *α2chimaerin* mutant mice

Wild type and conditional *α2chimaerin* mutant mice walked exclusively with ALT gait. In contrast, full *α2chimaerin* mutants displayed additionally to ALT gait, MIX and synHOP gait. Pictures on TreadScan at belt speed of 16cm/s.

In a detailed gait type analysis, the percentages of ALT, TS, MIX and synHOP gait types per trial are illustrated according to the gait classification (see chapter 3.1.2.1) as box and whisker plots (Fig. 26). The percentages of the four gait types in the conditional *α2chimaerin* mutants resembled the one of wild type mice at belt speeds of 12, 16 and 20 cm/s since the majority of steps consisted of ALT gait type (Fig. 26 A and B; all median values see Table 1.14). In the conditional *α2chimaerin* mutant mice, hardly any MIX and synHOP gait types were observed. On the contrary, in the full *α2chimaerin* mutant, mainly synHOP gait but in addition a high frequency of MIX and ALT gait types were found at all three tested belt speeds (Fig. 26 C; median values see Table 1.15).

In a further statistical analysis, MIX and synHOP gait types were pooled together as HOP gait (see all median values in Table 1.16). Percentages of HOP gait were compared between the speeds within each genotype of wild type, conditional and full *α2chimaerin* mutant mice by a Kruskal Wallis rank sum test. No significant difference was found between 12, 16 and 20 cm/s within each of the three genotypes (WT: P=0.057; Con *α2chimaerin*: P=0.797; *α2chimaerin*: P=0.307; see also Table 2.12). Moreover, HOP gait was compared between the genotypes within one speed by a Kruskal Wallis rank sum test and resulted in an overall significant difference between all three genotypes at 12 (P=0.0024), 16 (P=0.0007) and 20 cm/s (P=0.0002) (Fig. 27). In a further post-hoc pairwise Wilcoxon test, no significant difference was found in the frequency of HOP gait between conditional *α2chimaerin* mutants and wild type mice at all three belt speeds (Table 2.13). In contrast, the frequency of HOP gait in the full *α2chimaerin* mutant was significantly increased in comparison to conditional *α2chimaerin* mutant and wild type mice at all tested speeds (Fig. 27, Table 2.13). Taken together, the gait type analysis of conditional *α2chimaerin* mutants showed no overall difference in gait behavior in comparison to wild type mice.

In summary, against our expectations in the beginning of this study, conditional *α2chimaerin* mutant mice did not display similar anatomical and gait behavioral phenotypes as we have found in the conditional *EphA4* mutant. Interestingly, the full *α2chimaerin* mutant exhibited no constant hopping gait as it was seen in the full *EphA4* mutant (Wegmeyer 2007; Asante 2010).

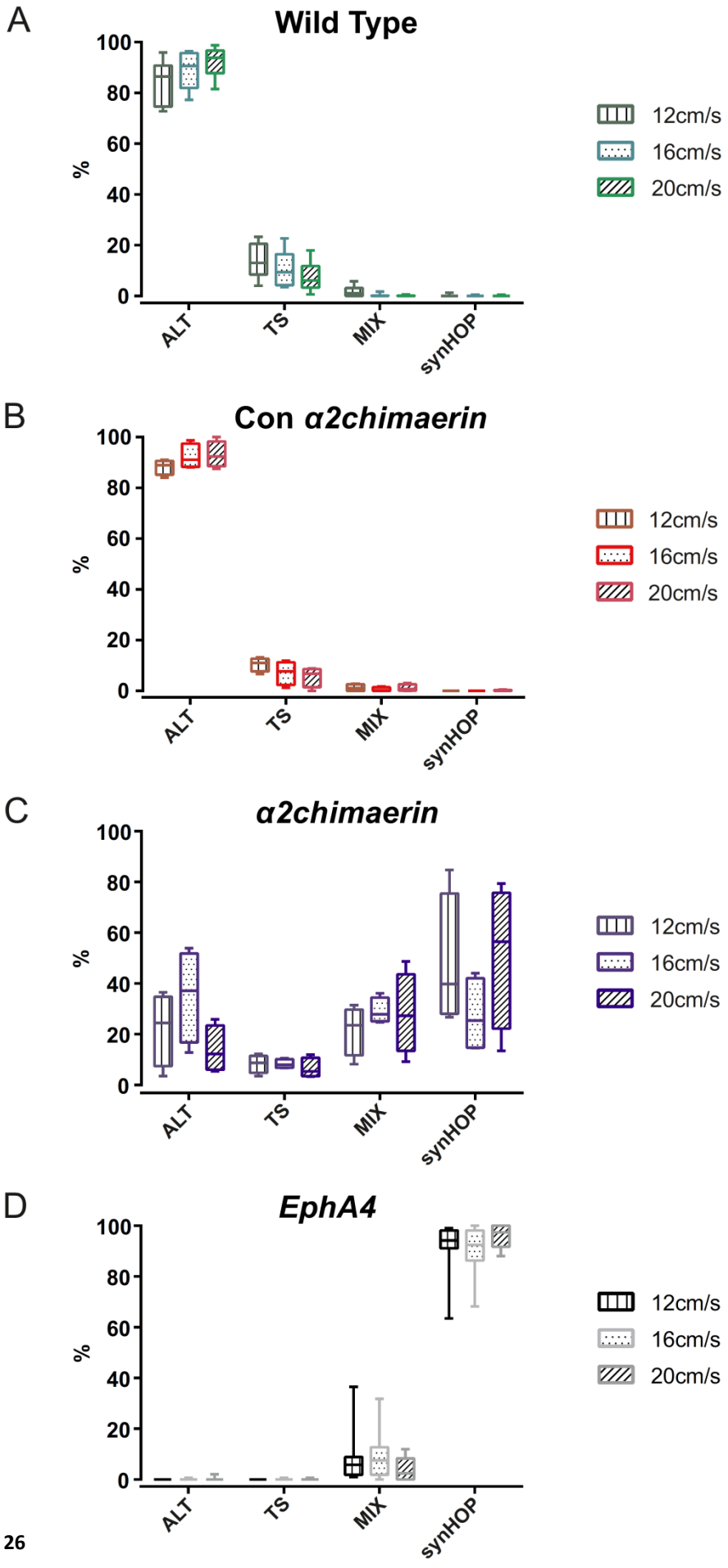
A
Wild Type
B
Con α2chimaerin
C
α2chimaerin
D
EphA4
%
100
80
60
40
20
0
ALT
TS
MIX
synHOP
12cm/s
16cm/s
20cm/s

Figure 26

Figure 26. Percentage of gait types during a 20s trial of adult wild type, conditional and full *α2chimaerin* mutant mice

Box and whisker plots showing percentages of ALT, TS, MIX and synHOP gait types at belt speeds of 12, 16 and 20 cm/s on the TreadScan of adult wild type (A), conditional (B) and full *α2chimaerin* (C) mutants in comparison to the full *EphA4* mutant mouse (D).

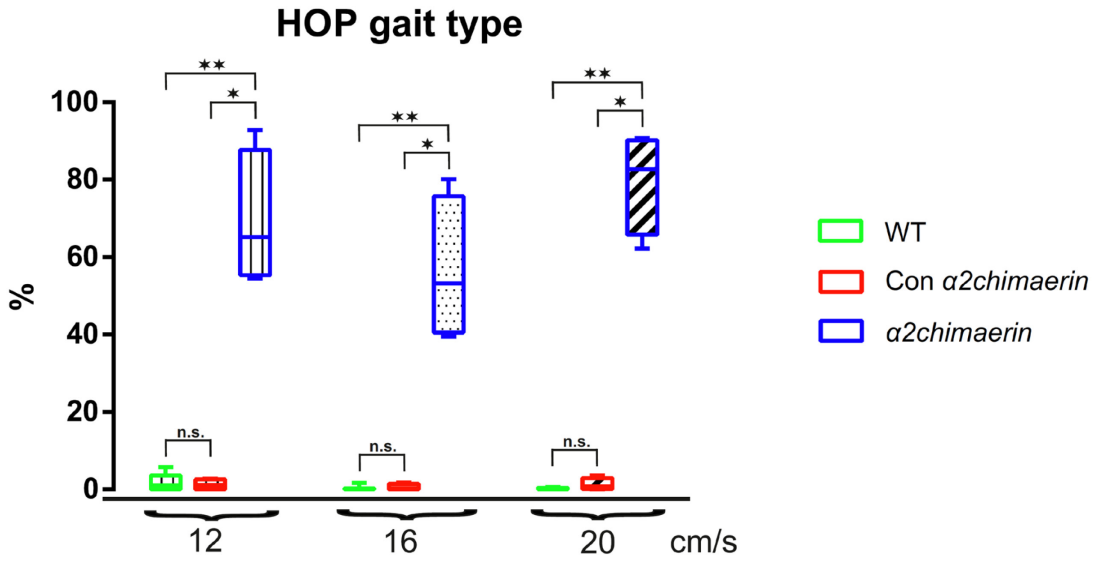

Figure 27. Comparison of HOP gait frequency between wild type, conditional and full *α2chimaerin* mutant mice

In the full *α2chimaerin* mutant, frequency of HOP gait was significantly increased in comparison to wild type and conditional *α2chimaerin* mutant mice at all tested speeds. No significant difference was found between wild type and conditional *α2chimaerin* mutants. Box and whisker plot. Kruskal Wallis rank sum test was performed with a post-hoc paired Wilcoxon test (significant difference when FDR<0.05).

3.3.3 Less frequency of HOP gait in full *α2chimaerin* mutant mice compared to full *EphA4* mutants

Since full *α2chimaerin* mutants did not always performed synchronous hindlimb movements, we therefore wanted to directly compare the frequency of hopping gait between full *α2chimaerin* and full *EphA4* mutant mice. Applying a Mann Whitney rank sum test, the percentage of HOP gait per trial was significantly decreased in the full *α2chimaerin* mutant compared to the full *EphA4* mutant mouse at 12, 16 and 20 cm/s (Fig. 28A, P values see Table 2.14, median values see Table 1.16). In addition, the frequency of synHOP gait was statistically tested in order to observe a possible difference in synchronous hindlimb movement between both full mutants. Likewise, the full *EphA4* mutant mouse displayed a significantly increased frequency of synHOP gait in comparison to the full *α2chimaerin* mutant at all three tested speeds (Fig. 28B, P values see Table 2.14).

In summary, the gait behavior phenotype in full *α2chimaerin* mutants showed less synchronous hindlimb movements compared to full *EphA4* mutant mice. Despite the deletion of solely one of the EphA4 effectors, α2chimaerin, the animal was still able to maintain the performance of some alternating steps (Wegmeyer 2007; Asante 2010). In contrast, the deletion of the entire EphA4 receptor resulted in a complete loss of alternating locomotion (Akay 2006).

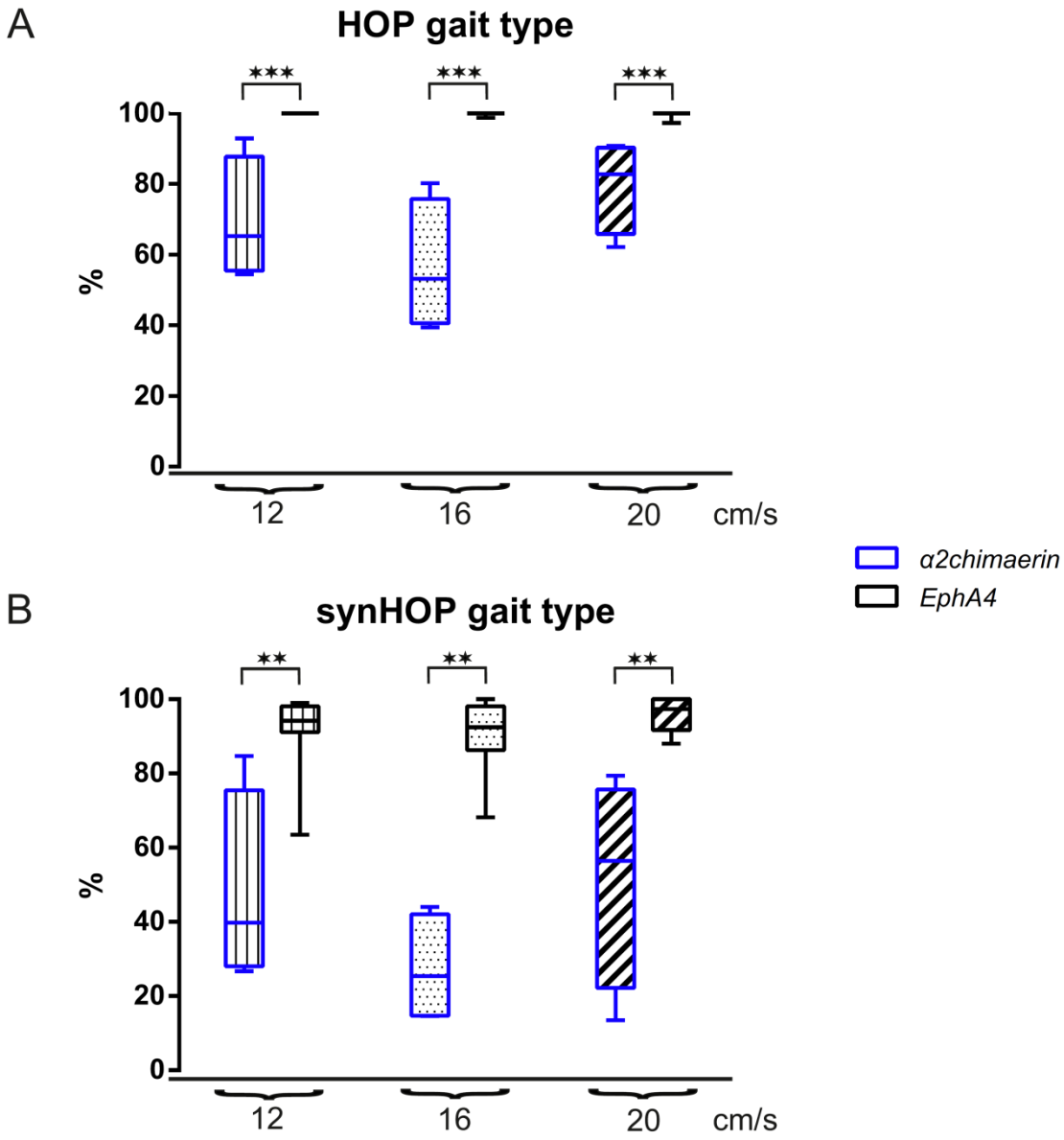

Figure 28. Comparison of HOP and synHOP gait frequency between full *α2chimaerin* and full *EphA4* mutant mice

A: Frequency of HOP gait was significantly decreased in full *α2chimaerin* mutants in comparison to full *EphA4* mutant mice at 12, 16 and 20 cm/s. B: Likewise, full *α2chimaerin* mutants showed a significant lower frequency in synchronous hindlimb movement compared to full *EphA4* mutants at all tested speeds. Box and whisker plots. Values were compared by a Mann Whitney rank sum test (significant difference when $P<0.05$).

4. Discussion

First work describing an abnormal hopping gait in full *EphA4*$^{-/-}$ and *ephrinB3*$^{-/-}$ mutant mice proposed that the abnormal gait was the result of an aberrantly recrossing of corticospinal tract fibers across the spinal midline (Dottori 1998; Kullander 2001a). However, following tracing experiments combined with fictive locomotion of isolated spinal cords showed that the hopping gait in the full *EphA4* mutant is the consequence of aberrantly midline-crossing axons from excitatory ventral spinal neurons that normally project ispilaterally (Kullander 2003; Butt 2005; Restrepo 2011). Further studies in the spinal cord by means of cell-ablation and genetic markers revealed that ventral subpopulations but also dorsally derived neurons play a role in coordinating locomotion (Pierani 2001; Lanuza 2004; Wilson 2005; Gosgnach 2006; Lundfald 2007; Crone 2008; Zhang 2008; Rabe 2009; Andersson 2012; Paixao 2013; Talpalar 2013). However, it remained unclear which misguided interneuron subtypes in the spinal cord are involved in the hopping gait of the full *EphA4* mutant mouse and, thereby, playing a role in the locomotor CPG.

In this study, we aimed to understand which subpopulation of spinal interneurons contributes to the misguidance of axons in the full *EphA4* mutant mouse that causes an inbalance between excitation and inhibition across the spinal midline. Here, we examined the premotor interneuron distribution from specific muscles in conditional *EphA4* and *α2chimaerin* mutant mice, in which the *EphA4* receptor or its effector *α2chimaerin* was deleted in Lbx1-expressing neurons, respectively. We also analyzed the gait behavior on a treadmill of the conditional mutant mice and compared their properties with control and full *EphA4* mutants.

First, we have shown that some dorsal Lbx1-expressing interneurons are monosynaptically connected to motor neurons innervating different muscles, including Q, TA and GS, at P13-15. Second, we revealed that axons of dorsal Lbx1-positive neurons aberrantly cross the spinal midline and innervate contralateral motor neurons in conditional *EphA4* mutant mice whose Lbx1-positive cells lack the EphA4 receptor. Third, a deletion of *EphA4* in Lbx1-expressing cells resulted in a slight aberrant HOP gait of hindlimbs at higher speeds of 3-week old and at lower speeds of adult conditional *EphA4* mutant mice. Fourth, the conditional *EphA4* mutant, either walking with ALT or HOP gait, exhibited a shorther

swing time compared to wild type mice suggesting a defect of flexion muscle innervations. Therefore, we assume a minor involvement of the Lbx1-expressing subpopulation in pattern and rhythm generation. Fifth, the gait of forelimbs was additionally affected in the conditional *EphA4* mutant and ranged between alternating and synchronous coordination of both forelimbs. Sixth, a deletion of the *EphA4* receptor in inhibitory neurons of the conditional $EphA4^{flox/-}vGAT^{Cre/+}$ mice resulted in a partial synHOP gait in addition to ALT gait. Seventh, the ablation of *α2chimaerin*, an EphA4 effector, in Lbx1-expressing neurons in conditional *α2chimaerin* mutants showed no overall difference in premotor interneuron distribution and in gait behavior in comparison to wild type mice. Eighthly, the full *α2chimaerin* mutant displayed a partial HOP gait beside ALT gait and, thereby, differs to the full *EphA4* mutant that showed a complete loss of ALT gait.

4. 1 Premotor interneuron distribution of conditional and full *EphA4* mutant mice

4.1.1 Variability of the premotor interneuron distribution in the full *EphA4* mutant

As a first approach to address our question, we started to investigate the premotor interneuron distribution of the full *EphA4* mutant mice. Surprisingly, we found a high variability in the distribution of premotor interneurons in the full *EphA4* mutant: while some mutant animals displayed a wild type distribution, others showed a significant increase of premotor neurons specifically in the dorsal contralateral spinal quadrant to the injection (% dorsal contralateral cells [full *EphA4*: 24.85, 8.1, 6.22, 4.59, 4.45, 4.16, 4.12]). There are several possible explanations for this finding. First, growing axons respond to a variety of different repulsive and attractive guidance cues during their migration and the axons themselves activate and deactivate various receptors at different time points (Dodd 1988; Kidd 1998; Imondi 2000). Some axons, missing the EphA4 receptor, might receive stronger attractive guidance cues and they migrate towards the correct direction, whereas other axons are less attracted and, therefore, directed towards the midline where they migrate in the contralateral side. Second, additionally to the misguided axons in the full *EphA4* mutant,

the cell position of various neurons might be aberrant since it was previously shown that cell bodies of migrating interneurons follow their axons (Marin 2010; O`Leary 2011). Paixao et al. (2013) revealed a relocation of dorsal interneurons in the spinal cord lacking the *EphA4* receptor. A shift of the dorsal cell position might lead to different innervations from other neurons due to competition and various interactions between the neurons resulting in a variety of aberrant networks. Another study by Coonan et al. (2001) in the full *EphA4* mutant described a ventral displacement of the termination zone of corticospinal tract axons in the spinal cord due to missing expression of *EphA4* in the intermediate zone. Corticospinal tract fibers might, therefore, innervate other neurons located more ventrally in the spinal cord. Lastly, even though animals were regenotyped several times, one should consider the possibility that some of the analyzed mice might in fact not have been bona fide mutants by genotype.

In general, full *EphA4* mutants are a difficult model to study the effect of *EphA4* receptor deletion, since *EphA4* is expressed in the entire body (Greferath 2002). In full *EphA4* mutants, descending tract fibers from the cortex are affected (Dottori 1998; Coonan 2001; Egea 2005; Canty 2006); certain motor neuron pools innervating specific muscles of the hindlimb are caudally displaced (Coonan 2003) and, additionally, the projection of motor neurons towards the muscles are misguided (Helmbacher 2000). Given the variety of defects in the full *EphA4* mutant, it would be difficult to link neuronal circuit properties to behavioral defects. This is the reason why we decided to study the connectivity and motor behavior of conditional *EphA4* mutant mice instead where an assignment of cell types to phenotypes will be cleaner than in the full mutant mouse strain.

4.1.2 Wider shape of the dorsal funiculus in full and conditional *EphA4* mutant mice

Previous studies reported that the dorsal funiculus in the full *EphA4* mutant exhibited a wider and broader shape in contrast to wild type mice (Dottori 1998; Kullander 2001b; Restrepo 2011; Paixao 2013; Borgius 2014). For this reason, we decided to quantify the shape of the dorsal funiculus in the conditional *EphA4* mutant and compared it with wild type and full mutant mice. We found that the dorsal funiculus in the conditional *EphA4*

mutant mice showed a similar wide shape compared to full *EphA4* mutants. Our findings are in agreement with the study of Paixao (2013), who revealed that removal of *EphA4* specifically from the dorsal spinal cord neurons affected the dorsal funiculus morphology. Specifically, they showed that in full and conditional *EphA4* mutants, axons from a subpopulation of Lbx1 neurons (dIL_B - Zic^{2+} neurons), which normally project into the ascending tract of the dorsal funiculus, instead cross the dorsal midline and their cell bodies relocate to a more medial position leading to a gap between the ephrinB3-expressing midline cells and the ventral tip of the dorsal funiculus. They suggested that crossing axons and cells at medial positions might prevent the dorsal funiculus from extending more ventrally. Moreover, in another study of Restrepo et al. (2011), an intercalated cell position of inhibitory and excitatory neurons in the dorsal commissure was reported in the full *EphA4* mutant. From previous studies and our own findings, we conclude that the misguidance of dorsal Lbx1-expressing neurons cause the shortening of the dorsal funiculus.

4.1.3 Premotor interneuron distribution in conditional *EphA4* mutants

The monosynaptic rabies tracing approach allowed the visualization of premotor interneurons from specific muscles in the spinal cord. Taking advantage of this technology, we demonstrated that the conditional *EphA4* mutant exhibited an aberrant increase of premotor interneurons localized in the dorsal contralateral part of the spinal cord independently of the injected muscle (Q, TA or GS). The distribution pattern in the dorsal contralateral side of TA and GS premotor interneurons confirmed our findings of the Q premotor interneuron distribution with a low number of animals. Further injections have to be performed to confirm this finding and allow a statistical comparison with wild type and full *EphA4* mutant mice. The same change in the premotor distribution pattern was found when Q muscle was injected in some of the full *EphA4* mutants, further supporting our findings. In addition, we showed that most of the ectopic dorsal contralateral interneurons innervating Q motor neurons express Lbx1. Moreover, in a previous study it was shown that on average 30% of Lbx1-positive cells express *EphA4* and that the number of axons crossing the dorsal midline in conditional *EphA4* mutant mice was doubled compared to control mice

(Paixao 2013). We, therefore, conclude that when dorsal Lbx1-expressing neurons lack the EphA4 receptor, their axons are misguided across the spinal midline and connect to contralateral motor neurons.

Interestingly, the GS premotor interneuron distribution revealed a shift of the percentage of cells in all four parts of the spinal cord in the conditional *EphA4* mutant that was not found in TA injections, indicating that either extensor GS premotor interneurons were misguided more extensively than flexor TA premotor interneurons or alternatively a reduction of the dorsal ipsilateral population raises the ratio of the ventral ipsilateral population. Moreover, the premotor distribution of another extensor motor neuron pool, Q, displayed a tendency to a decrease of neurons in the ventral ipsilateral side. Although more experiments are needed, these results suggest that a different contribution of Lbx1 neuronal subpopulation to flexor or extensor premotor circuits could explain our findings. Importantly, a previous study in the laboratory reported of a medio-lateral segregation of extensor GS and flexor TA premotor interneurons in the ipsilateral dorsal spinal cord of wild type mice where the majority of Lbx1-expressing neurons co-labeled with dorsal GS extensor premotor interneurons (Tripodi 2011). Future experiments could address our hypothesis through the visualization of all Lbx1-expressing neurons using conditional *EphA4* mutant mice containing a lacZ reporter gene (*EphA4*$^{flox/-}$*Lbx1*$^{Cre/+}$*Tau*$^{lox\text{-}stop\text{-}lox\text{-}SynGFP\text{-}INLA}$ and *EphA4*$^{flox/-}$*Lbx1*$^{Cre/+}$*Tau*$^{lox\text{-}stop\text{-}lox\text{-}FlpO\text{-}INLA}$ mutant mice) and its combination with retrograde monosynaptic rabies tracing from specific muscles. With this strategy, it will be possible to elucidate whether together with the aberrant axon guidance, the conditional Lbx1 mutant also shows a relocation of premotor neurons as it was previously reported for the non-premotor dIL_B subpopulation of Lbx1-expressing neurons (Paixao 2013).

4.2 Gait behavior of *EphA4* mutant mice

4.2.1 HOP gait at low frequency locomotion in adult conditional *EphA4* mutant mice

Since we revealed a misguidance of dorsal Lbx1-expressing cells across the midline of the spinal cord innervating contralateral motor neurons, we hypothesized that this anatomical

phenotype might result in a gait behavioral phenotype similar to the synchronous hopping seen in full *EphA4* mutants. We found that adult conditional *EphA4* mutant mice exhibited a milder hopping phenotype compared to full *EphA4* mutants, characterized by a minor increase in HOP gait at lower velocities of 12 to 20 cm/s on the treadmill compared to the absence of HOP gait in wild type mice. Moreover, when we analyzed the gait behavior of full *EphA4* mutant mice, we found that they displayed always HOP gait at all tested speeds, and this finding is in accordance with the detailed behavioral locomotion study of Akay et al. (2006). Previous reports addressed the effect of sectioning either the dorsal or ventral commissure in wild type and *EphA4* mutant mice and revealed an uncoupling of left-right coordination of isolated spinal cords only when the ventral commissure was sectioned (Kjaerulff 1996; Restrepo 2011). These findings are in agreement with our results in the conditional *EphA4* mutant that conserves an alternating gait with only a minor HOP gait.

In our study, the gait on the treadmill per trial was visually analyzed and classified into four gait types, ALT, TS, MIX and synHOP gait, depending on the position of the hind feet on the ground. MIX and synHOP gait were further distinguished by the timing between both hindlimbs when starting into the swing phase as we wanted to discriminate real synchronous hindlimb movement during the entire stride at synHOP gait from a less synchronous movement at MIX gait. During synHOP gait, both hindlimbs move synchronously during swing and stance phase beside the parallel position on the ground. The gait classification is in accordance with hindlimb coupling values obtained in the gait parameter analysis that is only calculating the time difference between both hindlimbs. Both gait classification and gait parameter analysis by TreadScan software revealed that conditional *EphA4* mutants walked with a less synchronous hindlimb movement when walking with HOP gait, whereas full *EphA4* mutants almost always exhibited synchronous hindlimb coupling. This finding suggests that the timing between both hindlimbs is not severly affected in the conditional *EphA4* mutant compared to full *EphA4* mutant mice.

The parallel placement of both hindlimbs during locomotion on the treadmill in the conditional *EphA4* mutant might be evoked directly by possible misguided Lbx1-positive interneurons in the spinal cord or alternatively by an indirect influence of descending fibers or sensory feedback. Importantly, it has been shown that dorsal Lbx1-positive interneurons are mainly co-located with extensor premotor neurons that receive propioceptive input

(Tripodi 2011). However, since conditional mutant mice are able to alternate their limbs while walking at different speeds, we conclude that the network for left-right alternation is still maintained. Therefore, the removal of *EphA4* in Lbx1-expressing neurons might have an effect on pattern generation by changing the network that selects between one or another mode of locomotion.

One important consideration is that by the retrograde monosynaptic rabies tracing method we are only able to visualize interneurons directly connected to motor neurons. Therefore, we cannot exclude that in the phenotype of the minor aberrant HOP gait in the conditional *EphA4* mutant other non-premotor Lbx1-expressing neurons are additionally involved. For example, Lbx1-expressing dIL_B interneurons lacking *EphA4* were reported to be misguided across the midline instead of projecting into the dorsal funiculus (Paixao 2013). In future, the link between crossing axons and partial aberrant gait has still to be proven.

4.2.2 Difference in HOP gait during development in conditional *EphA4* mutants

During development, we observed that 3-week old conditional *EphA4* mutant mice increased their HOP frequency at higher speeds of 30 to 50 cm/s whereas adult mutants showed only an increase in HOP frequency at lower speeds of 12 to 20 cm/s in comparison to wild type mice at according age. Regarding the development until adulthood in each animal, only some animals displayed a tendency for an increase in HOP frequency at higher speeds at the age of 3-weeks and at lower speeds at adulthood. A slightly stronger effect appears to ocurr on the gait behavior in 3-week old conditional *EphA4* mutant mice compared to adults, since the 3-week old mutants performed synHOP gait compared to MIX gait of adult mutants. The position of the hindlimbs is affected at both stages but the timing between the hindlimbs might be stronger affected in 3-week old mutant mice. Preliminary observations in the laboratory of neonatal conditional *EphA4* mutant mice performing swimming showed an uncoordinated hindlimb movement in comparison to alternating movements in wild types (Satoh et al., unpublished finding). Our findings suggest a compensation of uncoordinated hindlimb locomotion from neonatal age until adulthood which might be possible due to a remodulation of misguided axons of Lbx1-expressing

neurons in the spinal cord or by interaction from descending tracts originating in the hindbrain of the conditional *EphA4* mutant. Hence, Lbx1-positive cells might be involved in controlling the speed and could be a component of the rhythm generation. It has been shown that ipsilaterally projecting dI6 interneurons located close to the central canal oscillate intrinsically and, therefore, are thought to be involved in rhythm generation (Dyck 2012).

Wild type (C57BL/6) mice are indeed able to perform synchronous hindlimb movement but only under certain circumstances when achieving a high velocity as during flight response (Serradj 2009). The authors reported of a gait transition period from alternating to synchronous hindlimb movement at high speeds of locomotion, between 70 and 90 cm/s. In our study, conditional *EphA4* mutant mice switch the gait within the same speed on the treadmill and within the same trial. Previous models have suggested two different CPG networks, one for alternation, the other for synchronous hindlimb locomotion in the spinal cord (Kiehn 2010; Rybak 2013). The question remains how the switch between the two different networks occurs. Previous work in rat and decerebrate cat showed that with an increase of stimulation intensity in the mesencephalic locomotor region and the medioventral medulla, a transition from walk over trot to gallop (hopping) can be evoked (reviewed in Grillner (1975); (Atsuta 1990)). Furthermore, Lbx1 is also expressed in several nuclei of the hindbrain (Sieber 2007; Pagliardini 2008). An involvement of descending hindbrain tracts in the spinal cord cannot be excluded and further recordings from isolated spinal cords will have to be performed in future.

4.2.3 Reduced swing time in conditional *EphA4* mutants

In a detailed behavioral locomotion study of full *EphA4* mutant mice, a significantly decreased swing time and swing amplitude was reported in comparison to wild type mice (Akay 2006). This finding is in accordance with the results from our gait parameter analysis showing a reduced swing time in conditional and full *EphA4* mutant mice walking with a HOP gait (not statistically tested in comparison to wild type). However, we also observed a significantly decreased swing time in the conditional *EphA4* mutant walking with ALT gait

compared to wild type indicating that flexor muscles, which are mainly active during swing phase, are affected (Shik 1976).

In a previous study by Tripodi et al. (2011), it was demonstrated that the Lbx1-expressing neurons reside in the extensor and flexor premotor interneuron distribution pattern even if there was a distribution bias towards extensor population. Hence, it might be a possible explanation that Lbx1-expressing neurons are involved in the timing of flexion and extension. Future kinematic analysis of the joints would help to understand further locomotor differences of conditional *EphA4* mutants compared to wild type mice.

4.2.4 Coupling between fore- and hindlimbs in conditional *EphA4* mutants

In our gait parameter analysis, the coordination between hindlimbs resembled the one between forelimbs of ALT and HOP gait in wild type, conditional and full *EphA4* mutant mice (not statistically tested). Furthermore, the swing time of the forelimb in the conditional *EphA4* mutants was significantly decreased compared to wild type as it was seen for the hindlimbs. This finding indicates that the gait of forelimbs was also affected by the removal of *EphA4* in Lbx1-expressing neurons. This observation might be due to an independent change in the network of the cervical spinal cord by the deletion of *EphA4* or, alternatively, the reason might be coordination between fore- and hindlimbs as it was previously reported (Juvin 2005). Their findings in newborn rat revealed an interconnection of locomotor CPG via propiospinal tracts from rhythmogenic lumbar to cervical cord. They showed that an evoked synchronous bilateral lumbar activity induced by synaptic inhibition caused bilateral synchronous activity at the unblocked cervical level (Juvin 2005). On the contrary, behavioral locomotion studies in adult full *EphA4* mutants (Dottori 1998; Akay 2006) and in full *α2chimaerin* mutants (Asante 2010) revealed less synchronous coordination between forelimbs compared to the almost synchronous coordination between hindlimbs. However, in our gait parameter analysis, 9-11 consistent hindlimb steps were selected for an analysis and showed similar phase coupling values as observed for forelimbs. It still remains to be investigated to which extent forelimb gait pattern is coupled to hindlimb gait pattern. Taken together, forelimb gait is also affected in the conditional *EphA4* mutant mice.

4.2.5 Lbx1-expressing neurons in conditional *EphA4* mutants

We have shown that the deletion of *EphA4* in Lbx1-expressing neurons caused anatomical and gait behavioral phenotypes. However, Lbx1 is expressed in dI4, dI5, dI6 and dIL_A and dIL_B interneurons (Gross 2002; Muller 2002). It is highly possible that the different Lbx1-expressing interneuron subtypes exhibit different functions and axonal projection pattern in the spinal cord. In future experiments, it would be interesting to identify which subpopulations of the Lbx1-positive neurons are involved in aberrant axon migration and gait behavior. A first approach might be to identify whether indeed excitatory interneurons are misguided across the dorsal midline in the conditional *EphA4* mutant as it was previously suggested for the full *EphA4* mutant (Kullander 2003; Restrepo 2011). Retrograde monosynaptic rabies tracing combined with immunostaining, *in-situ* hybridization or the use of transgenic animals would help to detect the location of possible co-expression of excitatory (by expression of vGLUT2) and inhibitory (by expression of vGAT, GlyT2 or GAD67) markers with Lbx1-positive neurons.

One interesting Lbx1 subpopulation is the inhibitory dI6 interneurons which are commissural interneurons mainly located in lamina VIII and important for left-right alternation (Gross 2002; Rabe 2009). A deletion of the Dmrt3-expressing subpopulation of dI6 interneurons resulted in an uncoordinated fictive locomotion of neonatal pups (Andersson 2012). Importantly, two dI6 interneuron populations were recently distinguished by their different electrophysiological properties (Dyck 2012). The first dI6 population is thought to be located close to the central canal generating locomotor rhythm together with other cell types in this area and provide input onto the more ventrally located second dI6 population innervating directly motor neurons. The second population is involved in the pattern generation among other cells. These findings suggest that also dorsally derived interneurons contribute to the production of alternating left-right CPG activity and not as previously thought only the ventrally derived interneuron populations (Kjaerulff 1996; Kullander 2003). Since in our study we found that the dorsal Lbx1-expressing neurons are misguided and cross at the level of the dorsal spinal cord, it is possible that the dorsal dI6 subpopulation is affected in the conditional *Eph4* mutant contributing to the partial hopping phenotype.

From the other Lbx1-expressing subpopulations, there is much less anatomical and functional information. The dI5 interneurons are excitatory (Cheng 2004) and although their axonal projection pattern has not been reported, they are thought to be commissural according to their location in the intermediate spinal cord in lamina VIII (Gross 2002; Rabe 2009). Recently, Xu et al. (2013) revealed a subset of dI5 and dIL_B interneurons in laminae I and II which are involved in processing pain-related and itch-related information, as well as to generate the touch-evoked escape response. Moreover, the subset of dI5 neurons located in the deep laminae were suggested to be involved in the processing for sense of innocuous cold and warm (Xu 2013). In summary, dI5 interneurons are likely involved in pain and sensory pathways but a further locomotor function still remains to be investigated.

Finally, the inhibitory dI4 interneurons were shown to develop into association interneurons of the substantia gelatinosa rather than commissural interneurons (Gross 2002; Rabe 2009). Furthermore, it has been revealed that different subsets of Ptf1a-derived dI4 interneurons contact synaptic terminals of cutaneous afferents in the dorsal spinal cord and propioceptive terminals in the ventral horn (Betley 2009). Ptf1a-positive neurons form high selective GABA presynaptic contacts with propioceptive sensory terminals, thereby, filtering sensory signals to motor neurons by presynaptic inhibition (Betley 2009). Given the fact that dI4 neurons are revealed to be ipsilateral interneurons and might express EphA4*,* dI4 interneurons could be involved in the misguided dorsal Lbx1-expressing neurons. It has been shown that some ipsilateral inhibitory neurons in the spinal cord also express EphA4 (Butt 2005; Lundfald 2007). The function of dI4 interneurons and a possible role in locomotor behavior has not yet been investigated.

So far, it remains unclear which subpopulations of Lbx1-positive interneurons are involved in the anatomical and gait behavioral phenotypes in the conditional *EphA4* mutant. In the future, it would be necessary to specifically identify the axonal projection pattern and locomotor function of dI4, dI5 and dI6 interneurons allowing a possible further subclassification in commissural and ipsilateral interneurons.

4.2.6 Gait behavior of conditional *EphA4$^{flox/-}$vGAT$^{Cre/+}$* mutant mice

In previous studies, it was demonstrated that ipsilateral excitatory interneurons in the spinal cord aberrantly cross the midline and cause the hopping gait in the full *EphA4* mutant mouse (Kullander 2003; Restrepo 2011). An ablation of *EphA4* in all excitatory neurons in conditional *EphA4$^{flox/-}$ vGLUT2$^{Cre/+}$* mice was shown to result in a hopping gait at all frequencies of locomotion with occasional alternation of hindlimbs at low frequencies (Borgius 2014). Moreover, it has been revealed that inhibitory neurons play an important role in left-right and flexor-extensor alternation during locomotion (Kiehn 2010; Kiehn 2011; Talpalar 2011). We, therefore, wanted to investigate whether inhibitory neurons are also involved in the hopping gait of full *EphA4* mutant mice since EphA4 was shown to be expressed additionally in inhibitory interneurons (Lundfald 2007; Restrepo 2011). Moreover, Lbx1 is expressed by both excitatory and inhibitory neurons in the spinal cord (Cheng 2005) and, therefore, might also play an important role in the conditional *EphA4* mutant, we investigated in this study. Hence, we obtained two conditional *EphA4$^{flox/-}$vGAT$^{Cre/+}$* mutant mice whose *EphA4* receptor was deleted in all inhibitory neurons exhibiting a partial hopping gait. These mice maintained partly ALT gait and additionally performed synHOP and MIX steps. Possible misguided inhibitory neurons by the deletion of *EphA4* can cause a partial but not an almost complete hopping gait as it was seen for full *EphA4* mutant mice. This suggests an involvement of both inhibitory and excitatory neurons in the complete hopping gait of the full *EphA4* mutant and, therefore, it might be possible that ipsilateral inhibitory interneurons cross the midline in the spinal cord or, alternatively, they misconnect to misguided excitatory neurons. Further gait behavior experiments with an increased number of animals combined with tracing techniques need to be perfomed to verify misguidance of inhibitory interneurons across the spinal midline. In summary, an intact inhibitory network is important for the conservation of left-right alternation.

4.3 Less anatomical and gait defects in conditional and full *α2chimaerin* mutant mice compared to both *EphA4* mutants

Since α2chimaerin is a downstream effector of the EphA4 receptor (Beg 2007; Wegmeyer 2007) and the full *α2chimaerin* mutant mice performed a hopping gait (Beg 2007), we therefore expected a similar phenotype in the premotor interneuron distribution and gait behavior of the conditional *α2chimaerin* mutant as it was found in the conditional *EphA4* mutant mice. In the conditional *α2chimaerin* mutant, an ablation of *α2chimaerin* in Lbx1-expressing neurons resulted in no anatomical and gait behavioral phenotypes in comparison to wild type. To obtain the conditional *α2chimaerin* mutant in my study, *α2chimaerin*$^{+/-}$*Lbx1*$^{Cre/+}$ mutants were mated with homozygous *α2chimaerin*$^{flox/flox}$ mutant mice which are still poorly characterized (Scheiffele, unpublished). A complete deletion of the *α2chimaerin* allele in the conditional *α2chimaerin* mutant has not been investigated in this study. Further experiments still need to be performed in future to demonstrate a complete ablation. However, full *α2chimaerin* mutant mice were investigated in terms of their behavioral gait analysis as a full knockout control. Interestingly, our detailed gait behavioral analysis of the full *α2chimaerin* mutant revealed only a partial synHOP gait in addition to a maintained ALT and MIX gait. An uncomplete synchronous hopping locomotion in full *α-chimaerin* and *α2chimaerin* mutants was previously reported by fictive locomotion of L2 ventral roots from isolated spinal cords in neonatal mice (Wegmeyer 2007) and by locomotion on a treadmill (Asante 2010), respectively. We provided a direct comparison of a detailed gait analysis of hindlimbs between full *EphA4* and full *α2chimaerin* mutant mice. The full *α2chimaerin* mutant exhibited a significantly reduced synchronous hindlimb movement in comparison to an almost complete synchronous hopping gait in the full *EphA4* mutant mice. In both conditional and full *α2chimaerin* mutants, the effect of the removal of *α2chimaerin* either in Lbx1-expressing neurons or in all cells is reduced in comparison to the deletion of its *EphA4* receptor in the conditional and full *EphA4* mutants, respectively.

Following explanations might interpret the reduced phenotypes of the conditional and full *α2chimaerin* mutants. First, further studies still need to prove whether *α2chimaerin* is indeed a downstream EphA4 effector in Lbx1-positive cells or not. A lack of α2chimaerin-

expression in Lbx1-positive cells could explain the wild type-phenotypes in the conditional *α2chimaerin* mutant. However, *α2chimaerin* is expressed throughout the entire dorsal and ventral spinal cord (Beg 2007; Wegmeyer 2007), therefore, it is to assume that also Lbx1-positive neurons might express *α2chimaerin*. Second, previous studies suggested that a single GAP or GEF effector can bind to various receptors in a cell-specific manner (reviewed in Beg (2007)). The study of Wegmeyer et al. (2007) revealed that α2chimaerin binds additionally to EphB1 receptors previously shown to be expressed in commissural interneurons (Imondi 2000). The axonal guidance of commissural interneurons might additionally be affected to the one of ipsilateral neurons in full *α2chimaerin* mutant mice resulting in a possible different phenotype than observed in the full *EphA4* mutant.

Third, α2chimaerin is one of several effectors of the EphA4 receptor and, hence, other effectors might still be activated in both conditional and full *α2chimaerin* mutants and might, therefore, lead to reduced fiber crossing across the midline of the spinal cord in comparison to conditional and full *EphA4* mutant mice, respectively. For instance, other EphA4 effectors, such as ephexin or Vav2 (GEFs), might continue to mediate axonal growth cone collapse as they activate RhoA which then in turn has an inhibitory effect on actin polymerization in the growth cones (Shamah 2001; Cowan 2005; Sahin 2005; Iwasato 2007). On the contrary, it was shown that *ephexin1*$^{-/-}$ and the *Vav2/3*$^{-/-}$ mutant mice did not display any hopping gait (Cowan 2005; Sahin 2005). However, other GEFs such as various ephexin subtypes may have a more pronounced effect on RhoA activation and, thereby, in axonal growth cone collapse in the spinal cord (Shamah 2001; Sahin 2005), since the study of Katayama et al. (2012) showed that a deletion of RhoA in the dorsal and ventral spinal cord resulted in aberrant neuronal projections and a hopping gait. A relation to EphA4 receptor activation still needs to be proven in future. In a further investigation by Toyoda et al. (2013), the actin nucleator and polymerization factor mDia, that is regulated by GTPase Rho, was proposed as a possible mechanism in which ephexin might indirectly activate mDia through the activation of Rho upon EphA4 stimulation. An ablation of *mDia* resulted in impaired left-right limb coordination and aberrant dorsal midline crossing of axons of corticospinal neurons and spinal cord interneurons (Toyoda 2013). However, Fawcett et al. (2007) showed that another EphA4 downstream effector, Nck, interacts with α2chimaerin and links to actin regulatory proteins. A deletion of *Nck* caused a hopping gait defect in the spinal CPG (Fawcett 2007). In

summary, a variety of EphA4 downstream effectors might compensate to a certain degree the loss of α2chimaerin in conditional and full *α2chimaerin* mutant mice.

4.4 Future experiments

So far, we have shown that dorsal premotor Lbx1-expressing neurons are misconnected in the spinal cord of conditional *EphA4* mutants at P13-15 by a retrograde monosynaptic tracing method. Regarding the gait behavior, the adult conditional *EphA4* mutant displayed a minor defect, exhibiting HOP gait at low velocities and a decreased swing time compared to wild type mice. Further questions remain to be answered in future experiments, especially whether there is a link between the misguided axons of dorsal Lbx1-expressing neurons at younger developmental stages and the adult gait phenotype of a minor HOP gait.

Therefore, first, it is planned to investigate whether axons aberrantly cross the midline in the spinal cord of adult conditional *EphA4* mutants in comparison to control mice. Previously trained and tested conditional *EphA4*$^{flox/-}$*Lbx1*$^{Cre/+}$ *Tau*$^{lox\text{-}stop\text{-}lox\text{-}FlpO\text{-}INLA}$ mutant mice on the TreadScan apparatus will be injected with AAV-FRT-GFP in one side of the spinal cord in order to visualize the axon projection pattern and cell bodies of Lbx1-expressing neurons in the spinal cord. These experiments will answer the question of whether there are still axons of dorsal Lbx1-positive neurons misguided across the dorsal midline in adult conditional *EphA4* mutant mice. Further, one can investigate whether there is a correlation between gait behavior (frequency of HOP gait) and anatomy by the number of crossing axons in the spinal cord of each animal. We would assume that less axons cross the spinal midline in adult conditional *EphA4* mutants as it was seen at P13-15 and this possible finding would indicate to a reorganization of misguided dorsal Lbx1-positive cells in adulthood. In future, one can combine tracing and gait behavioral experiments at different developmental stages in conditional *EphA4* mutant mice.

Second, it is necessary to know whether Lbx1-expressing neurons are indeed involved in locomotor activity. Hence, the locomotor activity will be examined by the co-expression of Lbx1 and the marker for neuronal activity, c-fos, (Dragunow 1989; Al-Mosawie 2007) in trained (one hour running on treadmill before perfusion) and untrained conditional *EphA4*$^{flox/-}$*Lbx1*$^{Cre/+}$ *Tau*$^{lox\text{-}stop\text{-}lox\text{-}SynGFP\text{-}INLA}$ mutants and control mice.

Third, we observed a possible decrease of the aberrant gait behavior during development, from neonatal over 3-week old mice until adulthood in the conditional *EphA4* mutant. To test this hypothesis, we will have to start examining the coordination of hindlimbs of neonatal mice by airstepping and swimming behavior experiments of conditional *EphA4* mutants in comparison to wild type mice and continue investigating gait behavior until adulthood of the same animals. A possible decrease in the gait defect during development could indicate to compensational effects of the misguided axons by reorganization in the neuronal network of either spinal interneurons or descending tracts from the hindbrain. It has been shown that in full *Lbx1*$^{-/-}$ mutants, ascending and descending tracts from and towards the spinal cord were misrouted (Pagliardini 2008).

Fourth, Lbx1 is also expressed in several nuclei of the hindbrain (Sieber 2007; Pagliardini 2008). In order to exclude a general involvement of hindbrain input on locomotion in the conditional *EphA4* mutant, it would be necessary to perform fictive locomotion experiments from isolated spinal cords by recording from ventral roots in neonatal conditional *EphA4* mutant mice and controls. Recording between the right and left L2 or L5 ventral roots enables to investigate the coordination between hindlimbs, and between L2 and L5 of the same side allows to study the coordination between flexor and extensor muscles. Moreover, flexor and extensor activity might be important to study since we have revealed a reduced swing time in adult conditional *EphA4* mutants. These experiments could be also combined with a prior gait behavior analysis of neonatal mice.

Fifth, it might be interesting to delete Lbx1-expressing neurons only in the spinal cord and investigate the locomotor behavior in adult mice since full *Lbx1*$^{-/-}$ mice die at birth as the breathing center in the hindbrain is affected (Pagliardini 2008). Moreover, original Lbx1-positive cells acquire a different cell fate (Gross 2002; Muller 2002; Glasgow 2005) and muscles were severly reduced (Brohmann 2000; Gross 2002) in full *Lbx1*$^{-/-}$ mutants. To avoid any interference with the development of spinal neurons and muscle precursor cells, Lbx1 could be ablated in adult mice. Therefore, one future approach might be to inject AAV-flex-DTR (containing diphtheria toxin receptor) in the lumbar spinal cord of *Lbx1*^{Cre} adult mice and following two weeks of virus transport time, diphtheria toxin will be injected intraperitoneally (Esposito 2014). In this way, the breathing center of the hindbrain will not be affected. Alternatively, the generation of *Lbx1*$^{loxP\text{-}STOP\text{-}loxP\text{-}DTR}$ mutant mice crossed with

Hoxb8^{Cre} mice will produce *Hoxb8*^{Cre} *Lbx1*$^{LSL\text{-}DTR}$ mutant offspring, in which Cre recombination is restricted to spinal segments caudal to cervical segment 4 and leaving out the hindbrain (Witschi 2010). A further injection of diphtheria toxin intraperitoneally in adults will cause an ablation of Lbx1 cells in the lower cervical and lumbar spinal cord. These two methods would result in an ablation of Lbx1-expressing neurons in the spinal cord at adulthood. No compensational effect or neuronal reorganization during development would interfer. The ablation of Lbx1-expressing neurons in the spinal cord of adult mice could be studied in anatomical and gait behavioral experiments in future and will show whether a gait defect occurs.

Sixth, in future experiments, it might be important to identify the role of Lbx1-expressing subpopulations, such as dI4, dI5 and dI6, in the misguidance defect in the spinal cord and the aberrant gait behavior of the conditional *EphA4* mutant. Hence, the *EphA4* receptor could be deleted in single Lbx1-expressing subpopulations or the single subpopulations could be entirely ablated in the spinal cord. The transcription factor Ptf1a might be targeted for dI4 and dIL_A neurons, Lmx1b for dI5 and dIL_B neurons and Wt1 for dI6 interneurons (reviewed in Alaynick et al. (2011)).

Seventh, further muscle injections by rabies GFP complemented with AAV-glycoprotein need to be performed bilaterally in both hindlimbs to reveal possible aberrant interneurons projecting to motorneurons on both sides of the body in conditional *EphA4* mutants. Moreover, retrograde rabies tracing from forelimbs could be investigated whether the anatomical defect is less severe in the cervical than in the lumbar spinal cord since forelimb coordination was less affected compared to the hindlimb coordination in the full *EphA4* mutant (Akay 2006).

4.5 Conclusion and general outlook

In this study, we have shown that the EphA4 receptor in Lbx1-expressing neurons is important to keep the axonal projection of those neurons to the ipsilateral side of the spinal cord and to maintain a complete alternating gait. A deletion of *EphA4* in Lbx1-positive interneurons resulted in an aberrant axonal misguidance of dorsal neurons across the midline as it was also seen in some full *EphA4* mutants (Fig. 29A). In general, the behavioral

gait phenotype of the conditional *EphA4* mutant mice differed mainly to the full *EphA4* mutant. Furthermore, we have revealed that minor gait defects such as a slight frequency in hopping gait and a reduced swing time occurred in the conditional *EphA4* mutant mouse compared to wild type (Fig. 29B and C). Hence, the dorsally-derived Lbx1-expressing neurons might be one component of several cell types contributing to the locomotor CPG. In future, more experiments will have to identify the location, projection pattern and function of further spinal interneuron populations and will, thereby, provide insight into the CPG network. This knowledge will be helpful to understand the human CPG network and enable the discovery of therapeutic treatments in future.

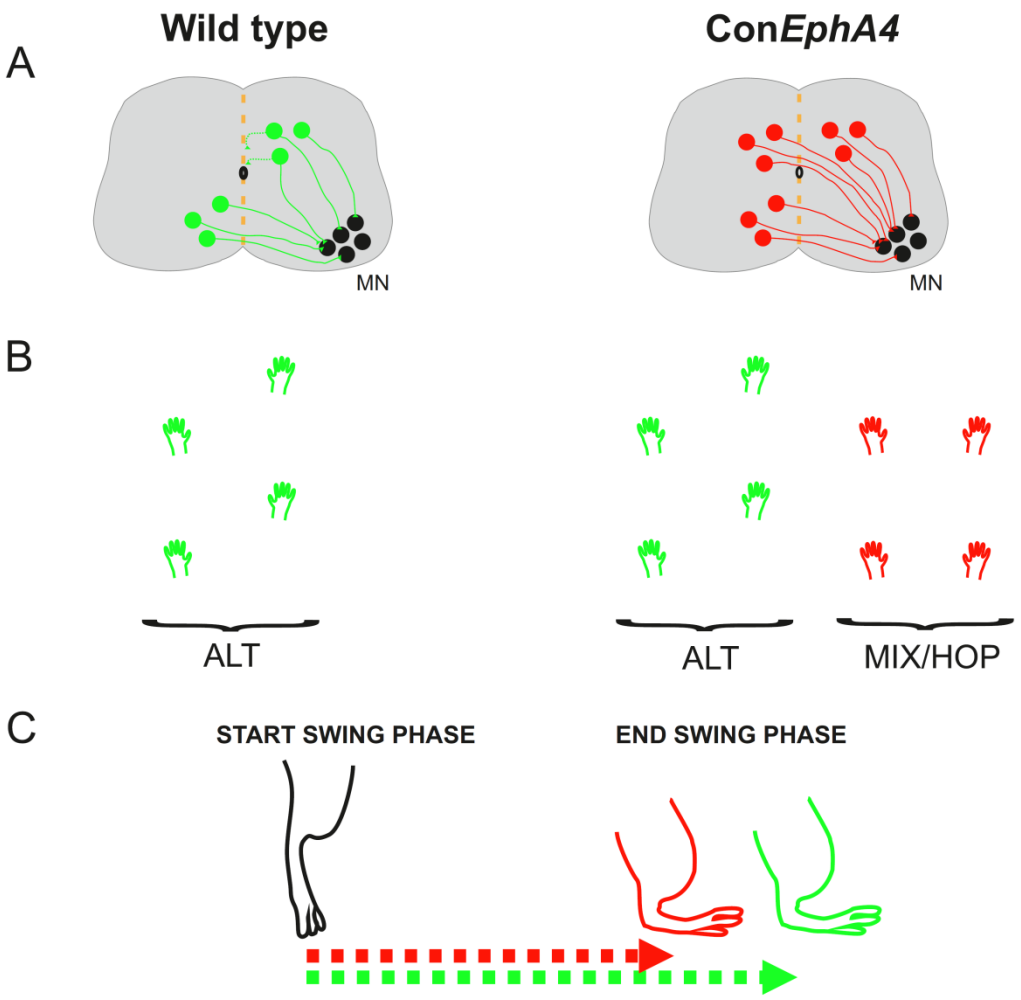

Figure 29. The EphA4 receptor in Lbx1-expressing neurons is important to maintain an ipsilateral axonal projection and to conserve a complete alternating gait

A: Presence of the EphA4 receptor in wild type results in repelling of axons from the spinal midline whereas an ablation of *EphA4* in Lbx1-positive interneurons revealed misguidance of axons across the dorsal midline connecting to contralateral motor neurons. B: Gait analysis in the conditional *EphA4* mutant showed a low frequency of HOP gait in addition to the maintained ALT gait. C: The swing time was significantly reduced in conditional *EphA4* mutant mice walking with ALT gait in comparison to wild type mice.

5. Experimental Procedures

5.1. Mouse genetics

The following various transgenic mouse lines were used to study the premotor interneuron distribution pattern in the spinal cord and the gait behavior. Wild type mice were maintained on a mixed genetic background (129/C57BL/6). The above described full *EphA4*$^{-/-}$ mutant mouse was an *EphA4*$^{lacZ/lacZ}$ mutant whose lacZ was expressed under the promoter of *EphA4* and was provided by P. Schwab, Zürich. The full *EphA4* knockout mouse was generated by Helmbacher et al. (2000). The transgenic *Lbx1*^{Cre} mouse was received from C. Birchmeier, Berlin (Sieber 2007). Further, the *EphA4*^{flox} mutant mouse was obtained from O. Kiehn, Stockholm and was previously generated by Herrmann et al. (2010). The generation of *Tau*$^{lox\text{-}stop\text{-}lox\text{-}SynGFP\text{-}INLA}$ mutant (Tripodi 2011) and *Tau*$^{lox\text{-}stop\text{-}lox\text{-}FlpO\text{-}INLA}$ mutant (Pivetta 2014) mice were performed in our laboratory using a strategy described previously (Hippenmeyer 2005). We bred and obtained a conditional *EphA4*$^{flox/-}$*Lbx1*$^{Cre/+}$ mutant mouse whose Lbx1-expressing cells lack the EphA4 receptor. Full *EphA4* mutant mice were first bred with *Lbx1*^{Cre} mice to obtain *EphA4*$^{+/-}$*Lbx1*$^{Cre/+}$ mutants that were then further mated with homozygous *EphA4*$^{flox/flox}$ mutant mice. As *Lbx1* is mainly expressed in a short time window in the embryonic stage of mice (Gross 2002; Muller 2002), the Cre-recombinase enzyme expression under the control of the *Lbx1* promoter might not have been efficient enough to flox the *EphA4* gene in two alleles. Therefore, we bred a conditional mouse in which one *EphA4* allele was already deleted and the second *EphA4* allele solely needed to be floxed. In the gait behavior analysis, *EphA4*$^{+/-}$*Lbx1*$^{Cre/+}$ males were mated with *EphA4*$^{flox/flox}$*Tau*$^{lox\text{-}stop\text{-}lox\text{-}SynGFP\text{-}INLA}$ or *EphA4*$^{flox/flox}$*Tau*$^{lox\text{-}stop\text{-}lox\text{-}FlpO\text{-}INLA}$ females. The Cre-recombinase enzyme, expressed under the control of the *Lbx1* promoter, additionally floxed the loxP-stop-loxP cassette of the *Tau* genomic locus resulting in the expression of LacZ in Lbx1-positive cells and, thereby, enabling the visualization of Lbx1-expressing neurons by a subsequent immunohistochemical staining of the spinal cord in conditional *EphA4* mutant mice. Finally, conditional *EphA4*$^{flox/-}$*Lbx1*$^{Cre/+}$*Tau*$^{lox\text{-}stop\text{-}lox\text{-}SynGFP\text{-}INLA}$ and *EphA4*$^{flox/}$*Lbx1*$^{Cre/+}$*Tau*$^{lox\text{-}stop\text{-}lox\text{-}FlpO\text{-}INLA}$ mutant mice were obtained. Furthermore, the *vGAT*$^{IRES\text{-}Cre}$ mouse was generated by B. Lowell, Harvard (Vong 2011).

The effect of the deletion of α2chimaerin, a downstream effector of the EphA4 receptor, was studied. The full *α2chimaerin*$^{-/-}$ mutant (Beg 2007) and the *α2chimaerin*^{flox} mutant mice (unpublished) were obtained by P. Scheiffele, Basel. A conditional *α2chimaerin*$^{flox/-}$ *Lbx1*$^{Cre/+}$ mutant mouse was bred as described above for the conditional *EphA4* mutant mouse.

5.2 Monosynaptically retrograde virus tracing

5.2.1 Virus production

5.2.1.1 AAV-glycoprotein production

In nitrogen frozen T293 HEK (human embryonic kidney) cells (ATCC company, Manassas, VA, USA) were thawed and placed in a small petri dish (10 cm diameter) with 10% FBS/DMEM medium (FBS: fetal bovine serum (Sigma Aldrich, St. Louis, USA); DMEM: Dulbecco`s modified eagle medium, FMI media kitchen). DMEM is a growing medium for mammalian cells containing different nutrients like anorganic salts, amino acids and vitamins. FBS was added since it consists of embryonic growth promoting factors in order to support specific metabolic requirements. Confluent petri dishes with HEK cells were split several times in order to obtain 30 or 60 big petri dishes (15 cm diameter) for two or four viral tube productions, respectively. Splitting cells required a washing step with PBS (phosphate buffered saline) before adding 0.05% trypsin (Gibco Life Technologies, Carlsbad, CA, USA) for 2 minutes at 37°C. Trypsin is a serine protease and hydrolyses proteins. In cell culture, it is used to remove adherent cells from the dish surface. After 2 minutes of trypsin incubation, 10% FBS/DMEM medium was quickly added to inhibit further tryptic activity and, thereby, avoiding cell damage. Cells were resuspended and mixed by pipetting up and down before collecting them in a falcon tube. Cells were added to the medium in a higher number of petri dishes and were grown at 37°C in a 5% CO_2 incubator. At circa 80% confluence, cells were transfected with PEI (polyethylenimine). Following substrates were added to a warmed up DMEM without FBS: 70 µg/µl AAV helper plasmid (serotype pAAV2/6, Plasmid Factory GmbH & Co.KG, Bielefeld, Germany), 70 µg/µl AAV vector (pAAV-CMV-Gly, Plasmid Factory) containing the glycoprotein genome, 200 µg/µl pHGTI-adeno1 (provides adenoviral helper function, Plasmid Factory) and 1360 µl PEI (1:4 ratio of DNA:PEI, Polyscience AG, Cham,

Switzerland). Transfection with PEI enables high viral titers as it condenses DNA into particles which are transported into the cell by endocytosis. After 15 minutes incubation time at room temperature, 5 ml of transformation mix was added per plate. The dishes were incubated at 37°C for 48-50 hours until cell collection was performed. Cells were removed from the dish surface by pipetting up and down. Medium and cells with AAV were collected in a falcon tube and centrifuged at 2000 rpm for 10 minutes (5804R, Eppendorf, Hamburg, Germany). The supernatant was removed and the remaining cell pellet was stored at -80°C.

The frozen cell pellet was thawed in a water bath at 37°C and then re-suspended in 15 ml lysis buffer (150mM NaCl, 20mM Tris, pH 8.0). Further, cells with AAV were freeze-thawed three times between dry ice/ethanol and 37°C water bath before vortexing in order to destroy the cells. 1mM $MgCl_2$ and benzonase (Sigma Aldrich) were added for DNA removal and incubated at 37°C for 15 minutes (the DNA/protein aggregate which formed in the thaw/freeze cycle should have dissolved). The cell debris was centrifuged at 4000 rpm at 4°C for 20 minutes (5804R, Eppendorf). The supernatant containing the virus was collected after centrifugation.

AAV was concentrated and purified by Iodixanol gradients. The gradients were formed in an Optiseal tube (Beckman Coulter, Washington D.C., USA) starting with 5ml of 60%, then 6ml of 40%, 6ml of 25% and 5ml of 17% Iodixanol solution (see Appendix, Table 3). The solutions were applied drop by drop with a needle and syringe. The virus supernatant was added on the top and the Optiseal tube was filled up by lysis buffer if required. It was essential to close the tube without any air bubbles for a further centrifugation in an ultracentrifuge for 90 minutes at 48-50,000 rpm (Optima L-90, Beckman Coulter, Washington D.C., USA) at 16°C. The virus was purified through the layers and was then concentrated in the 40% Iodixanol solution. The 40% solution containing the virus was harvested by inserting a needle into the intersection of 40 and 60% solutions through the Optiseal tube. 15ml 1x PBS was added to the virus fraction and transferred to a filter tube (Millipore Amicon 100K columns, EMD Millipore Corporation, Billerica, MA, USA) and centrifuged several times at 3500 rpm at 4°C for 30 minutes. This step was repeated until the virus fraction consisted only of a volume of 150-250 µl in the filter. The virus solution was collected in tubes and stored at 4°C for further muscle injections. AAV glycoprotein virus was produced at a titer of approximately $3e10^{12}$.

5.2.1.2 Modified rabies virus production

Modified rabies virus was produced in BHK-SADGly-NLS-GFP cells (Callaway, Salk Institute, USA) originating from BHK21 (baby hamster kidney) cells (ATCC company, Manassas, VA, USA). Therefore, BHK cells stably express a GFP reporter gene and glycoprotein (Wickersham 2007a; Wickersham 2007b; Marshel 2010; Wickersham 2010). One vial of in nitrogen-frozen BHK-SADGly-NLS-GFP cells were thawed and plated on a 10 cm diameter petri dish with 10% FBS/DMEM that was then stored at 37°C in a 5% CO_2 incubator. The following day, the medium was exchanged. When the cells were confluent, cells were split into a higher number of dishes. The medium was removed and the cells were washed with PBS. Then, 2ml of 0.25% trypsin (Sigma Aldrich) was applied for 5 minutes at 37°C in order to detach the cells from the dish surface. Trypsin was inactivated by adding 2ml of medium. The cells were re-suspended, collected and splitted into 10 plates. Two to three days later, the cells were repeatedly collected. The number of cells was counted with a Neubauer Improved slide (Hatfield, PA, USA). Approximately $4.5*10^6$ cells were plated in each petri dish. 20 plates were used for one production. At circa 80% confluence, cells were infected with the modified rabies virus (delta glycoprotein rabies GFP/ mCherry; supernatant of a previous cell production was used). The medium was changed to 2% FBS/DMEM medium. Circa 100 µl of frozen rabies GFP or mCherry virus from an old stock was applied to each plate. The inoculated cells were cultured at 35°C in a 3% CO_2 incubator.

Eight to nine days after transfection, GFP or mCherry expression of the virus was controlled under a fluorescence microscope (SZX16, Olympus, Hamburg, Germany). When most of the cells expressed the fluorescent protein and were 100% confluent, the first virus collection was performed. The supernatant of all 20 plates was collected into a falcon tube and centrifuged for 10 minutes at 4000 rpm (5430R, Eppendorf, Hamburg, Germany). 2% FBS/DMEM was added to the plates prior a further incubation at 35°C. After centrifugation, the supernatant was collected and transferred to six Beckman centrifuge tubes (Beckman Coulter, Washington D.C., USA). 5ml of 20 % sucrose was applied carefully to the bottom of the tube as a cushion. All steps were performed on ice. The Beckmann tubes were then placed in an ultracentrifuge (Optima L-80XP, Beckman Coulter, Washington D.C., USA) at 4°C at a speed of 25,000 rpm for 4 to 5 hours. Following centrifugation, the supernatant was removed and the tube placed upside down in order to ensure that all medium was removed.

The pellet containing the virus remained in the tube and was re-suspended by vortexing gently with 400 µl ice-cold PBS starting in the first tube. The re-suspended pellet was transferred to the next tube for a further re-suspension until the last one. Then, the re-suspended pellets were collected, mixed again and aliquoted in small tubes for muscle injection. The aliquoted tubes were immediately frozen on dry ice until storage at -80°C. A second batch was collected by re-suspending the remaining pellets another time in the Beckmann tubes.

The following two days, the second and third collection was performed in the same manner as described above. Modified rabies virus was produced at a titer of approximately $1e10^8$ (FACS analysis was performed by Monika Mielich).

5.2.2 Retrograde virus injection in muscle

The technique of retrograde rabies virus tracing allowed the visualization of monosynaptically connected neurons to the primarily infected cell. The modified rabies virus vector is derived from an attenuated strain and possesses a genomic substitution in the gene encoding the envelope glycoprotein G by a fluorescent marker protein. The envelope glycoprotein G is important for the transport across synapses. Due to the lack of the glycoprotein G, rabies virus is not able to spread from the infected cell. However, complementation by an independently derived gene for the glycoprotein G into an infected neuron results in monosynaptic spread of the virus to its pre-synaptic partners but not any further. Infected neurons express a marker protein such as GFP or mCherry and, thus, can be visualized (Wickersham 2007a; Wickersham 2007b).

In this project, we studied the premotor interneuron network in the spinal cord by investigating monosynaptic tracing from particular motor neuron pools. Modified rabies virus (ΔG protein rabies) was, therefore, injected into particular muscles to infect retrogradely the connected motor neurons through their axons. Additionally, AAV carrying the gene for the glycoprotein G (AAV-G-protein) was injected into the same muscle in order to complement expression in motor neurons. This method allowed the identification of monosynaptically connected interneurons to the corresponding motor neuron pool in the spinal cord (Stepien 2010).

Mice age P5-7 were anaesthetized by placing them on ice and the Q muscle was exposed. Rabies GFP or mCherry was mixed together with AAV glycoprotein in a ratio 1:1. Circa 5 µl of the mixed virus solution was injected into the Q muscle by a glass pipette (TW100-4, borosilicate glass capillaries, World Precision Instruments Inc., Sarasota, FL, USA; glass pipette was pulled by PC-10 Narishige group, Tokyo, Japan) connected to a picospritzer with several pulses of 8 µs (Parker Hannifin corporation, general valave operation, Cleveland, OH, USA). Skin closure was performed by polypropylene suture (Prolene, Ethicon, LLC., San Lorenzo, Puerto Rico). Following eight days of virus transport time, mice were sacrificed using initially isoflurane anaesthesia (Attane, Minrad, Inc., Buffalo, N.Y., USA) and then perfusion fixation (ice-cold PBS followed by 4% PFA (paraformaldehyde), Microstain Division, Martinego, Italy). Spinal cord and muscles were dissected and kept in PFA overnight. The precision of Quadriceps injection was verified under a fluorescence dissection microscope (MVX10, Olympus, Hamburg, Germany). Spinal cords were washed in PBS before transferring them to a 30% sucrose solution for 1-2 days. This step was essential for cryoprotection of the tissue. Spinal cords were then frozen in tissue tek (Sakura Finetek Europe B.V., Alphen aan den Rijn, Netherlands) at -20°C. Results of wild type (n=4), conditional *EphA4* mutants (n=2), full *EphA4* mutants (n=7) and conditional *α2chimaerin* mutant mice (n=3) were used for this study.

Additionally, TA and GS muscle injections with rabies GFP or mCherry complemented by AAV-glycoprotein were performed by Dr. Daisuke Satoh and conducted as described above. Wild type mice (n=5) were used for each of TA and GS muscle injections (see data in Dougherty et al. (2013)). Furthermore, TA and GS muscles were injected in conditional *EphA4* mutant mice (TA: n=4 and GS: n=3).

5.2.3 Immunohistochemistry and imaging

Spinal cords frozen in tissue tek (Sakura Finetek Europe B.V.) were mounted on a cryostat stage (cryostat, Histocom AG, Zug, Switzerland). 40 µm thick slices were sectioned from middle thoracic to sacral spinal segments and transferred in PBS in a rostral to caudal order. Spinal cord slices were then incubated overnight at 4°C in the first primary antibody against GFP and/or RFP corresponding to the rabies virus used. This step was necessary in order to

block rabies GFP or mCherry and, therefore, avoiding further unspecific stainings. Chicken anti-GFP (Molecular Probes, Eugene, Oregon, USA) and/or rabbit anti-RFP (Rockland, Gilbertsville, PA, USA) were diluted 1:1,000 and 1:5,000, respectively in a blocking buffer consisting of 1% BSA (bovine serum albumin, Sigma Aldrich, St. Louis, USA) and 0.1% triton X-100 (Sigma Aldrich) in PBS. To avoid unspecific background staining, BSA was essential to block endogenous proteins in the tissue. Triton is a detergent and, therefore, provoked a more permeable membrane for antibodies. The following day, further primary antibodies were applied after rinsing spinal cord slices in PBS. Goat anti-ChAT (choline acetyltransferase) 1:1,000 (Chemicon International, Temecula, CA, USA) and guinea pig anti-Lbx1 1:10,000 (provided by C. Birchmeier, Berlin (Muller 2002)) in blocking buffer were used to visualize motor neurons and Lbx1-expressing cells, respectively. Antibodies were incubated for 3 days at 4°C. Then, the slices were repeatedly washed in PBS before secondary antibody incubation with donkey anti-chicken FITC (Jackson ImmunoResearch Laboratories, Inc, PA, USA)/ Alexa488 (Jackson ImmunoResearch, Milan Analytica AG, Rheinfelden, Switzerland), donkey anti-rabbit Cy3 (Jackson Milan), donkey anti-guineapig Cy3 (Jackson Milan), donkey anti-goat Alexa 647 (Jackson Milan), donkey anti-guinea pig Dyl 649 (Jackson) and donkey anti goat Dyl 405 (Jackson) (corresponding to the primary antibodies used) overnight at 4°C. Slices were rinsed several times in PBS, mounted on a glass slide (Roth GmbH, Karlsruhe, Germany) in a rostral to caudal order and, then, coverslipped with Airvol mounting medium (Airvol 205, Air Products GmbH, Bochum, Germany).

Single slices of the lumbar level were scanned at 20x using image stacks ranging between 0.3 and 0.5 µm to provide an overview of the dorsal spinal cord. The photos were imported and further processed in Imaris (version 7.4.0, Bitplane AG, Zurich, Switzerland) and Corel Photo-Paint X5 (Ottawa, Canada).

5.2.4 Interneuron reconstructions

Spinal cord slices for cell reconstruction were scanned in a rostral to caudal order either with a 4x or 10x objective by a confocal microscope (FV1000, Olympus Fluoview, Hamburg, Germany). Slices were imported and aligned in Image J (version 1.43m, Wayne Rasband,

National Institutes of Health, USA), Fiji Project (version 1.48, software based on Image J, imaging processing package) or Matlab (version7.11.0.584, The MathWorks, Inc., Natick, MA, USA). Regarding the reconstruction in Matlab, a custom-made plug-in "Reference Axes" running by image processing suite "Qu" was used for a three-dimensional reconstruction of the position of interneurons (previously described by Tripodi et al. (2011), full methods). In all reconstructions, interneurons and motor neurons were reconstructed in each slice. With the help of the ChAT staining, Q motor neurons were identified. The central canal was set to 0.0 and the y-axis parallel to the midline. The midline, dorsal and ventral funiculus served as landmarks for the alignment of all slices. To compare all spinal cords, slices from T11 until S1 segments were selected for the analysis. The segments were identified by ChAT staining and compared with the mouse spinal cord atlas (Watson 2008).

Analysis and plotting of the reconstructed cells was performed in R project (version 2.14.0, The R Foundation for Statistical Computing, Vienna, Austria). Kernel density for contour plots was estimated using the kde2D function in the "MASS" library. The two dimensional density plots were obtained using the R "density" function. Percentages of the premotor interneuron distribution in the spinal cord were plotted and statistically analyzed in graph pad prism (version 6, GraphPad Software, Inc., La Jolla, CA, USA; see chapter 5.4)

5.3. Behavior analysis

5.3.1 TreadScan gait behavior analysis

Adult mice older than 1.5 months were tested for the gait behavior analysis on the TreadScan apparatus (Clever Sys, Inc., Reston, VA, USA). Mice were trained for the first three days on a rodent treadmill (Robomedica, Inc., Irvine, CA, USA) for acclimatization on a moving belt at speeds of 12, 16 and 20 cm/s. The following days, all animals were trained on the TreadScan apparatus for ca. 10 minutes every day at the same speeds of 12, 16 and 20 cm/s for one to two weeks until they walked consistently. During training period, mice were set under food restriction. Animals received one chocolate treat as a reward after each training session. The testing of the mice consisted of a one-day recording session. In the beginning of gait behavior experiments, all animals were recorded at speeds of 12, 16 and

20 cm/s. Several trials of each belt speed were recorded. The lowest belt speed of 12 cm/s was selected as the animals started to display problems in walking consistently. 20 cm/s was chosen since the Robomedica treadmill only achieved the highest speed of 23 cm/s and the full *EphA4* mutant mice already struggled in keeping up this speed. In order to compare wild type and conditional *EphA4* mutants with full *EphA4* mutant mice, the speed of 20 cm/s was selected as the highest speed at the beginning of the behavioral gait experiments. Given that the gait type and gait parameter analysis of the first and second set of conditional *EphA4* mutants showed no striking differences between 16 and 20 cm/s, the following animals were recorded at higher speeds of 30, 40 and 50 cm/s. TreadScan apparatus allowed a maximum belt speed of 51 cm/s. Most of the mice refused to walk at higher speeds and needed, therefore, to be stimulated.

Hence, conditional *EphA4* mutants (n=6, $EphA4^{flox/-}Lbx1^{Cre/+}\ Tau^{lox\text{-}stop\text{-}lox\text{-}SynGFP\text{-}INLA}$ and $EphA4^{flox/-}Lbx1^{Cre/+}\ Tau^{lox\text{-}stop\text{-}\ lox\text{-}FlpO\text{-}INLA}$ mutants), full *EphA4* mutants (n=3) and wild type mice (n=3) were additionally tested at a speed of 30, 40 and 50 cm/s. In total, videos of wild type (n=10), conditional *EphA4* (n=6), full *EphA4* (n=10), conditional *α2chimaerin* (n=4) and full *α2chimaerin* (n=4) mutant mice were used for analysis at lower speeds of 12, 16 and 20 cm/s. In addition, two conditional $EphA4^{flox/-}vGAT^{Cre/+}$ mutants were recorded at 12, 16, 20, 30, 40, and 50 cm/s.

Furthermore, the same conditional *EphA4* mutant mice (n=6) were previously recorded without prior training at the age of 3-weeks at belt speeds of 12, 16, 20, 30, 40 and 50 cm/s. Likewise, 3-week old wild type mice (C57BL/6; n=3) were additionally tested as controls.

TreadScan apparatus enabled the detection of feet placement of mice and, thereby, allowed the analysis of gait pattern and gait parameters. Mice were walking on a transparent belt (operated by Exer-gait treadmill, Columbus Instruments, Columbus, Ohio, USA) while a camera (Basler Camera A602fc, Basler AG, Ahrensburg, Germany) detected the steps at 100 frames per second from underneath over a mirror. A video software (BCamCapture version2.0, CleverSys, Inc.) enabled recordings of a duration of 20 seconds per trial. The gait behavior analysis with the TreadScan software (version3.0, CleverSys, Inc.) consisted of two parts: gait type and gait parameter analysis.

In the gait type analysis, four different gait types were found and classified by the position and time of both hindlegs to each other. The four gait types consisted of 1. ALT (alternating),

2. TS (transitional step), 3. MIX (mixture) and 4. synHOP (synchronous Hopping) gaits. A further description of the gait types can be seen in chapter 3.1.2.1. Percentages of the classified gait types per trial were counted for the right hindleg. The average of three trials at a single speed was analyzed for each animal. Finally, animals of the same genotype were pooled. The gait type analysis of few litter mate controls of conditional *EphA4* and conditional *a2chimaerin* mutant mice (*EphA4*$^{flox/+}$*Tau*$^{lox\text{-}stop\text{-}lox\text{-}SynGFP\text{-}INLA}$, *EphA4*$^{flox/+}$*Tau*$^{lox\text{-}stop\text{-}lox\text{-}FlpO\text{-}INLA}$ and *a2chimaerin*$^{flox/+}$ mutants) showed a comparable percentage of ALT gait as in wild type mice and, therefore, were not further used for the analysis.

In the gait parameter analysis, TreadScan software (version3.0, CleverSys, Inc.) was used to automatically detect the steps on the treadmill and, thereby, recorded stance phase time, swing phase time and stance length of each hind- and forelimb. The recorded steps were manually examined and falsely detected steps were excluded. Nine to eleven steps consisting of at least two consistent steps were selected for each animal and gait type for a further analysis. The software calculated a variety of gait parameters such as stance phase time, swing phase time, stride length, stride frequency, limb track width and limb coupling. Values of the different gait parameters were taken for the right hind- and forelimb. Different gait parameters of ALT gait in wild type and conditional *EphA4* mutants at 16 and 40 cm/s and of HOP gait in conditional and full *EphA4* mutant mice at 16 cm/s were obtained and used for further statistical comparisons (see chapter 3.1.2.5 for a description of the gait parameters used in this study). In the gait parameter analysis following adult mice were used: wild type (ALT gait: n=10 at 16 cm/s, n=3 at 40 cm/s), full *EphA4* mutant (HOP gait: n=10 at 16 cm/s) and conditional *EphA4* mutant (ALT gait: n=6 at 16 and 40 cm/s, HOP gait: n=5 at 16 cm/s). As the conditional *EphA4* mutant mice did not show frequent steps of HOP gait, the number of 9-11 consistent steps for the gait parameter analysis could not always be achieved.

5.3.2 Open field behavior analysis

Adult wild type (n=4, C57BL/6) and conditional *EphA4* mutant mice (n=6, *EphA4*$^{flox/-}$*Lbx1*$^{Cre/+}$*Tau*$^{lox\text{-}stop\text{-}lox\text{-}SynGFP\text{-}INLA}$ and *EphA4*$^{flox/-}$*Lbx1*$^{Cre/+}$*Tau*$^{lox\text{-}stop\text{-}lox\text{-}FlpO\text{-}INLA}$ mutants)

were placed in a white and odourless 50 x 50 cm box for 10 minutes. A 1.2 lux lamp was used as low light source for video detection from above connected to a Debut Video Capture software (NCH Software, Inc., Greenwood Village CO, USA). The videos were further analyzed by Analysis Viewer 3 (version 3.0.1.339, Biobserve GmbH, St.Augustin, Germany) which automatically calculated different parameters. The parameters, average velocity and total track length, were used for a further statistical test in this study.

5.4 Analysis and statistics of premotor interneuron distribution and behavior experiments

For each genotype, the ratio of the length devided by the width of the dorsal funiculus and the ratio of the dorsal cord length devided by the dorsal gray matter were calculated from three to four spinal cord slices of lumbar segments. The values of the mean plus the standard error of mean (SEM) of the ratios (dorsal funiculus and dorsal gray matter) were plotted in a bar graph in Graph Pad Prism (version 6, GraphPad Software, Inc., La Jolla, CA, USA). Data of premotor interneuron distribution and behavior analysis was plotted as box and whisker graphs in Graph Pad Prism (version 6, GraphPad Software, Inc.). The box extended to the 25^{th} and 75^{th} percentile. The horizontal line in the box indicated the median value. The whiskers extended to the minimum and maximum values. All mean and median values are given in the Appendix in Tables 1.1 to 1.16. The numbers of interneurons in the four parts of the spinal cord and the numbers of the four gait types during a trial were calculated in percentages and, therefore, were considered as dependent. Hence, it was not possible to statistically compare all four parts together of the spinal cord and all four gait types together. The percentages of the dorsal contralateral part in the spinal cord and in addition the percentages of the ventral ipsilateral quadrant were statistically compared. Percentages of HOP gait (MIX and synHOP gait types pooled together) were used for further statistical tests.

All values were tested for a normal distribution by the Shapiro-Wilk normality test in Graph Pad Prism (version 6, GraphPad Software, Inc.) or in R project (version 2.14.0, The R Foundation for Statistical Computing). The values of the ratios of the dorsal funiculus and the dorsal gray matter were normally distributed and, therefore, parametric statistical tests

were performed. Unpaired t test with Welch`s correction was conducted to compare between two genotypes, whereas a one-way ANOVA test with post-hoc Tukey-Kramer multiple comparison test was performed to compare between three genotypes in Graph Pad Prism (version 6, GraphPad Software, Inc.). As some values of premotor interneuron distribution and gait behavior analysis were not normally distributed or n was too small, a non-parametric test was selected to obtain a fair and equal comparison between all groups. Regarding the premotor interneuron distribution, percentages of the dorsal contralateral or ventral ipsilateral quadrant were compared between the genotype groups. Concerning the gait types, percentages of the HOP gait were either compared between the genotypes within one speed or compared between the speeds within one genotype. When only two groups were compared, the Mann Whitney rank sum test was performed with Graph Pad Prism (significant difference when $P<0.05$). When three or more groups were compared with each other, the Kruskal Wallis rank sum test was completed with Graph Pad Prism (significant difference when $P<0.05$). A further post-hoc pairwise Wilcoxon test was conducted only when a significant difference was found in the Kruskal Wallis test. This post-hoc test was performed in R project (Wilcox_test from package “coin”) and required a P-value correction by a multiple testing correction according to Benjamin and Hochberg. This test uses a false discovery rate (FDR) which correlates with a P-value. The FDR value of 0.05 was selected as a significant difference cut-off in order to achieve a correlation to the P-values. To compare the percentages of HOP gait of each conditional *EphA4* mutant mouse at the age of 3-weeks and as adult at a certain speed, the Wilcoxon matched-paired signed rank test in Graph Pad Prism was performed (significant difference when $P<0.05$). In the gait parameter analysis, gait parameters of ALT and HOP gait types were compared between the genotypes within the belt speed of 16 and 40 cm/s, and parameters of ALT gait were compared between 16 and 40 cm/s within the genotype by a Mann Whitney rank sum test in Graph Pad Prism (significant difference when $P<0.05$). Given that the steps of ALT and HOP gait were already selected according to the gait type classification, solely ALT gait of conditional *EphA4* mutant mice was statistically compared with the ALT gait of wild type mice and HOP gait of conditional *EphA4* mutant mice was statistically compared with the HOP gait of full *EphA4* mutants for the different gait parameters. In the open field analysis, the values of average velocity and total track length were compared by a Mann Whitney rank sum test in Graph Pad Prism (significant difference when $P<0.05$).

All P and FDR values are given in Tables 2.1 to 2.14 in the Appendix. Finally, plots and graphs were further processed in Corel Draw Graphics Suite X5 (Ottawa, Canada). The significance level in the box and whisker plots was indicated as following: one star (*) when P or FDR < 0.05, two stars (**) when P or FDR < 0.01, three stars (***) when P or FDR < 0.001 and four stars (****) when P or FDR < 0.0001.

Appendix

1. Tables of median and mean values

Table 1.1 Dorsal funiculus and dorsal gray matter (mean ± SEM)

Ratio	WT	Con*EphA4*	*EphA4*	Con *α2chimaerin*
dorsal funiculus (Length/Width)	2.8 ± 0.19	0.46 ± 0.04	0.52 ± 0.04	2.56 ± 0.09
dorsal gray matter (Dorsal length/DGM length)	4.38 ± 0.41	1.4 ± 0.05	1.39 ± 0.03	3.77 ± 0.12

Table 1.2 Premotor interneuron distribution of Q motor neurons (median)

% interneurons	WT	Con*EphA4*	*EphA4*	Con *α2chimaerin*
dorsal ipsi	49.25	55.41	43.63	47.77
dorsal contra	3.45	13.95	4.59	3.42
ventral ipsi	30.35	17.94	33.14	30.40
ventral contra	17.37	12.70	17.38	15.92

Table 1.3 Premotor interneuron distribution of TA and GS motor neurons (median)

% interneurons	TA		GS	
	WT	Con*EphA4*	WT	Con*EphA4*
dorsal ipsi	61.54	56.18	65.30	46.86
dorsal contra	1.92	14.41	3.68	6.77
ventral ipsi	27.31	19.18	22.99	27.10
ventral contra	9.21	8.93	9.06	17.19

Table 1.4 Gait types of adult wild type mice (median)

% gait types	12 cm/s	16 cm/s	20 cm/s	30 cm/s	40 cm/s	50 cm/s
ALT	86.46	90.64	93.91	92.71	93.60	97.16
TS	13.02	9.36	6.09	6.92	6.40	2.84
MIX	1.01	0	0	0	0	0
synHOP	0	0	0	0.4	0	0

Table 1.5 Gait types of adult conditional *EphA4* mutants (median)

% gait types	12 cm/s	16 cm/s	20 cm/s	30 cm/s	40 cm/s	50 cm/s
ALT	76.26	81.71	88.30	97.02	99.03	99.25
TS	17.18	13.65	9.64	2.98	0.97	0.75
MIX	5.09	3.98	2.02	0	0	0
synHOP	0	0.24	0	0	0	0.26

Table 1.6 Gait types of adult full *EphA4* mutants (median)

% gait types	12 cm/s	16 cm/s	20 cm/s	30 cm/s	40 cm/s
ALT	0	0	0	0	0
TS	0	0	0	0	0
MIX	5.78	7.50	2.45	0.46	0
synHOP	94.22	92.50	97.39	99.54	100

Table 1.7 Gait types of 3-week old wild type mice (median)

% gait types	12 cm/s	16 cm/s	20 cm/s	30 cm/s	40 cm/s	50 cm/s
ALT	87.88	93.46	95.48	97.69	98.28	99.05
TS	11.51	6.54	4.52	2.31	1.72	0.42
MIX	0.54	0	0	0	0	0
synHOP	0	0	0	0	0	0

Table 1.8 Gait types of 3-week old conditional *EphA4* mutants (median)

% gait types	12 cm/s	16 cm/s	20 cm/s	30 cm/s	40 cm/s	50 cm/s
ALT	93.56	92.29	94.92	94.81	93.83	87.67
TS	5.91	7.00	4.02	3.63	3.01	5.27
MIX	0.26	0	0.15	0.56	0.65	1.39
synHOP	0.49	0.20	0.18	0.72	2.69	4.03

Table 1.9 Percentage of HOP gait of wild type and *EphA4* mutant mice (median)

% HOP gait type	12 cm/s	16 cm/s	20 cm/s	30 cm/s	40 cm/s	50 cm/s
adult WT	1.01	0	0	0.40	0	0
adult Con*EphA4*	6.18	4.77	2.18	0	0	0.26
adult *EphA4*	100	100	100	100	100	n/a
3-week WT	0.54	0	0	0	0	0
3-week Con*EphA4*	0.54	0.70	0.36	1.28	3.26	6.34

Table 1.10 Percentage of HOP gait for each conditional *EphA4* mutant mouse (mean of 3 trials)

% HOP gait type	12 cm/s		16 cm/s		20 cm/s	
mouse	3-week	adult	3-week	adult	3-week	adult
# 1	0.57	0	1.41	0.63	0.41	0
# 2	0	11.51	1.97	6.12	3.49	3.38
# 3	1.52	9.79	0	2.22	0.31	0.97
# 4	0.51	10.55	0	3.41	0.72	3.96
# 5	0.48	1.09	0	15.86	0	10.66
# 6	2.75	2.58	3.41	6.31	0	0.48

% HOP gait type	30 cm/s		40 cm/S		50 cm/s	
mouse	3-week	adult	3-week	adult	3-week	adult
# 1	0	0	n/a	0	n/a	0.53
# 2	1.00	0.74	19.41	0	n/a	0.52
# 3	0	0	14.39	0	n/a	0
# 4	2.12	0	3.26	0	6.34	0
# 5	5.12	2.23	3.16	3.80	11.46	5.65
# 6	1.57	0	0.79	0	3.49	0

Table 1.11 Gait parameters (median)

gait parameters	16 cm/s				40 cm/s	
	WT ALT	Con*EphA4* ALT	Con*EphA4* HOP	*EphA4* HOP	WT ALT	Con*EphA4* ALT
Hindlimb Coupling	0.46	0.44	0.17	0.02	0.48	0.46
Diagonal Feet Coupling (HL)	0.10	0.12	0.18	0.36	0.03	0.08
Stride Length (HL) [mm]	53.01	55.13	42.02	48.87	67.05	68.56
Stride Frequency (HL) [Hz]	2.78	3.46	3.51	3.19	5.05	5.55
Stance Time (HL) [ms]	235	204.5	209.1	228.6	100	91.82
Swing Time (HL) [ms]	128	95.73	77.5	88.64	98.18	83.19
Swing Time Percentage HL [%]	35.92	32.18	27.15	27.77	49.66	47.17
Hindlimb Track Width [mm]	20.08	18.76	18.57	22.88	20.25	16.24
Forelimb Coupling	0.43	0.44	0.22	0.02	0.47	0.46
Stance Time (FL) [ms]	220	175.9	138.3	196.7	94.55	90.91
Swing Time (FL) [ms]	142.8	99.51	95	86.44	100	87.28

Table 1.12 Open field behavior (median)

10 min	WT	Con*EphA4*
Avg. Velocity [cm/s]	7.90	6.62
Track Length [m]	47.44	39.68

Table 1.13 Gait types of conditional *EphA4*$^{flox/-}$*vGAT*$^{Cre/+}$ mutants (mean of 3 trials)

% gait types	12 cm/s		16 cm/s		20 cm/s		30 cm/s	40 cm/s
mouse	# 1	# 2	# 1	# 2	# 1	# 2	# 1	# 1
ALT	36.08	9.66	19.63	11.11	12.61	5.41	9.81	1.19
TS	13.95	7.49	10.09	6.79	5.38	5.41	4.75	1.19
MIX	28.27	34.80	19.69	27.78	22.65	29.73	11.03	0.79
synHOP	21.70	48.04	50.58	54.32	59.37	59.46	74.41	96.83

Table 1.14 Gait types of conditional *α2chimaerin* mutants (median)

% gait types	12 cm/s	16 cm/s	20 cm/s
ALT	88.98	91.13	92.37
TS	11.02	7.67	6.81
MIX	1.10	0.31	0.82
synHOP	0	0	0

Table 1.15 Gait types of full *α2chimaerin* mutants (median)

% gait types	12 cm/s	16 cm/s	20 cm/s
ALT	24.42	37.11	12.22
TS	8.73	7.93	5.33
MIX	23.53	27.89	27.27
synHOP	39.83	25.35	56.49

Table 1.16 Percentage of HOP gait type of *α2chimaerin* mutants (median)

% HOP gait type	12 cm/s	16 cm/s	20 cm/s
WT	1.01	0	0
Con *α2chimaerin*	1.10	0.31	0.82
α2chimaerin	65.2	53.2	82.71
EphA4	100	100	100

2. Tables of statistical tests

(significant difference when P/FDR value < 0.05)

Table 2.1: Comparison of dorsal funiculus and dorsal gray matter in *EphA4* mutants and *α2chimaerin* mutants

Ratio	One-way ANOVA Test (P value)	post-hoc Tukey-Kramer Test (P value)			Unpaired t test (P value)
		WT vs Con*EphA4*	Con*EphA4* vs *EphA4*	WT vs *EphA4*	WT vs Con *α2chimaerin*
dorsal funiculus (Length/Width)	< 0.0001	< 0.0001	0.9431	< 0.0001	0.3165
dorsal gray matter (Dorsal length/GM length)	< 0.0001	0.0001	0.9997	< 0.0001	0.2352

Table 2.2: Comparison of interneuron distribution of Q motor neurons in *EphA4* mutants and *α2chimaerin* mutants

% interneurons	Kruskal Wallis Test (P value)	post-hoc Pairwise Wilcoxon Test (FDR value)			Mann-Whitney Test (P value)
		WT vs Con*EphA4*	Con*EphA4* vs *EphA4*	WT vs *EphA4*	WT vs Con *α2chimaerin*
dorsal contralateral	0.0095	0.06408	0.14323	0.02334	> 0.9999
ventral ipsilateral	0.2166	n/a	n/a	n/a	n/a

Table 2.3: Comparison of interneuron distribution of TA and GS motor neurons in conditional *EphA4* mutants

% interneurons	Mann-Whitney Test (P value)	
	TA WT vs Con*EphA4*	GS WT vs Con*EphA4*
dorsal contralateral	0.0159	0.0357
ventral ipsilateral	0.0635	0.0357

Table 2.4: Comparison of HOP gait of *EphA4* mutants between speeds within genotype

% HOP gait type	Kruskal Wallis Test (P value)	post-hoc Pairwise Wilcoxon Test (FDR value)			
		12 vs 16 cm/s	12 vs 20 cm/s	12 vs 30 cm/s	12 vs 40 cm/s
WT	0.0744	n/a	n/a	n/a	n/a
Con*EphA4*	0.0122	1	0.58799	0.09789	0.09789
EphA4	0.8183	n/a	n/a	n/a	n/a

% HOP gait type	post-hoc Pairwise Wilcoxon Test (FDR value)				
	12 vs 50 cm/s	16 vs 20 cm/s	16 vs 30 cm/s	16 vs 40 cm/s	16 vs 50 cm/s
WT	n/a	n/a	n/a	n/a	n/a
Con*EphA4*	0.1271	0.3935	0.07784	0.07784	0.07784
EphA4	n/a	n/a	n/a	n/a	n/a

% HOP gait type	post-hoc Pairwise Wilcoxon Test (FDR value)					
	20 vs 30 cm/s	20 vs 40 cm/s	20 vs 50 cm/s	30 vs 40 cm/s	30 vs 50 cm/s	40 vs 50 cm/s
WT	n/a	n/a	n/a	n/a	n/a	n/a
Con*EphA4*	0.1271	0.12334	0.36918	0.7725	0.7725	0.40182
EphA4	n/a	n/a	n/a	n/a	n/a	n/a

Table 2.5: Comparison of HOP gait of *EphA4* mutants between genotypes within speed

% HOP gait type	Kruskal Wallis Test (P value)	post-hoc Pairwise Wilcoxon Test (FDR value)		
		WT vs Con*EphA4*	Con*EphA4* vs *EphA4*	WT vs *EphA4*
12 cm/s	< 0.0001	0.15236	0.00018	0.00005
16 cm/s	< 0.0001	0.00118	0.00034	0.00004
20 cm/s	< 0.0001	0.01489	0.00034	0.00005
30 cm/s	0.0104	0.28071	0.01342	0.0369
40 cm/s	0.0242	0.4795	0.02092	0.0455
Mann-Whitney Test (P value)				
50 cm/s	n/a	0.5238	n/a	n/a

Table 2.6: Comparison of HOP gait of 3-week old conditional *EphA4* mutants between speeds within genotype

% HOP gait type	Kruskal Wallis Test (P value)	post-hoc Pairwise Wilcoxon Test (FDR value)			
		12 vs 16 cm/s	12 vs 20 cm/s	12 vs 30 cm/s	12 vs 40 cm/s
3-week WT	0.3435	n/a	n/a	n/a	n/a
3-week Con*EphA4*	0.024	0.86447	0.63011	0.75545	0.07551

% HOP gait type	post-hoc Pairwise Wilcoxon Test (FDR value)				
	12 vs 50 cm/s	16 vs 20 cm/s	16 vs 30 cm/s	16 vs 40 cm/s	16 vs 50 cm/s
3-week WT	n/a	n/a	n/a	n/a	n/a
3-week Con*EphA4*	0.07551	1	0.75545	0.14013	0.07551

% HOP gait type	post-hoc Pairwise Wilcoxon Test (FDR value)					
	20 vs 30 cm/s	20 vs 40 cm/s	20 vs 50 cm/s	30 vs 40 cm/s	30 vs 50 cm/s	40 vs 50 cm/s
3-week WT	n/a	n/a	n/a	n/a	n/a	n/a
3-week Con*EphA4*	0.63011	0.0843	0.07551	0.1867	0.09514	0.75545

Table 2.7: Comparison of HOP gait of 3-week old and adult conditional *EphA4* mutants between genotypes within speed

% HOP gait type	Mann-Whitney Test (P value)		Wilcoxon Matched-Paired Test (P value)
	WT vs Con*EphA4* (3-week)	3-week vs adult Con*EphA4*	3-week vs adult Con*EphA4*
12 cm/s	0.7738	0.1385	0.1563
16 cm/s	0.7024	0.0411	0.0625
20 cm/s	0.1667	0.1775	0.1563
30 cm/s	0.1667	0.2749	0.125
40 cm/s	0.0357	0.0216	0.125
50 cm/s	0.1	0.0357	0.25

Table 2.8: Comparison of gait parameters of *EphA4* mutants between genotypes within speed

Gait parameters	Belt speed	Mann-Whitney Test (P value)		
		WT(ALT) vs Con*EphA4*(ALT)	Con*EphA4*(HOP) vs *EphA4*(HOP)	Con*EphA4*(ALT) vs Con*EphA4*(HOP)
Hindlimb Coupling				
	16 cm/s	0.2624	0.0003	0.0043
	40 cm/s	0.0595	n/a	n/a
Diagonal Feet Coupling (hindlimb)				
	16 cm/s	0.3192	0.0023	0.1342
	40 cm/s	0.0357	n/a	n/a
Stride Length (hindlimb)				
	16 cm/s	0.7842	0.4109	n/a
	40 cm/s	0.619	n/a	n/a
Stride Frequency (hindlimb)				
	16 cm/s	0.0142	0.0033	n/a
	40 cm/s	0.5	n/a	n/a
Stance Time (hindlimb)				
	16 cm/s	0.1718	0.0423	n/a
	40 cm/s	0.4286	n/a	n/a
Swing Time (hindlimb)				
	16 cm/s	0.011	0.0523	n/a
	40 cm/s	0.1667	n/a	n/a
Swing Time Percentage (hindlimb)				
	16 cm/s	0.1746	0.4795	n/a
	40 cm/s	0.381	n/a	n/a
Hindlimb Track Width				
	16 cm/s	0.3511	0.0173	n/a
	40 cm/s	0,2619	n/a	n/a
Forelimb Coupling				
	16 cm/s	> 0.9999	0.0003	0.0022
	40 cm/s	0,119	n/a	n/a
Stance Time (forelimb)				
	16 cm/s	0.0209	0.0193	n/a
	40 cm/s	0.7143	n/a	n/a
Swing Time (forelimb)				
	16 cm/s	0.0225	0.5335	n/a
	40 cm/s	0.1905	n/a	n/a

Table 2.9: Comparison of hindlimb gait parameters between speeds of 16 and 40 cm/s within genotype

Gait parameter Hindlimb	Mann-Whitney Test (P value)			
	Hindlimb Coupling	Diagonal Feet Coupling (HL)	Stride Length (HL)	Stride Frequency (HL)
WT (ALT)	0.2483	0.007	0.007	0.007
Con*EphA4* (ALT)	0.3463	0.1385	0.026	0.0022

Gait parameter Hindlimb	Mann-Whitney Test (P value)			
	Stance Time (HL)	Swing Time (HL)	Swing Time % (HL)	Hindlimb Track Width
WT (ALT)	0.0035	0.049	0.007	> 0.9999
Con*EphA4* (ALT)	0.0022	0.3052	0.0022	> 0.9999

Table 2.10: Comparison of forelimb gait parameters between speeds of 16 and 40 cm/s within genotype

Gait parameter Forelimb	Mann-Whitney Test (P value)		
	Forelimb Coupling	Stance Time (FL)	Swing Time (FL)
WT (ALT)	0.0035	0.007	0.049
Con*EphA4* (ALT)	0.0216	0.0022	0.132

Table 2.11: Open Field Behavior

10 min	Mann-Whitney Test (P value)
	WT vs Con*EphA4*
Avg. Velocity	0.3524
Total Track Length	0.3524

Table 2.12: Comparison of HOP gait of *α2chimaerin* mutants between speeds within genotype

% HOP gait type	Kruskal Wallis Test (P value)	post-hoc Pairwise Wilcoxon Test (FDR value)		
		12 vs 16 cm/s	12 vs 20 cm/s	16 vs 20 cm/s
WT	0.0568	n/a	n/a	n/a
Con *α2chimaerin*	0.7974	n/a	n/a	n/a
α2chimaerin	0.307	n/a	n/a	n/a

Table 2.13: Comparison of HOP gait of *α2chimaerin* mutants between genotypes within speed

% HOP gait type	Kruskal Wallis Test (P value)	post-hoc Pairwise Wilcoxon Test (FDR value)		
		WT vs Con *α2chimaerin*	Con *α2chimaerin* vs *α2chimaerin*	WT vs *α2chimaerin*
12 cm/s	0.0024	0.55601	0.02016	0.00424
16 cm/s	0.0007	0.28785	0.02016	0.00173
20 cm/s	0.0002	0.05027	0.02092	0.00252

Table 2.14: Comparison of HOP and synHOP gait types between full *α2chimaerin* versus full *EphA4* mutants

Gait type	Mann-Whitney Test (P value)	
	% HOP	% synHOP
12 cm/s	0.001	0.004
16 cm/s	0.001	0.002
20 cm/s	0.001	0.002

3. AAV-glycoprotein production

Table 3: Preparation of Iodixanol solutions

	10xPBS (ml)	1M $MgCl_2$ (ml)	1M KCl (ml)	5M NaCl (ml)	Optiprep (Iodixanol, Sigma)(ml)	0,5%Phenol red (Sigma) (ml)	H_2O (ml)
17%	5	0.05	0.125	10	12.5	-	up to 50
25%	5	0.05	0.125	-	20	0.2	up to 50
40%	5	0.05	0.125	-	33.3	-	up to 50
60%	-	0.05	0.125	-	50	0.05	-

List of Figures

Abbreviations

AAV	adeno-associated virus
ALT	alternating gait type of hindlimbs
BHK	baby hamster kidney cells
BMP	bone morphogenetic protein
BSA	bovine serum albumin
C segment	cervical segment of spinal cord
CC	central canal in spinal cord
ChAT	choline acetyltransferase
Con*EphA4*	conditional EphA4 mutant mouse (*EphA4*$^{flox/-}$*Lbx1*$^{Cre/+}$ *Tau*$^{lox\text{-}stop\text{-}lox\text{-}SynGFP\text{-}INLA}$ and *EphA4*$^{flox/-}$*Lbx1*$^{Cre/+}$ *Tau*$^{lox\text{-}stop\text{-}lox\text{-}FlpO\text{-}INLA}$ mutant mice (figures)
conditional *EphA4*	*EphA4*$^{flox/-}$*Lbx1*$^{Cre/+}$ or *EphA4*$^{flox/-}$*Lbx1*$^{Cre/+}$ *Tau*$^{lox\text{-}stop\text{-}lox\text{-}SynGFP\text{-}INLA}$ or *EphA4*$^{flox/-}$*Lbx1*$^{Cre/+}$ *Tau*$^{lox\text{-}stop\text{-}lox\text{-}FlpO\text{-}INLA}$ mutant mice (text)
CPG	central pattern generator
DGM	dorsal gray matter
DMEM	dulbecco`s modified eagle medium
E	embryonic stage of development
EphA4	full *EphA4*$^{-/-}$ k.o. mutant mouse (figures)
FBS	foetal bovine serum
FDR	false discovery rate
full *EphA4*	full *EphA4*$^{-/-}$ k.o. mutant mouse (text)
G-protein	glycoprotein of rabies virus
GEF	guanine nucleotide exchange factor
GFP	green fluorescent protein
GS	Gastrocnemius muscle (extensor)
HEK	human embryonic kidney cells
HOP	hopping gait type of hindlimbs (includes synHOP and MIX gait types)
IN	interneuron

L segment	lumbar segment of spinal cord
MIX	mixture gait type of hindlimbs (mixture between alternating and hopping gait)
MN	motor neuron
P	postnatal stage of development
PBS	phosphate buffered saline
PCR	polymerase chain reaction
Q	Quadriceps muscle (extensor)
RFP	red fluorescent protein
S segment	sacral segments of spinal cord
SEM	standard error of the mean
Shh	sonic hedgehog
synHOP	synchronous hopping gait type of hindlimbs
T segment	thoracic segment of spinal cord
TA	Tibialis anterior muscle (flexor)
TS	transitional step of hindlimbs
WT	wild type (figures)

References

(1997). "Unified nomenclature for Eph family receptors and their ligands, the ephrins. Eph Nomenclature Committee." Cell **90**(3): 403-404.

Akay, T., H. J. Acharya, K. Fouad and K. G. Pearson (2006). "Behavioral and electromyographic characterization of mice lacking EphA4 receptors." J Neurophysiol **96**(2): 642-651.

Al-Mosawie, A., J. M. Wilson and R. M. Brownstone (2007). "Heterogeneity of V2-derived interneurons in the adult mouse spinal cord." Eur J Neurosci **26**(11): 3003-3015.

Alaynick, W. A., T. M. Jessell and S. L. Pfaff (2011). "SnapShot: spinal cord development." Cell **146**(1): 178-178.e171.

Alvarez, F. J. and R. E. Fyffe (2007). "The continuing case for the Renshaw cell." J Physiol **584**(Pt 1): 31-45.

Alvarez, F. J., P. C. Jonas, T. Sapir, R. Hartley, M. C. Berrocal, E. J. Geiman, A. J. Todd and M. Goulding (2005). "Postnatal phenotype and localization of spinal cord V1 derived interneurons." J Comp Neurol **493**(2): 177-192.

Andersson, L. S., M. Larhammar, F. Memic, H. Wootz, D. Schwochow, C. J. Rubin, K. Patra, T. Arnason, L. Wellbring, G. Hjalm, F. Imsland, J. L. Petersen, M. E. McCue, J. R. Mickelson, G. Cothran, N. Ahituv, L. Roepstorff, S. Mikko, A. Vallstedt, G. Lindgren, L. Andersson and K. Kullander (2012). "Mutations in DMRT3 affect locomotion in horses and spinal circuit function in mice." Nature **488**(7413): 642-646.

Armatas, C. A., J. J. Summers and J. L. Bradshaw (1994). "Mirror movements in normal adult subjects." J Clin Exp Neuropsychol **16**(3): 405-413.

Asante, C. O., A. Chu, M. Fisher, L. Benson, A. Beg, P. Scheiffele and J. Martin (2010). "Cortical control of adaptive locomotion in wild-type mice and mutant mice lacking the ephrin-Eph effector protein alpha2-chimaerin." J Neurophysiol **104**(6): 3189-3202.

Atsuta, Y., E. Garcia-Rill and R. D. Skinner (1990). "Characteristics of electrically induced locomotion in rat in vitro brain stem-spinal cord preparation." J Neurophysiol **64**(3): 727-735.

Augsburger, A., A. Schuchardt, S. Hoskins, J. Dodd and S. Butler (1999). "BMPs as mediators of roof plate repulsion of commissural neurons." Neuron **24**(1): 127-141.

Barbeau, H. and S. Rossignol (1987). "Recovery of locomotion after chronic spinalization in the adult cat." Brain Res **412**(1): 84-95.

Barthe, J. Y. and F. Clarac (1997). "Modulation of the spinal network for locomotion by substance P in the neonatal rat." Exp Brain Res **115**(3): 485-492.

Beg, A. A., J. E. Sommer, J. H. Martin and P. Scheiffele (2007). "alpha2-Chimaerin is an essential EphA4 effector in the assembly of neuronal locomotor circuits." Neuron **55**(5): 768-778.

Bergemann, A. D., L. Zhang, M. K. Chiang, R. Brambilla, R. Klein and J. G. Flanagan (1998). "Ephrin-B3, a ligand for the receptor EphB3, expressed at the midline of the developing neural tube." Oncogene **16**(4): 471-480.

Berkowitz, A. (2008). "Physiology and morphology of shared and specialized spinal interneurons for locomotion and scratching." J Neurophysiol **99**(6): 2887-2901.

Bermingham, N. A., B. A. Hassan, V. Y. Wang, M. Fernandez, S. Banfi, H. J. Bellen, B. Fritzsch and H. Y. Zoghbi (2001). "Proprioceptor pathway development is dependent on Math1." Neuron **30**(2): 411-422.

Betley, J. N., C. V. Wright, Y. Kawaguchi, F. Erdelyi, G. Szabo, T. M. Jessell and J. A. Kaltschmidt (2009). "Stringent specificity in the construction of a GABAergic presynaptic inhibitory circuit." Cell **139**(1): 161-174.

Bjursten, L. M., K. Norrsell and U. Norrsell (1976). "Behavioural repertory of cats without cerebral cortex from infancy." Exp Brain Res **25**(2): 115-130.

Borgius, L., H. Nishimaru, V. Caldeira, Y. Kunugise, P. Low, R. Reig, S. Itohara, T. Iwasato and O. Kiehn (2014). "Spinal Glutamatergic Neurons Defined by EphA4 Signaling Are Essential Components of Normal Locomotor Circuits." J Neurosci **34**(11): 3841-3853.

Brohmann, H., K. Jagla and C. Birchmeier (2000). "The role of Lbx1 in migration of muscle precursor cells." Development **127**(2): 437-445.

Brose, K., K. S. Bland, K. H. Wang, D. Arnott, W. Henzel, C. S. Goodman, M. Tessier-Lavigne and T. Kidd (1999). "Slit proteins bind Robo receptors and have an evolutionarily conserved role in repulsive axon guidance." Cell **96**(6): 795-806.

Brown, T. G. (1914). "On the nature of the fundamental activity of the nervous centres; together with an analysis of the conditioning of rhythmic activity in progression, and a theory of the evolution of function in the nervous system." J Physiol **48**(1): 18-46.

Bruckner, K., E. B. Pasquale and R. Klein (1997). "Tyrosine phosphorylation of transmembrane ligands for Eph receptors." Science **275**(5306): 1640-1643.

Butt, S. J., R. M. Harris-Warrick and O. Kiehn (2002). "Firing properties of identified interneuron populations in the mammalian hindlimb central pattern generator." J Neurosci **22**(22): 9961-9971.

Butt, S. J. and O. Kiehn (2003). "Functional identification of interneurons responsible for left-right coordination of hindlimbs in mammals." Neuron **38**(6): 953-963.

Butt, S. J., L. Lundfald and O. Kiehn (2005). "EphA4 defines a class of excitatory locomotor-related interneurons." Proc Natl Acad Sci U S A **102**(39): 14098-14103.

Canty, A. J., U. Greferath, A. M. Turnley and M. Murphy (2006). "Eph tyrosine kinase receptor EphA4 is required for the topographic mapping of the corticospinal tract." Proc Natl Acad Sci U S A **103**(42): 15629-15634.

Cazalets, J. R., Y. Sqalli-Houssaini and F. Clarac (1992). "Activation of the central pattern generators for locomotion by serotonin and excitatory amino acids in neonatal rat." J Physiol **455**: 187-204.

Chaudhry, F. A., R. J. Reimer, E. E. Bellocchio, N. C. Danbolt, K. K. Osen, R. H. Edwards and J. Storm-Mathisen (1998). "The vesicular GABA transporter, VGAT, localizes to synaptic vesicles in sets of glycinergic as well as GABAergic neurons." J Neurosci **18**(23): 9733-9750.

Cheng, H. J., M. Nakamoto, A. D. Bergemann and J. G. Flanagan (1995). "Complementary gradients in expression and binding of ELF-1 and Mek4 in development of the topographic retinotectal projection map." Cell **82**(3): 371-381.

Cheng, L., A. Arata, R. Mizuguchi, Y. Qian, A. Karunaratne, P. A. Gray, S. Arata, S. Shirasawa, M. Bouchard, P. Luo, C. L. Chen, M. Busslinger, M. Goulding, H. Onimaru and Q. Ma (2004). "Tlx3 and Tlx1 are post-mitotic selector genes determining glutamatergic over GABAergic cell fates." Nat Neurosci **7**(5): 510-517.

Cheng, L., O. A. Samad, Y. Xu, R. Mizuguchi, P. Luo, S. Shirasawa, M. Goulding and Q. Ma (2005). "Lbx1 and Tlx3 are opposing switches in determining GABAergic versus glutamatergic transmitter phenotypes." Nat Neurosci **8**(11): 1510-1515.

Cohen, A. H., L. Guan, J. Harris, R. Jung and T. Kiemel (1996). "Interaction between the caudal brainstem and the lamprey central pattern generator for locomotion." Neuroscience **74**(4): 1161-1173.

Coonan, J. R., P. F. Bartlett and M. P. Galea (2003). "Role of EphA4 in defining the position of a motoneuron pool within the spinal cord." J Comp Neurol **458**(1): 98-111.

Coonan, J. R., U. Greferath, J. Messenger, L. Hartley, M. Murphy, A. W. Boyd, M. Dottori, M. P. Galea and P. F. Bartlett (2001). "Development and reorganization of corticospinal projections in EphA4 deficient mice." J Comp Neurol **436**(2): 248-262.

Cowan, C. W., Y. R. Shao, M. Sahin, S. M. Shamah, M. Z. Lin, P. L. Greer, S. Gao, E. C. Griffith, J. S. Brugge and M. E. Greenberg (2005). "Vav family GEFs link activated Ephs to endocytosis and axon guidance." Neuron **46**(2): 205-217.

Cowley, K. C. and B. J. Schmidt (1995). "Effects of inhibitory amino acid antagonists on reciprocal inhibitory interactions during rhythmic motor activity in the in vitro neonatal rat spinal cord." J Neurophysiol **74**(3): 1109-1117.

Crago, P. E., J. C. Houk and W. Z. Rymer (1982). "Sampling of total muscle force by tendon organs." J Neurophysiol **47**(6): 1069-1083.

Crone, S. A., K. A. Quinlan, L. Zagoraiou, S. Droho, C. E. Restrepo, L. Lundfald, T. Endo, J. Setlak, T. M. Jessell, O. Kiehn and K. Sharma (2008). "Genetic ablation of V2a ipsilateral interneurons disrupts left-right locomotor coordination in mammalian spinal cord." Neuron **60**(1): 70-83.

Dai, X., B. R. Noga, J. R. Douglas and L. M. Jordan (2005). "Localization of spinal neurons activated during locomotion using the c-fos immunohistochemical method." J Neurophysiol **93**(6): 3442-3452.

Davis, S., N. W. Gale, T. H. Aldrich, P. C. Maisonpierre, V. Lhotak, T. Pawson, M. Goldfarb and G. D. Yancopoulos (1994). "Ligands for EPH-related receptor tyrosine kinases that require membrane attachment or clustering for activity." Science **266**(5186): 816-819.

Davy, A., N. W. Gale, E. W. Murray, R. A. Klinghoffer, P. Soriano, C. Feuerstein and S. M. Robbins (1999). "Compartmentalized signaling by GPI-anchored ephrin-A5 requires the Fyn tyrosine kinase to regulate cellular adhesion." Genes Dev **13**(23): 3125-3135.

Dodd, J., S. B. Morton, D. Karagogeos, M. Yamamoto and T. M. Jessell (1988). "Spatial regulation of axonal glycoprotein expression on subsets of embryonic spinal neurons." Neuron **1**(2): 105-116.

Dottori, M., L. Hartley, M. Galea, G. Paxinos, M. Polizzotto, T. Kilpatrick, P. F. Bartlett, M. Murphy, F. Kontgen and A. W. Boyd (1998). "EphA4 (Sek1) receptor tyrosine kinase is required for the development of the corticospinal tract." Proc Natl Acad Sci U S A **95**(22): 13248-13253.

Dougherty, K. J., L. Zagoraiou, D. Satoh, I. Rozani, S. Doobar, S. Arber, T. M. Jessell and O. Kiehn (2013). "Locomotor rhythm generation linked to the output of spinal shox2 excitatory interneurons." Neuron **80**(4): 920-933.

Dragunow, M. and R. Faull (1989). "The use of c-fos as a metabolic marker in neuronal pathway tracing." J Neurosci Methods **29**(3): 261-265.

Drescher, U., C. Kremoser, C. Handwerker, J. Loschinger, M. Noda and F. Bonhoeffer (1995). "In vitro guidance of retinal ganglion cell axons by RAGS, a 25 kDa tectal protein related to ligands for Eph receptor tyrosine kinases." Cell **82**(3): 359-370.

Drew, T., J. E. Andujar, K. Lajoie and S. Yakovenko (2008). "Cortical mechanisms involved in visuomotor coordination during precision walking." Brain Res Rev **57**(1): 199-211.

Dyck, J., G. M. Lanuza and S. Gosgnach (2012). "Functional characterization of dI6 interneurons in the neonatal mouse spinal cord." J Neurophysiol **107**(12): 3256-3266.

Egea, J., U. V. Nissen, A. Dufour, M. Sahin, P. Greer, K. Kullander, T. D. Mrsic-Flogel, M. E. Greenberg, O. Kiehn, P. Vanderhaeghen and R. Klein (2005). "Regulation of EphA 4 kinase activity is required for a subset of axon guidance decisions suggesting a key role for receptor clustering in Eph function." Neuron **47**(4): 515-528.

Eide, A. L., J. Glover, O. Kjaerulff and O. Kiehn (1999). "Characterization of commissural interneurons in the lumbar region of the neonatal rat spinal cord." J Comp Neurol **403**(3): 332-345.

Engberg, I. and A. Lundberg (1969). "An electromyographic analysis of muscular activity in the hindlimb of the cat during unrestrained locomotion." Acta Physiol Scand **75**(4): 614-630.

Esposito, M. S., P. Capelli and S. Arber (2014). "Brainstem nucleus MdV mediates skilled forelimb motor tasks." Nature.

Etienne-Manneville, S. and A. Hall (2002). "Rho GTPases in cell biology." Nature **420**(6916): 629-635.

Fawcett, J. P., J. Georgiou, J. Ruston, F. Bladt, A. Sherman, N. Warner, B. J. Saab, R. Scott, J. C. Roder and T. Pawson (2007). "Nck adaptor proteins control the organization of neuronal circuits important for walking." Proc Natl Acad Sci U S A **104**(52): 20973-20978.

Fazeli, A., S. L. Dickinson, M. L. Hermiston, R. V. Tighe, R. G. Steen, C. G. Small, E. T. Stoeckli, K. Keino-Masu, M. Masu, H. Rayburn, J. Simons, R. T. Bronson, J. I. Gordon, M. Tessier-Lavigne and R. A. Weinberg (1997). "Phenotype of mice lacking functional Deleted in colorectal cancer (Dcc) gene." Nature **386**(6627): 796-804.

Feldman, A. G. and G. N. Orlovsky (1975). "Activity of interneurons mediating reciprocal 1a inhibition during locomotion." Brain Res **84**(2): 181-194.

Finger, J. H., R. T. Bronson, B. Harris, K. Johnson, S. A. Przyborski and S. L. Ackerman (2002). "The netrin 1 receptors Unc5h3 and Dcc are necessary at multiple choice points for the guidance of corticospinal tract axons." J Neurosci **22**(23): 10346-10356.

Flanagan, J. G. and P. Vanderhaeghen (1998). "The ephrins and Eph receptors in neural development." Annu Rev Neurosci **21**: 309-345.

Frisen, J., J. Holmberg and M. Barbacid (1999). "Ephrins and their Eph receptors: multitalented directors of embryonic development." Embo j **18**(19): 5159-5165.

Gale, N. W., A. Flenniken, D. C. Compton, N. Jenkins, N. G. Copeland, D. J. Gilbert, S. Davis, D. G. Wilkinson and G. D. Yancopoulos (1996). "Elk-L3, a novel transmembrane ligand for the Eph family of receptor tyrosine kinases, expressed in embryonic floor plate, roof plate and hindbrain segments." Oncogene **13**(6): 1343-1352.

Gale, N. W. and G. D. Yancopoulos (1997). "Ephrins and their receptors: a repulsive topic?" Cell Tissue Res **290**(2): 227-241.

Garcia-Rill, E. and R. D. Skinner (1987). "The mesencephalic locomotor region. II. Projections to reticulospinal neurons." Brain Res **411**(1): 13-20.

Gezelius, H., A. Wallen-Mackenzie, A. Enjin, M. Lagerstrom and K. Kullander (2006). "Role of glutamate in locomotor rhythm generating neuronal circuitry." J Physiol Paris **100**(5-6): 297-303.

Glasgow, S. M., R. M. Henke, R. J. Macdonald, C. V. Wright and J. E. Johnson (2005). "Ptf1a determines GABAergic over glutamatergic neuronal cell fate in the spinal cord dorsal horn." Development **132**(24): 5461-5469.

Gosgnach, S., G. M. Lanuza, S. J. Butt, H. Saueressig, Y. Zhang, T. Velasquez, D. Riethmacher, E. M. Callaway, O. Kiehn and M. Goulding (2006). "V1 spinal neurons regulate the speed of vertebrate locomotor outputs." Nature **440**(7081): 215-219.

Goulding, M. (2009). "Circuits controlling vertebrate locomotion: moving in a new direction." Nat Rev Neurosci **10**(7): 507-518.

Goulding, M., G. Lanuza, T. Sapir and S. Narayan (2002). "The formation of sensorimotor circuits." Curr Opin Neurobiol **12**(5): 508-515.

Gowan, K., A. W. Helms, T. L. Hunsaker, T. Collisson, P. J. Ebert, R. Odom and J. E. Johnson (2001). "Crossinhibitory activities of Ngn1 and Math1 allow specification of distinct dorsal interneurons." Neuron **31**(2): 219-232.

Greferath, U., A. J. Canty, J. Messenger and M. Murphy (2002). "Developmental expression of EphA4-tyrosine kinase receptor in the mouse brain and spinal cord." Mech Dev **119 Suppl 1**: S231-238.

Grillner, S. (1975). "Locomotion in vertebrates: central mechanisms and reflex interaction." Physiol Rev **55**(2): 247-304.

Grillner, S. (2003). "The motor infrastructure: from ion channels to neuronal networks." Nat Rev Neurosci **4**(7): 573-586.

Grillner, S. (2006). "Biological pattern generation: the cellular and computational logic of networks in motion." Neuron **52**(5): 751-766.

Grillner, S., T. Deliagina, O. Ekeberg, A. el Manira, R. H. Hill, A. Lansner, G. N. Orlovsky and P. Wallen (1995). "Neural networks that co-ordinate locomotion and body orientation in lamprey." Trends Neurosci **18**(6): 270-279.

Grillner, S. and T. Matsushima (1991). "The neural network underlying locomotion in lamprey--synaptic and cellular mechanisms." Neuron **7**(1): 1-15.

Grillner, S., A. McClellan and C. Perret (1981). "Entrainment of the spinal pattern generators for swimming by mechano-sensitive elements in the lamprey spinal cord in vitro." Brain Res **217**(2): 380-386.

Grillner, S. and S. Rossignol (1978). "On the initiation of the swing phase of locomotion in chronic spinal cats." Brain Res **146**(2): 269-277.

Gross, M. K., M. Dottori and M. Goulding (2002). "Lbx1 specifies somatosensory association interneurons in the dorsal spinal cord." Neuron **34**(4): 535-549.

Grossmann, K. S., A. Giraudin, O. Britz, J. Zhang and M. Goulding (2010). "Genetic dissection of rhythmic motor networks in mice." Prog Brain Res **187**: 19-37.

Gundersen, R. W. and J. N. Barrett (1979). "Neuronal chemotaxis: chick dorsal-root axons turn toward high concentrations of nerve growth factor." Science **206**(4422): 1079-1080.

Hagglund, M., L. Borgius, K. J. Dougherty and O. Kiehn (2010). "Activation of groups of excitatory neurons in the mammalian spinal cord or hindbrain evokes locomotion." Nat Neurosci **13**(2): 246-252.

Hall, C., C. Monfries, P. Smith, H. H. Lim, R. Kozma, S. Ahmed, V. Vanniasingham, T. Leung and L. Lim (1990). "Novel human brain cDNA encoding a 34,000 Mr protein n-chimaerin, related to both the regulatory domain of protein kinase C and BCR, the product of the breakpoint cluster region gene." J Mol Biol **211**(1): 11-16.

Hall, C., W. C. Sin, M. Teo, G. J. Michael, P. Smith, J. M. Dong, H. H. Lim, E. Manser, N. K. Spurr, T. A. Jones and et al. (1993). "Alpha 2-chimerin, an SH2-containing GTPase-activating protein for the ras-related protein p21rac derived by alternate splicing of the human n-chimerin gene, is selectively expressed in brain regions and testes." Mol Cell Biol **13**(8): 4986-4998.

Hammar, I., B. A. Bannatyne, D. J. Maxwell, S. A. Edgley and E. Jankowska (2004). "The actions of monoamines and distribution of noradrenergic and serotoninergic contacts on different subpopulations of commissural interneurons in the cat spinal cord." Eur J Neurosci **19**(5): 1305-1316.

Hammar, I., K. Stecina and E. Jankowska (2007). "Differential modulation by monoamine membrane receptor agonists of reticulospinal input to lamina VIII feline spinal commissural interneurons." Eur J Neurosci **26**(5): 1205-1212.

Helmbacher, F., S. Schneider-Maunoury, P. Topilko, L. Tiret and P. Charnay (2000). "Targeting of the EphA4 tyrosine kinase receptor affects dorsal/ventral pathfinding of limb motor axons." Development **127**(15): 3313-3324.

Helms, A. W. and J. E. Johnson (1998). "Progenitors of dorsal commissural interneurons are defined by MATH1 expression." Development **125**(5): 919-928.

Helms, A. W. and J. E. Johnson (2003). "Specification of dorsal spinal cord interneurons." Curr Opin Neurobiol **13**(1): 42-49.

Henkemeyer, M., D. Orioli, J. T. Henderson, T. M. Saxton, J. Roder, T. Pawson and R. Klein (1996). "Nuk controls pathfinding of commissural axons in the mammalian central nervous system." Cell **86**(1): 35-46.

Herrmann, J. E., M. A. Pence, E. A. Shapera, R. R. Shah, C. G. Geoffroy and B. Zheng (2010). "Generation of an EphA4 conditional allele in mice." Genesis **48**(2): 101-105.

Hildebrand, M. (1989). “The quadrupedal gaits of vertebrates.” BioScience **39** (11): 766-775

Hippenmeyer, S., E. Vrieseling, M. Sigrist, T. Portmann, C. Laengle, D. R. Ladle and S. Arber (2005). "A developmental switch in the response of DRG neurons to ETS transcription factor signaling." PLoS Biol **3**(5): e159.

Holland, S. J., N. W. Gale, G. Mbamalu, G. D. Yancopoulos, M. Henkemeyer and T. Pawson (1996). "Bidirectional signalling through the EPH-family receptor Nuk and its transmembrane ligands." Nature **383**(6602): 722-725.

Hulliger, M. (1984). "The mammalian muscle spindle and its central control." Rev Physiol Biochem Pharmacol **101**: 1-110.

Hultborn, H., E. Jankowska and S. Lindstrom (1971). "Recurrent inhibition of interneurones monosynaptically activated from group Ia afferents." J Physiol **215**(3): 613-636.

Imondi, R., C. Wideman and Z. Kaprielian (2000). "Complementary expression of transmembrane ephrins and their receptors in the mouse spinal cord: a possible role in constraining the orientation of longitudinally projecting axons." Development **127**(7): 1397-1410.

Iwasato, T., H. Katoh, H. Nishimaru, Y. Ishikawa, H. Inoue, Y. M. Saito, R. Ando, M. Iwama, R. Takahashi, M. Negishi and S. Itohara (2007). "Rac-GAP alpha-chimerin regulates motor-circuit formation as a key mediator of EphrinB3/EphA4 forward signaling." Cell **130**(4): 742-753.

Jagla, K., P. Dolle, M. G. Mattei, T. Jagla, B. Schuhbaur, G. Dretzen, F. Bellard and M. Bellard (1995). "Mouse Lbx1 and human LBX1 define a novel mammalian homeobox gene family related to the Drosophila lady bird genes." Mech Dev **53**(3): 345-356.

Jankowska, E., I. Hammar, B. Chojnicka and C. H. Heden (2000). "Effects of monoamines on interneurons in four spinal reflex pathways from group I and/or group II muscle afferents." Eur J Neurosci **12**(2): 701-714.

Jessell, T. M. (2000). "Neuronal specification in the spinal cord: inductive signals and transcriptional codes." Nat Rev Genet **1**(1): 20-29.

Jessell, T. M., P. Bovolenta, M. Placzek, M. Tessier-Lavigne and J. Dodd (1989). "Polarity and patterning in the neural tube: the origin and function of the floor plate." Ciba Found Symp **144**: 255-276; discussion 276-280, 290-255.

Jordan, L. M. (1998). "Initiation of locomotion in mammals." Ann N Y Acad Sci **860**: 83-93.

Jordan, L. M., R. M. Brownstone and B. R. Noga (1992). "Control of functional systems in the brainstem and spinal cord." Curr Opin Neurobiol **2**(6): 794-801.

Jordan, L. M., J. Liu, P. B. Hedlund, T. Akay and K. G. Pearson (2008). "Descending command systems for the initiation of locomotion in mammals." Brain Res Rev **57**(1): 183-191.

Julius, D. and A. I. Basbaum (2001). "Molecular mechanisms of nociception." Nature **413**(6852): 203-210.

Juvin, L., J. Simmers and D. Morin (2005). "Propriospinal circuitry underlying interlimb coordination in mammalian quadrupedal locomotion." J Neurosci **25**(25): 6025-6035.

Kadison, S. R., T. Makinen, R. Klein, M. Henkemeyer and Z. Kaprielian (2006). "EphB receptors and ephrin-B3 regulate axon guidance at the ventral midline of the embryonic mouse spinal cord." J Neurosci **26**(35): 8909-8914.

Kania, A. and T. M. Jessell (2003). "Topographic motor projections in the limb imposed by LIM homeodomain protein regulation of ephrin-A:EphA interactions." Neuron **38**(4): 581-596.

Kaprielian, Z., E. Runko and R. Imondi (2001). "Axon guidance at the midline choice point." Dev Dyn **221**(2): 154-181.

Katayama, K., J. R. Leslie, R. A. Lang, Y. Zheng and Y. Yoshida (2012). "Left-right locomotor circuitry depends on RhoA-driven organization of the neuroepithelium in the developing spinal cord." J Neurosci **32**(30): 10396-10407.

Katz, P. S. (1995). "Intrinsic and extrinsic neuromodulation of motor circuits." Curr Opin Neurobiol **5**(6): 799-808.

Kennedy, T. E., T. Serafini, J. R. de la Torre and M. Tessier-Lavigne (1994). "Netrins are diffusible chemotropic factors for commissural axons in the embryonic spinal cord." Cell **78**(3): 425-435.

Kidd, T., K. Brose, K. J. Mitchell, R. D. Fetter, M. Tessier-Lavigne, C. S. Goodman and G. Tear (1998). "Roundabout controls axon crossing of the CNS midline and defines a novel subfamily of evolutionarily conserved guidance receptors." Cell **92**(2): 205-215.

Kiehn, O. (2006). "Locomotor circuits in the mammalian spinal cord." Annu Rev Neurosci **29**: 279-306.

Kiehn, O. (2011). "Development and functional organization of spinal locomotor circuits." Curr Opin Neurobiol **21**(1): 100-109.

Kiehn, O., K. J. Dougherty, M. Hagglund, L. Borgius, A. Talpalar and C. E. Restrepo (2010). "Probing spinal circuits controlling walking in mammals." Biochem Biophys Res Commun **396**(1): 11-18.

Kjaerulff, O. and O. Kiehn (1996). "Distribution of networks generating and coordinating locomotor activity in the neonatal rat spinal cord in vitro: a lesion study." J Neurosci **16**(18): 5777-5794.

Kjaerulff, O. and O. Kiehn (1997). "Crossed rhythmic synaptic input to motoneurons during selective activation of the contralateral spinal locomotor network." J Neurosci **17**(24): 9433-9447.

Kolodkin, A. L. (1996). "Growth cones and the cues that repel them." Trends Neurosci **19**(11): 507-513.

Kriellaars, D. J., R. M. Brownstone, B. R. Noga and L. M. Jordan (1994). "Mechanical entrainment of fictive locomotion in the decerebrate cat." J Neurophysiol **71**(6): 2074-2086.

Kudo, N. and T. Yamada (1987). "N-methyl-D,L-aspartate-induced locomotor activity in a spinal cord-hindlimb muscles preparation of the newborn rat studied in vitro." Neurosci Lett **75**(1): 43-48.

Kullander, K., S. J. Butt, J. M. Lebret, L. Lundfald, C. E. Restrepo, A. Rydstrom, R. Klein and O. Kiehn (2003). "Role of EphA4 and EphrinB3 in local neuronal circuits that control walking." Science **299**(5614): 1889-1892.

Kullander, K., S. D. Croll, M. Zimmer, L. Pan, J. McClain, V. Hughes, S. Zabski, T. M. DeChiara, R. Klein, G. D. Yancopoulos and N. W. Gale (2001a). "Ephrin-B3 is the midline barrier that prevents corticospinal tract axons from recrossing, allowing for unilateral motor control." Genes Dev **15**(7): 877-888.

Kullander, K., N. K. Mather, F. Diella, M. Dottori, A. W. Boyd and R. Klein (2001b). "Kinase-dependent and kinase-independent functions of EphA4 receptors in major axon tract formation in vivo." Neuron **29**(1): 73-84.

Lakke, E. A. (1997). "The projections to the spinal cord of the rat during development: a timetable of descent." Adv Anat Embryol Cell Biol **135**: I-xiv, 1-143.

Lanuza, G. M., S. Gosgnach, A. Pierani, T. M. Jessell and M. Goulding (2004). "Genetic identification of spinal interneurons that coordinate left-right locomotor activity necessary for walking movements." Neuron **42**(3): 375-386.

Lee, K. J. and T. M. Jessell (1999). "The specification of dorsal cell fates in the vertebrate central nervous system." Annu Rev Neurosci **22**: 261-294.

Liu, J., T. Akay, P. B. Hedlund, K. G. Pearson and L. M. Jordan (2009). "Spinal 5-HT7 receptors are critical for alternating activity during locomotion: in vitro neonatal and in vivo adult studies using 5-HT7 receptor knockout mice." J Neurophysiol **102**(1): 337-348.

Lundfald, L., C. E. Restrepo, S. J. Butt, C. Y. Peng, S. Droho, T. Endo, H. U. Zeilhofer, K. Sharma and O. Kiehn (2007). "Phenotype of V2-derived interneurons and their relationship to the axon guidance molecule EphA4 in the developing mouse spinal cord." Eur J Neurosci **26**(11): 2989-3002.

Luo, L. (2000). "Rho GTPases in neuronal morphogenesis." Nat Rev Neurosci **1**(3): 173-180.

Luo, L. (2002). "Actin cytoskeleton regulation in neuronal morphogenesis and structural plasticity." Annu Rev Cell Dev Biol **18**: 601-635.

Luria, V., D. Krawchuk, T. M. Jessell, E. Laufer and A. Kania (2008). "Specification of motor axon trajectory by ephrin-B:EphB signaling: symmetrical control of axonal patterning in the developing limb." Neuron **60**(6): 1039-1053.

MacKay-Lyons, M. (2002). "Central pattern generation of locomotion: a review of the evidence." Phys Ther **82**(1): 69-83.

Marin, O., M. Valiente, X. Ge and L. H. Tsai (2010). "Guiding neuronal cell migrations." Cold Spring Harb Perspect Biol **2**(2): a001834.

Marshel, J. H., T. Mori, K. J. Nielsen and E. M. Callaway (2010). "Targeting single neuronal networks for gene expression and cell labeling in vivo." Neuron **67**(4): 562-574.

Martone, M. E., J. A. Holash, A. Bayardo, E. B. Pasquale and M. H. Ellisman (1997). "Immunolocalization of the receptor tyrosine kinase EphA4 in the adult rat central nervous system." Brain Res **771**(2): 238-250.

McHanwell, S. and T. J. Biscoe (1981). "The localization of motoneurons supplying the hindlimb muscles of the mouse." Philos Trans R Soc Lond B Biol Sci **293**(1069): 477-508.

Menzel, P., F. Valencia, P. Godement, V. C. Dodelet and E. B. Pasquale (2001). "Ephrin-A6, a new ligand for EphA receptors in the developing visual system." Dev Biol **230**(1): 74-88.

Meyrand, P., J. Simmers and M. Moulins (1991). "Construction of a pattern-generating circuit with neurons of different networks." Nature **351**(6321): 60-63.

Mori, T., A. Wanaka, A. Taguchi, K. Matsumoto and M. Tohyama (1995). "Differential expressions of the eph family of receptor tyrosine kinase genes (sek, elk, eck) in the developing nervous system of the mouse." Brain Res Mol Brain Res **29**(2): 325-335.

Muller, T., H. Brohmann, A. Pierani, P. A. Heppenstall, G. R. Lewin, T. M. Jessell and C. Birchmeier (2002). "The homeodomain factor lbx1 distinguishes two major programs of neuronal differentiation in the dorsal spinal cord." Neuron **34**(4): 551-562.

Nieto, M. A., P. Gilardi-Hebenstreit, P. Charnay and D. G. Wilkinson (1992). "A receptor protein tyrosine kinase implicated in the segmental patterning of the hindbrain and mesoderm." Development **116**(4): 1137-1150.

Noren, N. K. and E. B. Pasquale (2004). "Eph receptor-ephrin bidirectional signals that target Ras and Rho proteins." Cell Signal **16**(6): 655-666.

O`Leary, C. J. and K. W. McDermott (2011). "Spinal cord neuroepithelial progenitor cells display developmental plasticity when co-cultured with embryonic spinal cord slices at different stages of development." Dev Dyn **240**(4): 785-795.

Pagliardini, S., J. Ren, P. A. Gray, C. Vandunk, M. Gross, M. Goulding and J. J. Greer (2008). "Central respiratory rhythmogenesis is abnormal in lbx1- deficient mice." J Neurosci **28**(43): 11030-11041.

Paixao, S., A. Balijepalli, N. Serradj, J. Niu, W. Luo, J. H. Martin and R. Klein (2013). "EphrinB3/EphA4-mediated guidance of ascending and descending spinal tracts." Neuron **80**(6): 1407-1420.

Panayi, H., E. Panayiotou, M. Orford, N. Genethliou, R. Mean, G. Lapathitis, S. Li, M. Xiang, N. Kessaris, W. D. Richardson and S. Malas (2010). "Sox1 is required for the specification of a novel p2-derived interneuron subtype in the mouse ventral spinal cord." J Neurosci **30**(37): 12274-12280.

Parker, D. and S. Grillner (1996). "Tachykinin-mediated modulation of sensory neurons, interneurons, and synaptic transmission in the lamprey spinal cord." J Neurophysiol **76**(6): 4031-4039.

Pearlstein, E., F. Ben Mabrouk, J. F. Pflieger and L. Vinay (2005). "Serotonin refines the locomotor-related alternations in the in vitro neonatal rat spinal cord." Eur J Neurosci **21**(5): 1338-1346.

Pearson, K. G. (1993). "Common principles of motor control in vertebrates and invertebrates." Annu Rev Neurosci **16**: 265-297.

Pearson, K. G. (1995). "Proprioceptive regulation of locomotion." Curr Opin Neurobiol **5**(6): 786-791.

Pierani, A., L. Moran-Rivard, M. J. Sunshine, D. R. Littman, M. Goulding and T. M. Jessell (2001). "Control of interneuron fate in the developing spinal cord by the progenitor homeodomain protein Dbx1." Neuron **29**(2): 367-384.

Pivetta, C., M. S. Esposito, M. Sigrist and S. Arber (2014). "Motor-circuit communication matrix from spinal cord to brainstem neurons revealed by developmental origin." Cell **156**(3): 537-548.

Proske, U. and S. C. Gandevia (2012). "The proprioceptive senses: their roles in signaling body shape, body position and movement, and muscle force." Physiol Rev **92**(4): 1651-1697.

Quinlan, K. A. and O. Kiehn (2007). "Segmental, synaptic actions of commissural interneurons in the mouse spinal cord." J Neurosci **27**(24): 6521-6530.

Rabe Bernhardt, N., F. Memic, H. Gezelius, A. L. Thiebes, A. Vallstedt and K. Kullander (2012). "DCC mediated axon guidance of spinal interneurons is essential for normal locomotor central pattern generator function." Dev Biol **366**(2): 279-289.

Rabe, N., H. Gezelius, A. Vallstedt, F. Memic and K. Kullander (2009). "Netrin-1-dependent spinal interneuron subtypes are required for the formation of left-right alternating locomotor circuitry." J Neurosci **29**(50): 15642-15649.

Restrepo, C. E., L. Lundfald, G. Szabo, F. Erdelyi, H. U. Zeilhofer, J. C. Glover and O. Kiehn (2009). "Transmitter-phenotypes of commissural interneurons in the lumbar spinal cord of newborn mice." J Comp Neurol **517**(2): 177-192.

Restrepo, C. E., G. Margaryan, L. Borgius, L. Lundfald, D. Sargsyan and O. Kiehn (2011). "Change in the balance of excitatory and inhibitory midline fiber crossing as an explanation for the hopping phenotype in EphA4 knockout mice." Eur J Neurosci **34**(7): 1102-1112.

Romanes, G. J. (1964). "THE MOTOR POOLS OF THE SPINAL CORD." Prog Brain Res **11**: 93-119.

Rossignol, S. (1996). "Visuomotor regulation of locomotion." Can J Physiol Pharmacol **74**(4): 418-425.

Rybak, I. A., N. A. Shevtsova and O. Kiehn (2013). "Modelling genetic reorganization in the mouse spinal cord affecting left-right coordination during locomotion." J Physiol **591**(Pt 22): 5491-5508.

Sahin, M., P. L. Greer, M. Z. Lin, H. Poucher, J. Eberhart, S. Schmidt, T. M. Wright, S. M. Shamah, S. O'Connell, C. W. Cowan, L. Hu, J. L. Goldberg, A. Debant, G. Corfas, C. E. Krull and M. E. Greenberg (2005). "Eph-dependent tyrosine phosphorylation of ephexin1 modulates growth cone collapse." Neuron **46**(2): 191-204.

Sakai, N. and Z. Kaprielian (2012). "Guidance of longitudinally projecting axons in the developing central nervous system." Front Mol Neurosci **5**: 59.

Sapir, T., E. J. Geiman, Z. Wang, T. Velasquez, S. Mitsui, Y. Yoshihara, E. Frank, F. J. Alvarez and M. Goulding (2004). "Pax6 and engrailed 1 regulate two distinct aspects of renshaw cell development." J Neurosci **24**(5): 1255-1264.

Schreyer, D. J. and E. G. Jones (1982). "Growth and target finding by axons of the corticospinal tract in prenatal and postnatal rats." Neuroscience **7**(8): 1837-1853.

Schubert, F. R., S. Dietrich, R. C. Mootoosamy, S. C. Chapman and A. Lumsden (2001). "Lbx1 marks a subset of interneurons in chick hindbrain and spinal cord." Mech Dev **101**(1-2): 181-185.

Serafini, T., S. A. Colamarino, E. D. Leonardo, H. Wang, R. Beddington, W. C. Skarnes and M. Tessier-Lavigne (1996). "Netrin-1 is required for commissural axon guidance in the developing vertebrate nervous system." Cell **87**(6): 1001-1014.

Serradj, N. and M. Jamon (2009). "The adaptation of limb kinematics to increasing walking speeds in freely moving mice 129/Sv and C57BL/6." Behav Brain Res **201**(1): 59-65.

Shamah, S. M., M. Z. Lin, J. L. Goldberg, S. Estrach, M. Sahin, L. Hu, M. Bazalakova, R. L. Neve, G. Corfas, A. Debant and M. E. Greenberg (2001). "EphA receptors regulate growth cone dynamics through the novel guanine nucleotide exchange factor ephexin." Cell **105**(2): 233-244.

Shik, M. L. and G. N. Orlovsky (1976). "Neurophysiology of locomotor automatism." Physiol Rev **56**(3): 465-501.

Sieber, M. A., R. Storm, M. Martinez-de-la-Torre, T. Muller, H. Wende, K. Reuter, E. Vasyutina and C. Birchmeier (2007). "Lbx1 acts as a selector gene in the fate determination of somatosensory and viscerosensory relay neurons in the hindbrain." J Neurosci **27**(18): 4902-4909.

Smith, C. L. and E. Frank (1988). "Peripheral specification of sensory connections in the spinal cord." Brain Behav Evol **31**(4): 227-242.

Snider, W. D. and S. B. McMahon (1998). "Tackling pain at the source: new ideas about nociceptors." Neuron **20**(4): 629-632.

Srour, M., J. B. Riviere, J. M. Pham, M. P. Dube, S. Girard, S. Morin, P. A. Dion, G. Asselin, D. Rochefort, P. Hince, S. Diab, N. Sharafaddinzadeh, S. Chouinard, H. Theoret, F. Charron and G. A. Rouleau (2010). "Mutations in DCC cause congenital mirror movements." Science **328**(5978): 592.

Stanfield, B. B. (1992). "The development of the corticospinal projection." Prog Neurobiol **38**(2): 169-202.

Stepien, A. E., M. Tripodi and S. Arber (2010). "Monosynaptic rabies virus reveals premotor network organization and synaptic specificity of cholinergic partition cells." Neuron **68**(3): 456-472.

Stoeckli, E. T., P. Sonderegger, G. E. Pollerberg and L. T. Landmesser (1997). "Interference with axonin-1 and NrCAM interactions unmasks a floor-plate activity inhibitory for commissural axons." Neuron **18**(2): 209-221.

Stokke, M. F., U. V. Nissen, J. C. Glover and O. Kiehn (2002). "Projection patterns of commissural interneurons in the lumbar spinal cord of the neonatal rat." J Comp Neurol **446**(4): 349-359.

Swett, J. E. and T. W. Schoultz (1975). "Mechanical transduction in the Golgi tendon organ: a hypothesis." Arch Ital Biol **113**(4): 374-382.

Talpalar, A. E., J. Bouvier, L. Borgius, G. Fortin, A. Pierani and O. Kiehn (2013). "Dual-mode operation of neuronal networks involved in left-right alternation." Nature **500**(7460): 85-88.

Talpalar, A. E., T. Endo, P. Low, L. Borgius, M. Hagglund, K. J. Dougherty, J. Ryge, T. S. Hnasko and O. Kiehn (2011). "Identification of minimal neuronal networks involved in flexor-extensor alternation in the mammalian spinal cord." Neuron **71**(6): 1071-1084.

Tessier-Lavigne, M. and C. S. Goodman (1996). "The molecular biology of axon guidance." Science **274**(5290): 1123-1133.

Todd, A. J. and A. C. Sullivan (1990). "Light microscope study of the coexistence of GABA-like and glycine-like immunoreactivities in the spinal cord of the rat." J Comp Neurol **296**(3): 496-505.

Toyoda, Y., R. Shinohara, D. Thumkeo, H. Kamijo, H. Nishimaru, H. Hioki, T. Kaneko, T. Ishizaki, T. Furuyashiki and S. Narumiya (2013). "EphA4-dependent axon retraction and midline localization of Ephrin-B3 are disrupted in the spinal cord of mice lacking mDia1 and mDia3 in combination." Genes Cells **18**(10): 873-885.

Tran, T. S. and P. E. Phelps (2000). "Axons crossing in the ventral commissure express L1 and GAD65 in the developing rat spinal cord." Dev Neurosci **22**(3): 228-236.

Tresch, M. C. and O. Kiehn (1999). "Coding of locomotor phase in populations of neurons in rostral and caudal segments of the neonatal rat lumbar spinal cord." J Neurophysiol **82**(6): 3563-3574.

Tripodi, M., A. E. Stepien and S. Arber (2011). "Motor antagonism exposed by spatial segregation and timing of neurogenesis." Nature **479**(7371): 61-66.

Ugolini, G. (1995). "Specificity of rabies virus as a transneuronal tracer of motor networks: transfer from hypoglossal motoneurons to connected second-order and higher order central nervous system cell groups." J Comp Neurol **356**(3): 457-480.

Ugolini, G. (2008). "Use of rabies virus as a transneuronal tracer of neuronal connections: implications for the understanding of rabies pathogenesis." Dev Biol (Basel) **131**: 493-506.

Ugolini, G. (2010). "Advances in viral transneuronal tracing." J Neurosci Methods **194**(1): 2-20.

Vallstedt, A. and K. Kullander (2013). "Dorsally derived spinal interneurons in locomotor circuits." Ann N Y Acad Sci **1279**: 32-42.

Vong, L., C. Ye, Z. Yang, B. Choi, S. Chua, Jr. and B. B. Lowell (2011). "Leptin action on GABAergic neurons prevents obesity and reduces inhibitory tone to POMC neurons." Neuron **71**(1): 142-154.

Wallen-Mackenzie, A., H. Gezelius, M. Thoby-Brisson, A. Nygard, A. Enjin, F. Fujiyama, G. Fortin and K. Kullander (2006). "Vesicular glutamate transporter 2 is required for central respiratory rhythm generation but not for locomotor central pattern generation." J Neurosci **26**(47): 12294-12307.

Watson C., G. Paxinos, G. Kayalioglu (2008). "The spinal cord." Elsevier Ltd, Oxford: 308-379

Weber, I., G. Veress, P. Szucs, M. Antal and A. Birinyi (2007). "Neurotransmitter systems of commissural interneurons in the lumbar spinal cord of neonatal rats." Brain Res **1178**: 65-72.

Wegmeyer, H., J. Egea, N. Rabe, H. Gezelius, A. Filosa, A. Enjin, F. Varoqueaux, K. Deininger, F. Schnutgen, N. Brose, R. Klein, K. Kullander and A. Betz (2007). "EphA4-dependent axon guidance is mediated by the RacGAP alpha2-chimaerin." Neuron **55**(5): 756-767.

Wells, C. D., J. P. Fawcett, A. Traweger, Y. Yamanaka, M. Goudreault, K. Elder, S. Kulkarni, G. Gish, C. Virag, C. Lim, K. Colwill, A. Starostine, P. Metalnikov and T. Pawson (2006). "A Rich1/Amot complex regulates the Cdc42 GTPase and apical-polarity proteins in epithelial cells." Cell **125**(3): 535-548.

Wichmann, T. and M. R. DeLong (1996). "Functional and pathophysiological models of the basal ganglia." Curr Opin Neurobiol **6**(6): 751-758.

Wickersham, I. R., S. Finke, K. K. Conzelmann and E. M. Callaway (2007a). "Retrograde neuronal tracing with a deletion-mutant rabies virus." Nat Methods **4**(1): 47-49.

Wickersham, I. R., D. C. Lyon, R. J. Barnard, T. Mori, S. Finke, K. K. Conzelmann, J. A. Young and E. M. Callaway (2007b). "Monosynaptic restriction of transsynaptic tracing from single, genetically targeted neurons." Neuron **53**(5): 639-647.

Wickersham, I. R., H. A. Sullivan and H. S. Seung (2010). "Production of glycoprotein-deleted rabies viruses for monosynaptic tracing and high-level gene expression in neurons." Nat Protoc **5**(3): 595-606.

Wilson, D. M. and R. J. Wyman (1965). "MOTOR OUTPUT PATTERNS DURING RANDOM AND RHYTHMIC STIMULATION OF LOCUST THORACIC GANGLIA." Biophys J **5**: 121-143.

Wilson, J. M., R. Hartley, D. J. Maxwell, A. J. Todd, I. Lieberam, J. A. Kaltschmidt, Y. Yoshida, T. M. Jessell and R. M. Brownstone (2005). "Conditional rhythmicity of ventral spinal interneurons defined by expression of the Hb9 homeodomain protein." J Neurosci **25**(24): 5710-5719.

Witschi, R., T. Johansson, G. Morscher, L. Scheurer, J. Deschamps and H. U. Zeilhofer (2010). "Hoxb8-Cre mice: A tool for brain-sparing conditional gene deletion." Genesis **48**(10): 596-602.

Wong, K., X. R. Ren, Y. Z. Huang, Y. Xie, G. Liu, H. Saito, H. Tang, L. Wen, S. M. Brady-Kalnay, L. Mei, J. Y. Wu, W. C. Xiong and Y. Rao (2001). "Signal transduction in neuronal migration: roles of GTPase activating proteins and the small GTPase Cdc42 in the Slit-Robo pathway." Cell **107**(2): 209-221.

Wu, L., P. M. Sonner, D. J. Titus, E. P. Wiesner, F. J. Alvarez and L. Ziskind-Conhaim (2011). "Properties of a distinct subpopulation of GABAergic commissural interneurons that are part of the locomotor circuitry in the neonatal spinal cord." J Neurosci **31**(13): 4821-4833.

Xu, Q., G. Alldus, N. Holder and D. G. Wilkinson (1995). "Expression of truncated Sek-1 receptor tyrosine kinase disrupts the segmental restriction of gene expression in the Xenopus and zebrafish hindbrain." Development **121**(12): 4005-4016.

Xu, Q., G. Alldus, R. Macdonald, D. G. Wilkinson and N. Holder (1996). "Function of the Eph-related kinase rtk1 in patterning of the zebrafish forebrain." Nature **381**(6580): 319-322.

Xu, Q., G. Mellitzer and D. G. Wilkinson (2000). "Roles of Eph receptors and ephrins in segmental patterning." Philos Trans R Soc Lond B Biol Sci **355**(1399): 993-1002.

Xu, Y., C. Lopes, H. Wende, Z. Guo, L. Cheng, C. Birchmeier and Q. Ma (2013). "Ontogeny of excitatory spinal neurons processing distinct somatic sensory modalities." J Neurosci **33**(37): 14738-14748.

Yang, L. and G. J. Bashaw (2006). "Son of sevenless directly links the Robo receptor to rac activation to control axon repulsion at the midline." Neuron **52**(4): 595-607.

Yokoyama, N., M. I. Romero, C. A. Cowan, P. Galvan, F. Helmbacher, P. Charnay, L. F. Parada and M. Henkemeyer (2001). "Forward signaling mediated by ephrin-B3 prevents contralateral corticospinal axons from recrossing the spinal cord midline." Neuron **29**(1): 85-97.

Zagoraiou, L., T. Akay, J. F. Martin, R. M. Brownstone, T. M. Jessell and G. B. Miles (2009). "A cluster of cholinergic premotor interneurons modulates mouse locomotor activity." Neuron **64**(5): 645-662.

Zhang, Y., S. Narayan, E. Geiman, G. M. Lanuza, T. Velasquez, B. Shanks, T. Akay, J. Dyck, K. Pearson, S. Gosgnach, C. M. Fan and M. Goulding (2008). "V3 spinal neurons establish a robust and balanced locomotor rhythm during walking." Neuron **60**(1): 84-96.

Zheng, J. Q., M. Felder, J. A. Connor and M. M. Poo (1994). "Turning of nerve growth cones induced by neurotransmitters." Nature **368**(6467): 140-144.

Acknowledgements

First of all, I would like to thank Prof. Dr. Silvia Arber for giving me the opportunity to perform my PhD thesis in her lab, for mentoring, for fruitful advices and for proofreading this thesis.

Next, I am grateful to my PhD comitee members, Prof. Dr. Peter Scheiffele and Prof. Dr. Markus Affolter, for their helpful advices and discussions.

And I would like to thank Dr. Daisuke Satoh, who joined and continues my project, for helpful discussions and for proofreading my thesis.

I am also grateful to all members of the lab for support and encouragement discussions, especially Dr. Soledad Esposito and Emanuela Basaldella.

Special thank goes to Moritz Kirschmann from the Facility for Advanced Imaging and Microscopy and Michael Stadler from Bioinformatics at the FMI for their support in image processing and statistical analysis.

Additionally, I am thankful to the Lüthi group at the FMI who allowed me to share their open field assay.

Furthermore, I would like to thank the Werner-Siemens Foundation for their financial support during my PhD thesis.

Last but not least, I am very thankful to my parents and all my friends who have continuously supported and encouraged me throughout the whole time of my PhD thesis.